Electronic Supplementary Material (ESI) for Dalton Transactions.

Appendix A: Supporting Data

Pd(II) Complexes Bearing NNS Pincer Ligands: Unveiling Potent Cytotoxicity Against Breast and Pancreatic Cancer

Deepika Tanwar[a,b], Tashmeen Kaur[c], Athul Sudheendranath[d], Umesh Kumar[a]*, Deepika Sharma[c]*

[a]*Catalysis and Bioinorganic Research Lab, Department of Chemistry, Deshbandhu College, University of Delhi, New Delhi-110019, India.*
[b]*Department of Chemistry, University of Delhi, New Delhi-110007, India.*
[c]*Institute of Nano Science and Technology, Knowledge City, Mohali, Punjab-140306, India*
[d]*Department of Chemistry, Indian Institute of Technology, New Delhi-110016, India.*

Email: ukumar@db.du.ac.in, deepika@inst.ac.in

1. Materials and Methods

All reagents were purchased from Sigma-Aldrich. All organic chemicals, inorganic salts, and solvents were of analytical grade and were used without further purification. The solvents were distilled using drying agents before use. The compound 2-Bromo-*N*-quinolin-8-yl-acetamide (**A**) was prepared by following literature procedure.[1] The IR spectral data for the samples were obtained using an IR Affinity–1 Shimadzu FTIR spectrometer from powdered samples by the ATR method and on a Shimadzu IR435 spectrometer using KBr pellets, with data presented in the frequency range of 400–4000 cm^{-1}. Elemental analyses were analyzed on an Elementar AnalysenSysteme GmbH VarioEL V3.00. ^{1}H NMR and $^{13}C\{^{1}H\}$ NMR spectra were recorded on a Bruker AV-400 MHz/Jeol ECX 400 MHz spectrometer operating at field strengths of 400 and 100.5 MHz, respectively, and the chemical shifts are reported in ppm relative to TMS. Electrospray ionization mass spectra (ESI−MS) were recorded on a Waters Q-TOF Premier Micromass spectrometer with CH_3OH as the carrier solvent.

1.1 X-ray Diffraction Studies

Details of the data collection, structure solution, and refinement of structurally characterized compounds are presented in **Table S1**. X-ray crystallographic diffraction data for **C1** and **C4** were collected on Oxford Xcalibur S diffractometer (4-circle kappa goniometer, Sapphire−3 CCD detector, omega scans, graphite monochromator, and a single wavelength Enhance X-ray source with MoKα radiation) or Rigaku XtaLAB Synergy (4-circle goniometer, Hybrid Pixel Array Detector, omega scans, graphite monochromator, and PhotonJet (Mo) X-ray Source X-ray source type with micro-focus

sealed Xray tube).[2] Pre-experiment, data collection, data reduction, and absorption corrections were performed using the CrysAlisPro software suite.[3] The single-crystal X-ray diffraction data of **C3** was collected at 295K with a Bruker D8 Quest diffractometer equipped with microfocus sealed tube molybdenum source (Mo Kα, λ = 0.71073 Å) and PHOTON III photon counting detector.[4] The sample to detector distance was set to 50 mm, and the data reduction and multi-scan absorption were done using the program APEX4.[5] Further, the structure solution and refinement were carried out by the direct method in SHELXS97[6] and SHELXL[7] program in Olex2 package respectively.[8,9] All the non-hydrogen atoms were refined anisotropically, and hydrogen atoms were refined using the riding atom model in accordance with the default parameters in SHELXL. The non-covalent interactions were analyzed using Mercury software.

References:

1. W. Li, J. Luo and Z. Chen, *Dalton Trans.*, 2011, **40**, 484-488.
2. ENHANCE, Oxford Xcalibur Single Crystal Diffractometer, version 1.171.34.49, Oxford Diffraction Ltd: Oxford, U.K., 2006.
3. CrysAlisPro, version 1.171.34.49, Oxford Diffraction Ltd: Oxford, U.K., 2011.
4. B. Smart, Bruker Molecular Analysis Research Tool; Bruker AXS: 2000.
5. APEX4; Bruker AXS: 2002.
6. G. M. A. Sheldrick, Short History of SHELX. *Acta Crystallogr. Sect. A Found. Crystallogr*. 2008, **64** (1), 112−122.

7. G. M. Sheldrick, Crystal Structure Refinement with SHELXL. *Acta Crystallogr. Sect. C Struct. Chem*. 2015, **71** (1), 3−8.
8. O. V. Dolomanov, L. J. Bourhis, R. J. Gildea, J. A. K. Howard, H. Puschmann, OLEX2: a complete structure solution, refinement and analysis program. *J. Appl. Crystallogr*. 2009, **42**, 339−341.
9. L. J. Bourhis, O. V. Dolomanov, R. J. Gildea, J. A. K. Howard, H. Puschmann, The Anatomy of a Comprehensive Constrained, Restrained Refinement Program for the Modern Computing Environment-Olex2 Dissected. *Acta Crystallogr., Sect. A Found. Adv.* 2015, **71**, 59−75.

Tabe S1: Crystallographic data and structure refinement summary for complex C1, **C3** and **C4**.

Identification code	Complex **C1**	Complex **C3**	Complex **C4**
Empirical formula	$C_{17}H_{13}ClN_2OPdS$	$C_{18}H_{15}ClN_2OPdS$	$C_{18}H_{15}ClN_2O_2PdS$
Formula weight	435.20	449.266	465.23
Temperature/K	293.00(10)	295.00	293.00(16)
Crystal system	orthorhombic	monoclinic	monoclinic
Space group	Pbcn	$P2_1/c$	$P2_1/c$
a/Å	19.0594(5)	4.9586(6)	5.03180(10)
b/Å	10.4533(3)	14.645(2)	15.5130(4)
c/Å	16.3019(4)	23.907(4)	21.8863(6)
α/°	90	90	90
β/°	90	95.542(4)	94.618(2)
γ/°	90	90	90
Volume/Å^3	3247.89(15)	1728.0(4)	1702.86(7)
Z	8	4	4
ρ_{calc}g/cm^3	1.780	1.727	1.815
μ/mm^{-1}	1.440	1.356	1.384
F(000)	1728.0	893	928.0
Crystal size/mm^3	0.19 × 0.16 × 0.14	0.604 × 0.097 × 0.055	0.23 × 0.17 × 0.14
Radiation	Mo Kα (λ = 0.71073)	MoKα (λ = 0.71073)	Mo Kα (λ = 0.71073)
2Θ range for data collection/°	4.274 to 53.858	4.42 to 50	3.734 to 53.884
Index ranges	-23 ≤ h ≤ 23, -13 ≤ k ≤ 12, -20 ≤ l ≤ 15	-6 ≤ h ≤ 6, -19 ≤ k ≤ 19, -31 ≤ l ≤ 31	-6 ≤ h ≤ 6, -19 ≤ k ≤ 19, -27 ≤ l ≤ 26
Reflections collected	19837	50398	19671
Independent reflections	3391 [R_{int} = 0.0442, R_{sigma} = 0.0252]	3034 [R_{int} = 0.0682, R_{sigma} = 0.0349]	3571 [R_{int} = 0.0615, R_{sigma} = 0.0413]
Data/restraints/parameters	3391/0/196	3034/0/218	3571/0/221
Goodness-of-fit on F^2	1.076	1.072	1.078
Final R indexes [I>=2σ (I)]	R_1 = 0.0610, wR_2 = 0.1759	R_1 = 0.0377, wR_2 = 0.1047	R_1 = 0.0413, wR_2 = 0.1137
Final R indexes [all data]	R_1 = 0.0695, wR_2 = 0.1822	R_1 = 0.0469, wR_2 = 0.1141	R_1 = 0.0461, wR_2 = 0.1173
Largest diff. peak/hole / e Å^{-3}	2.47/-0.98	0.96/-0.49	0.74/-1.28

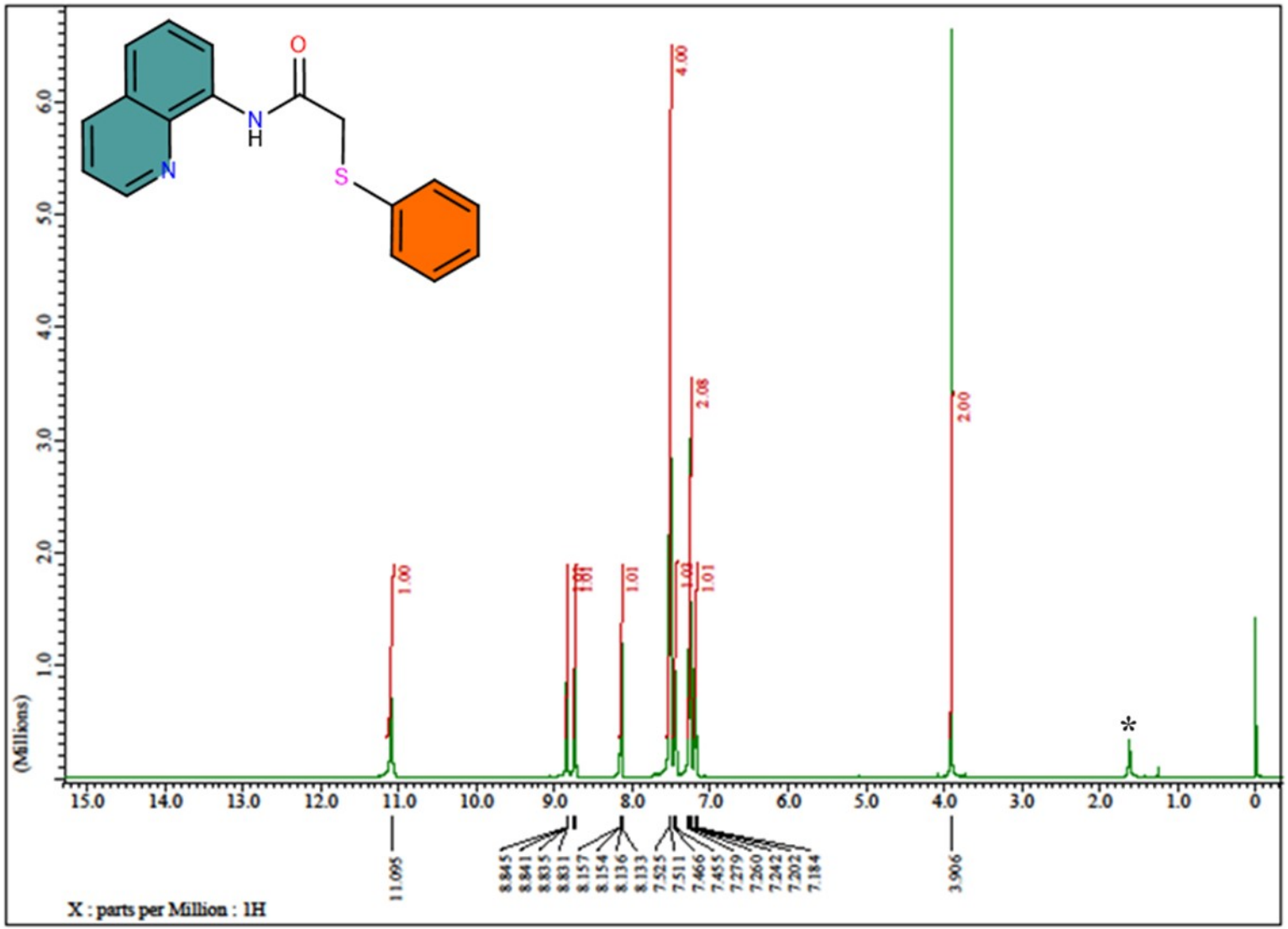

Fig. S1.[1]H NMR ($CDCl_3$, 400 MHz) spectrum of **L1** and asterisk (*) represents the solvent.

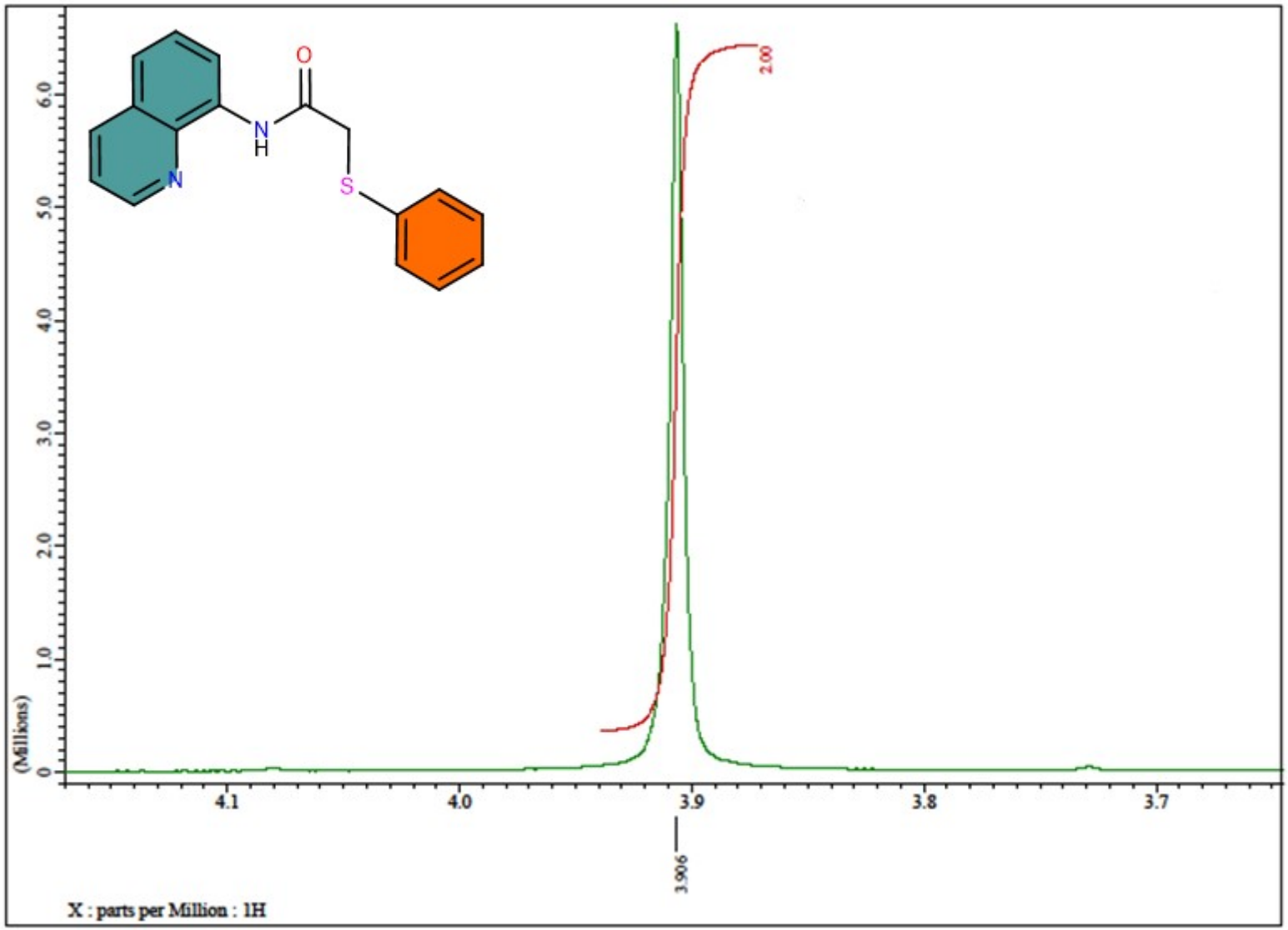

Fig. S2.^{1}H NMR ($CDCl_3$, 400 MHz) spectrum of **L1** in alkyl region.

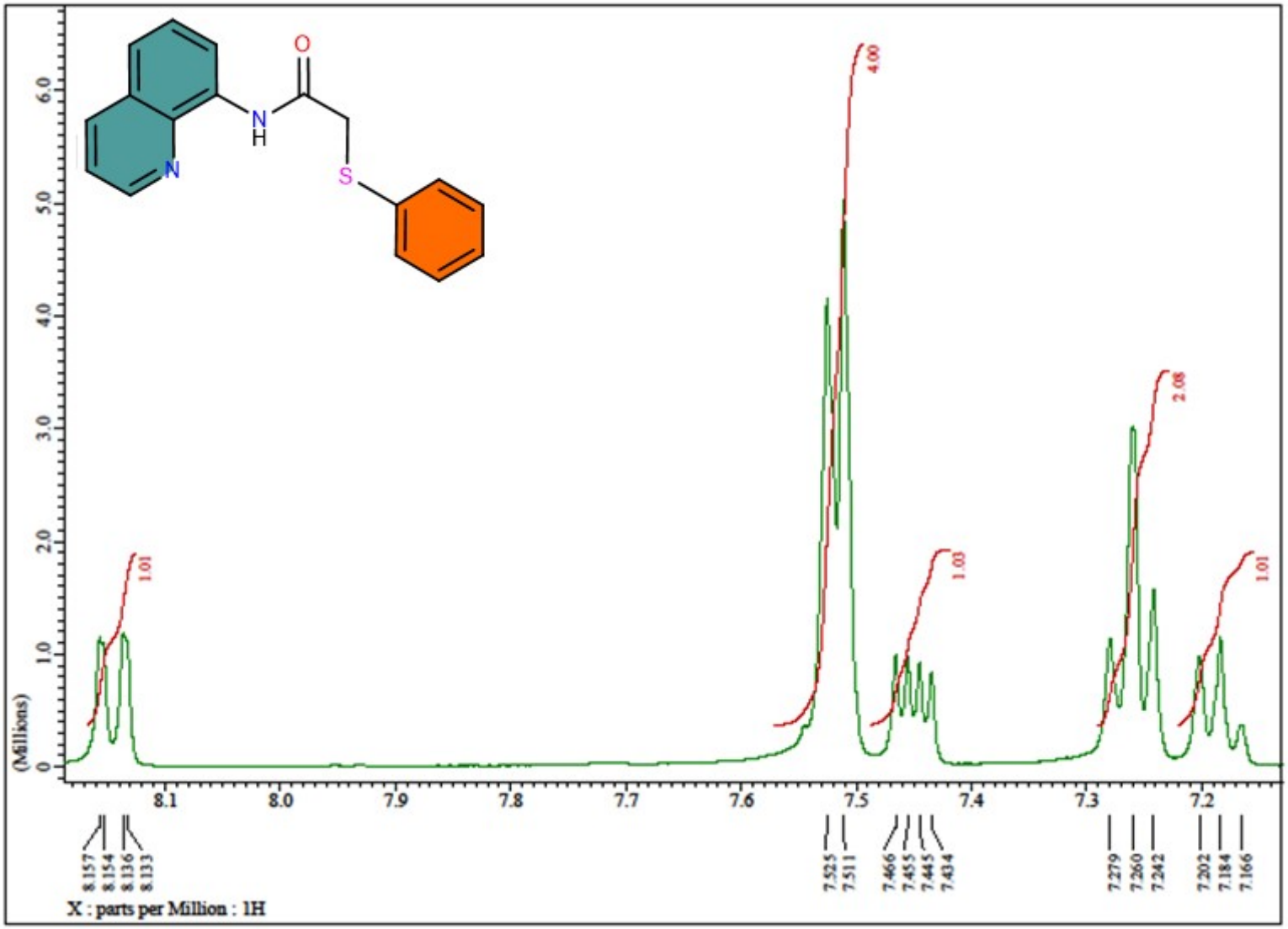

Fig. S3.^{1}H NMR ($CDCl_3$, 400 MHz) spectrum of **L1** in aryl region.

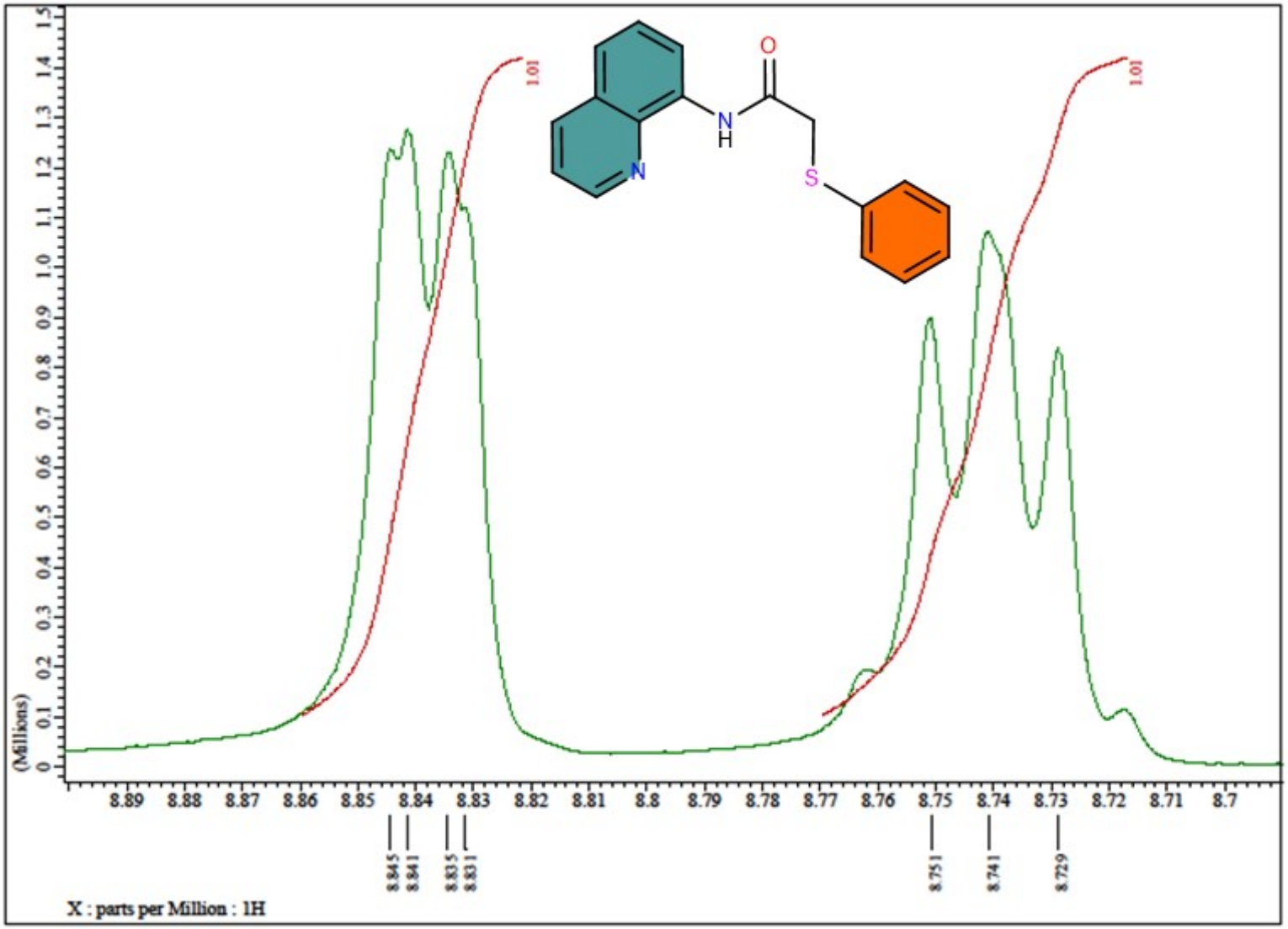

Fig. S4.[1]H NMR ($CDCl_3$, 400 MHz) spectrum of **L1** in aryl region.

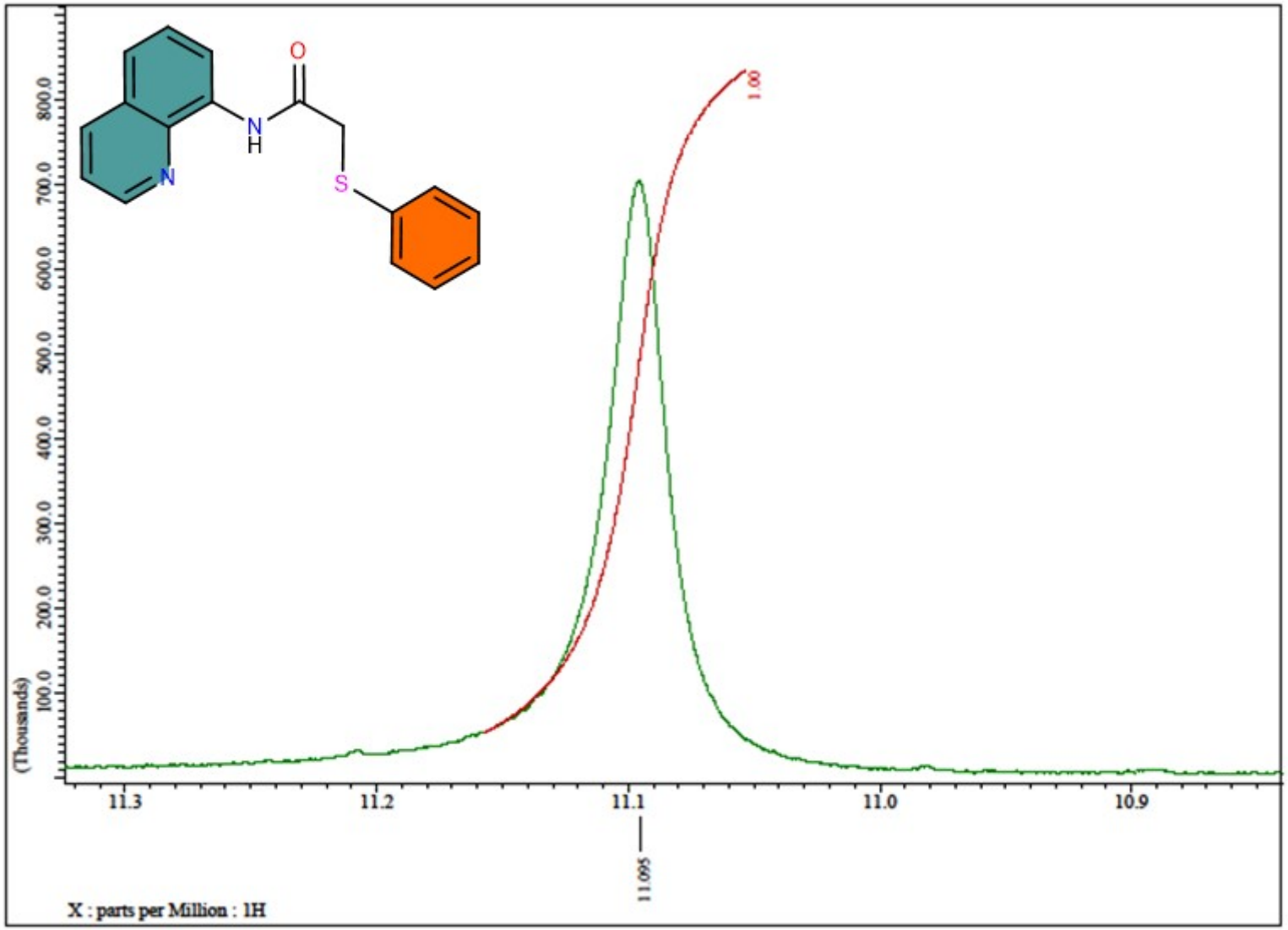

Fig. S5.^{1}H NMR ($CDCl_3$, 400 MHz) spectrum of **L1** in aryl region.

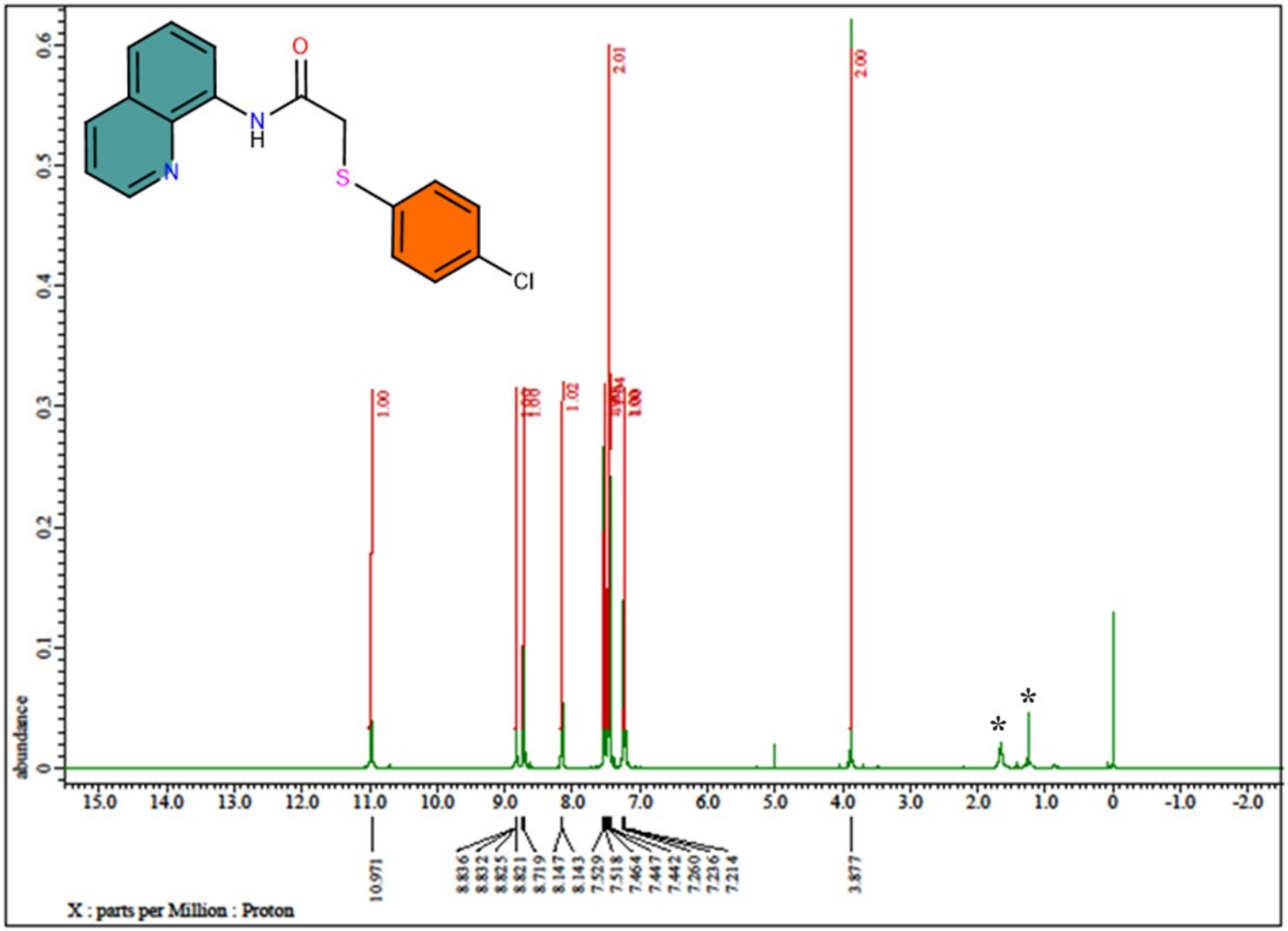

Fig. S6.[1]H NMR ($CDCl_3$, 400 MHz) spectrum of **L2** and asterisk (*) represents the solvents.

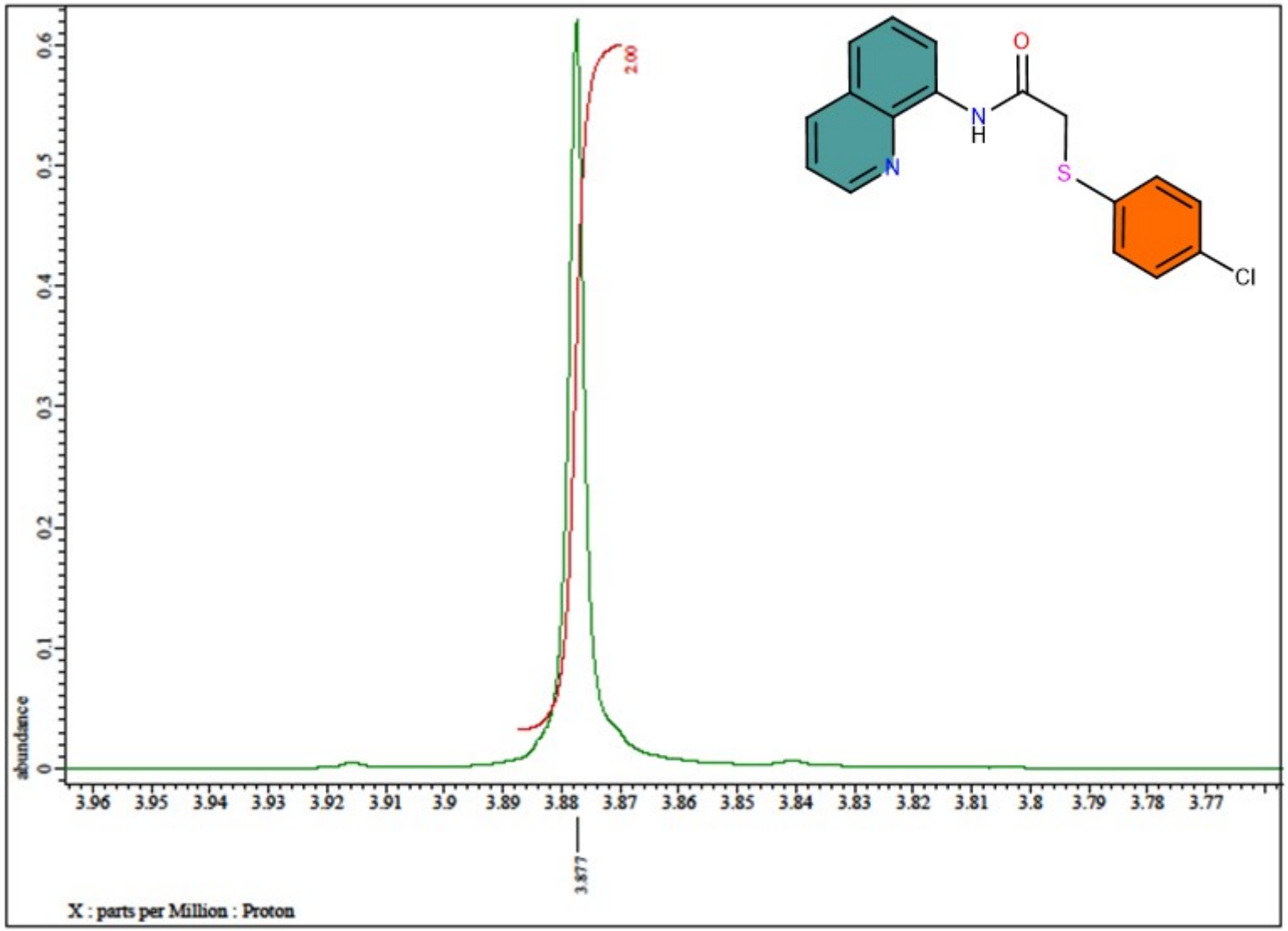

Fig. S7.^{1}H NMR ($CDCl_3$, 400 MHz) spectrum of **L2** in alkyl region.

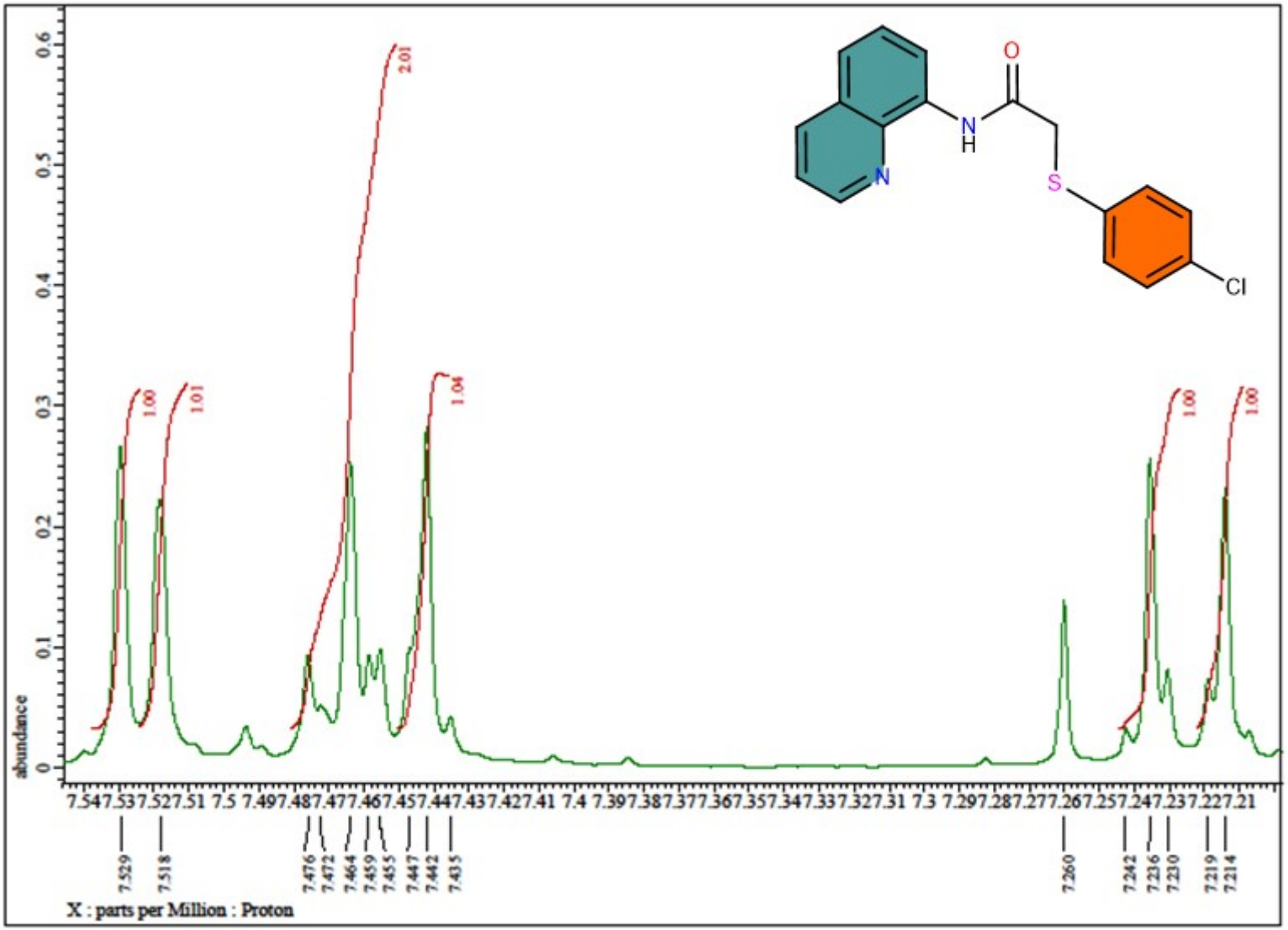

Fig. S8.^{1}H NMR ($CDCl_3$, 400 MHz) spectrum of **L2** in aryl region.

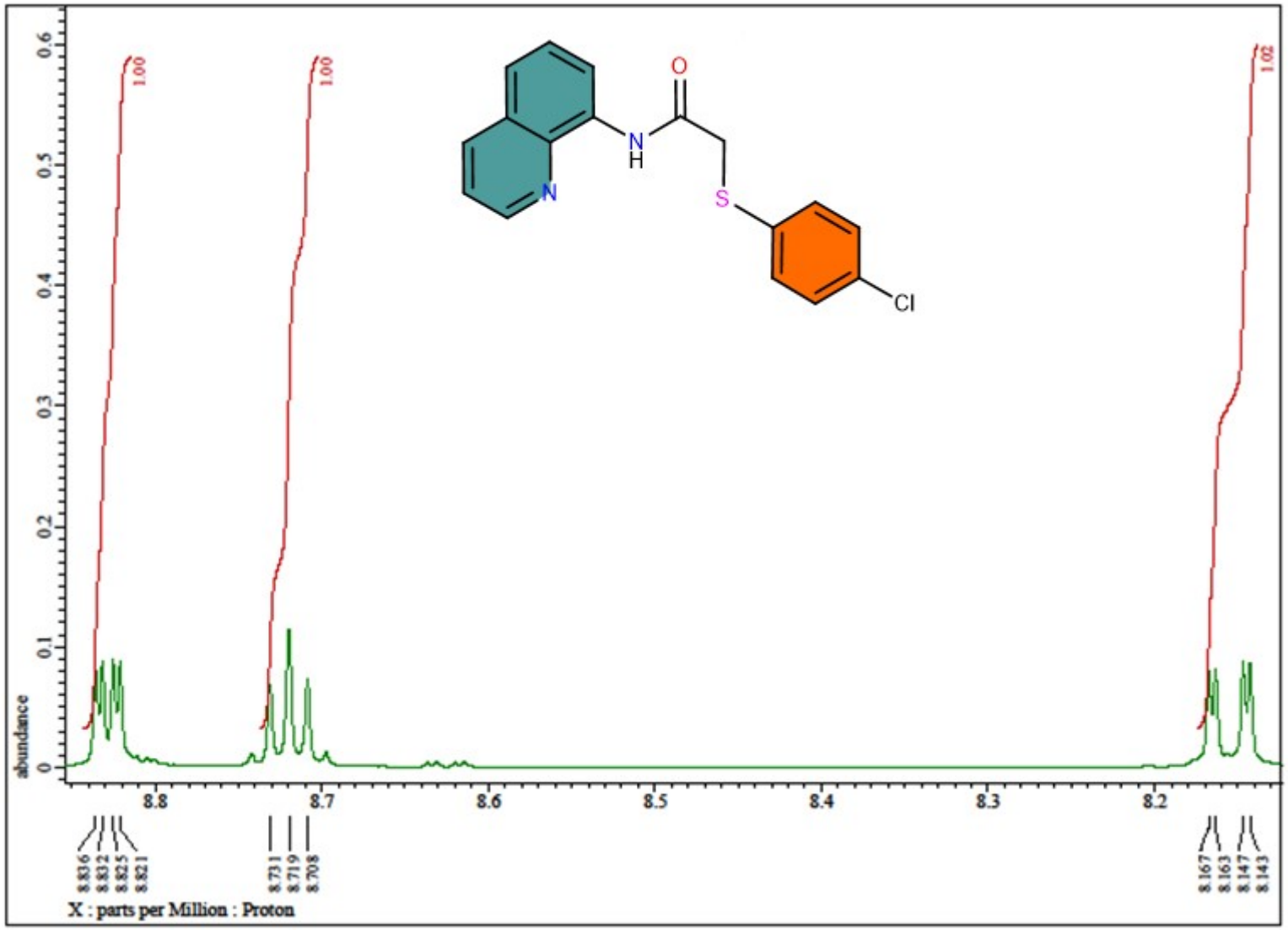

Fig. S9.[1]H NMR ($CDCl_3$, 400 MHz) spectrum of **L2** in aryl region.

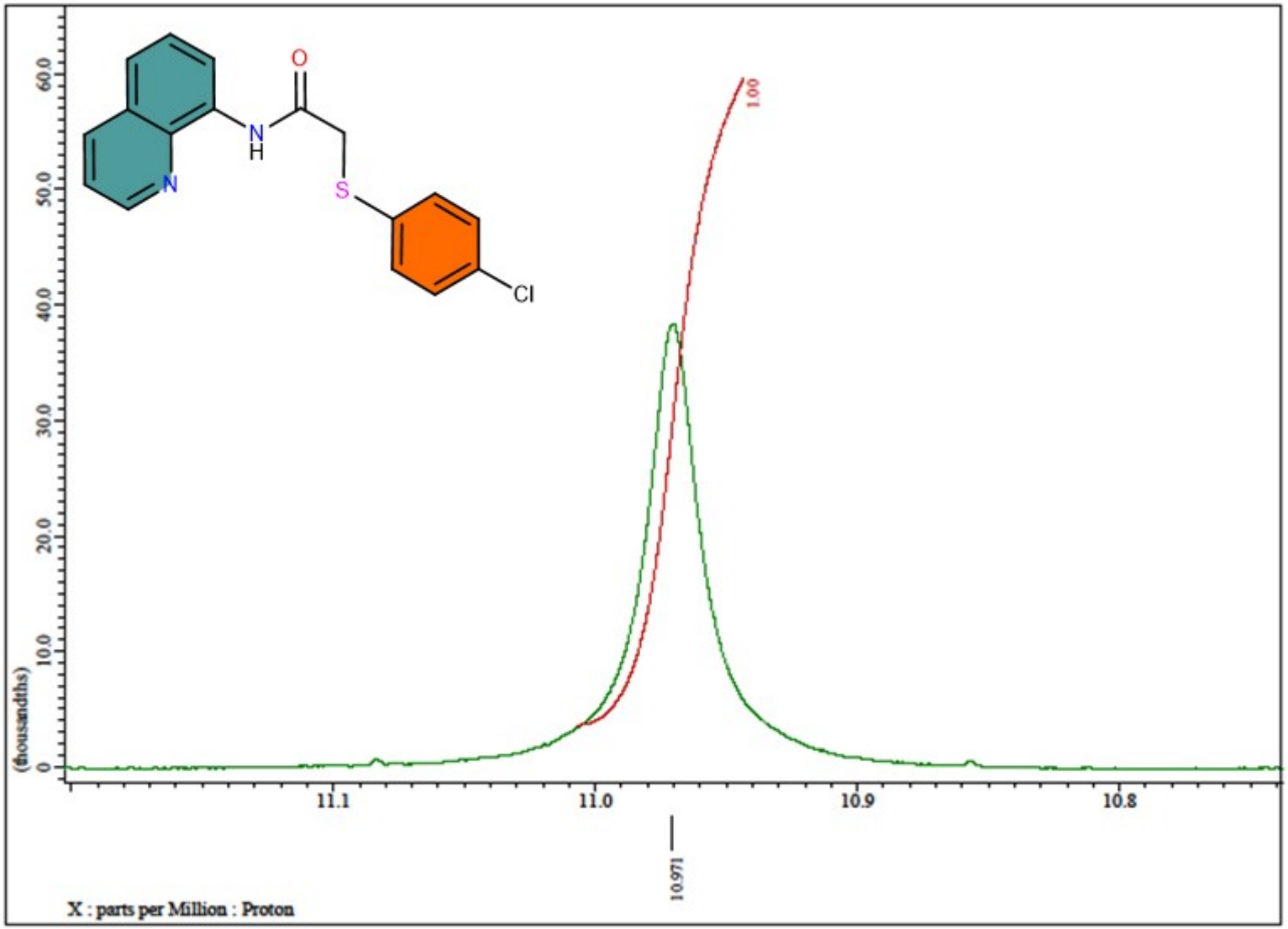

Fig. S10.[1]H NMR ($CDCl_3$, 400 MHz) spectrum of **L2** in aryl region.

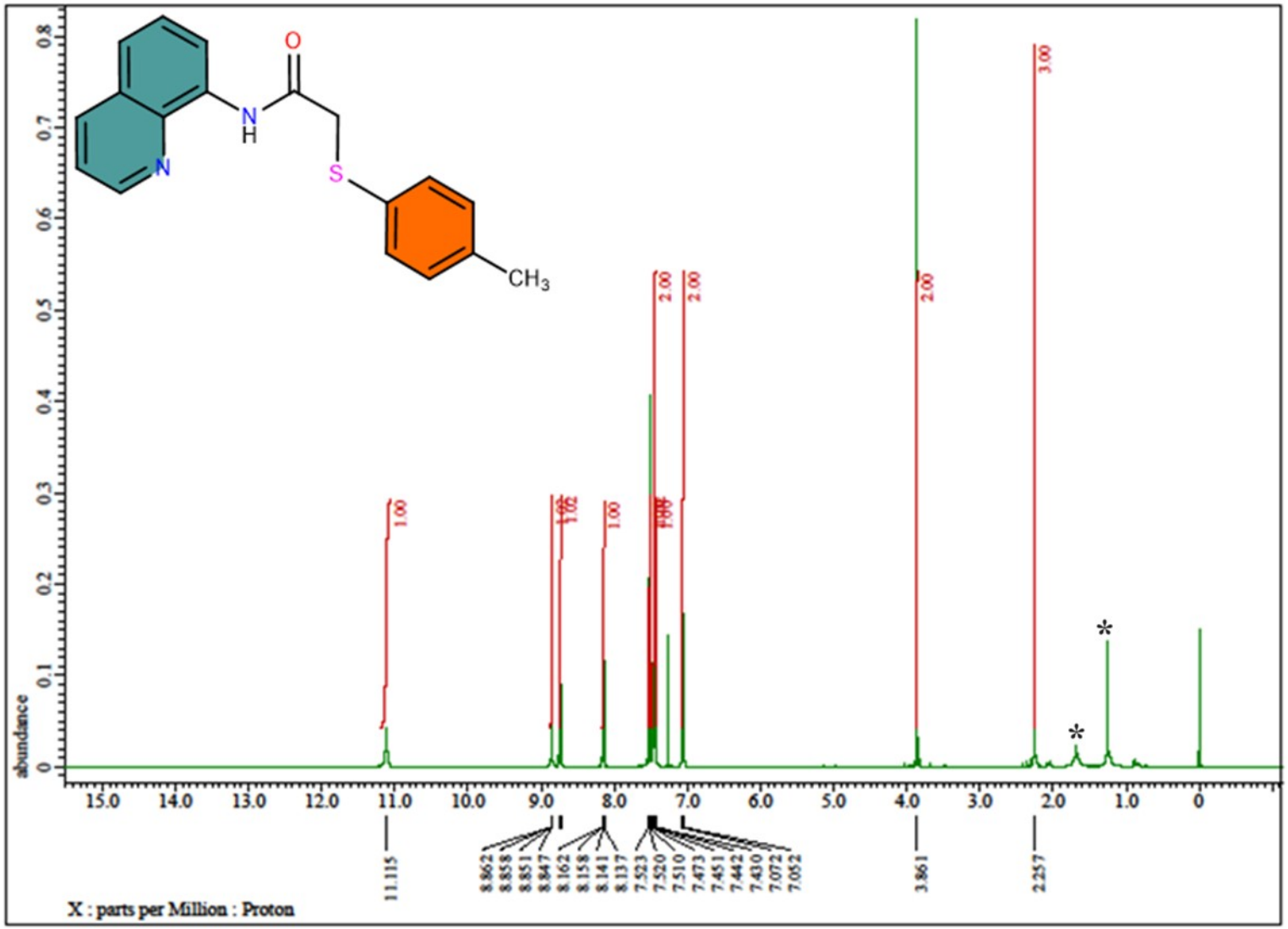

Fig. S11.[1]H NMR ($CDCl_3$, 400 MHz) spectrum of **L3** and asterisk (*) represents the solvents.

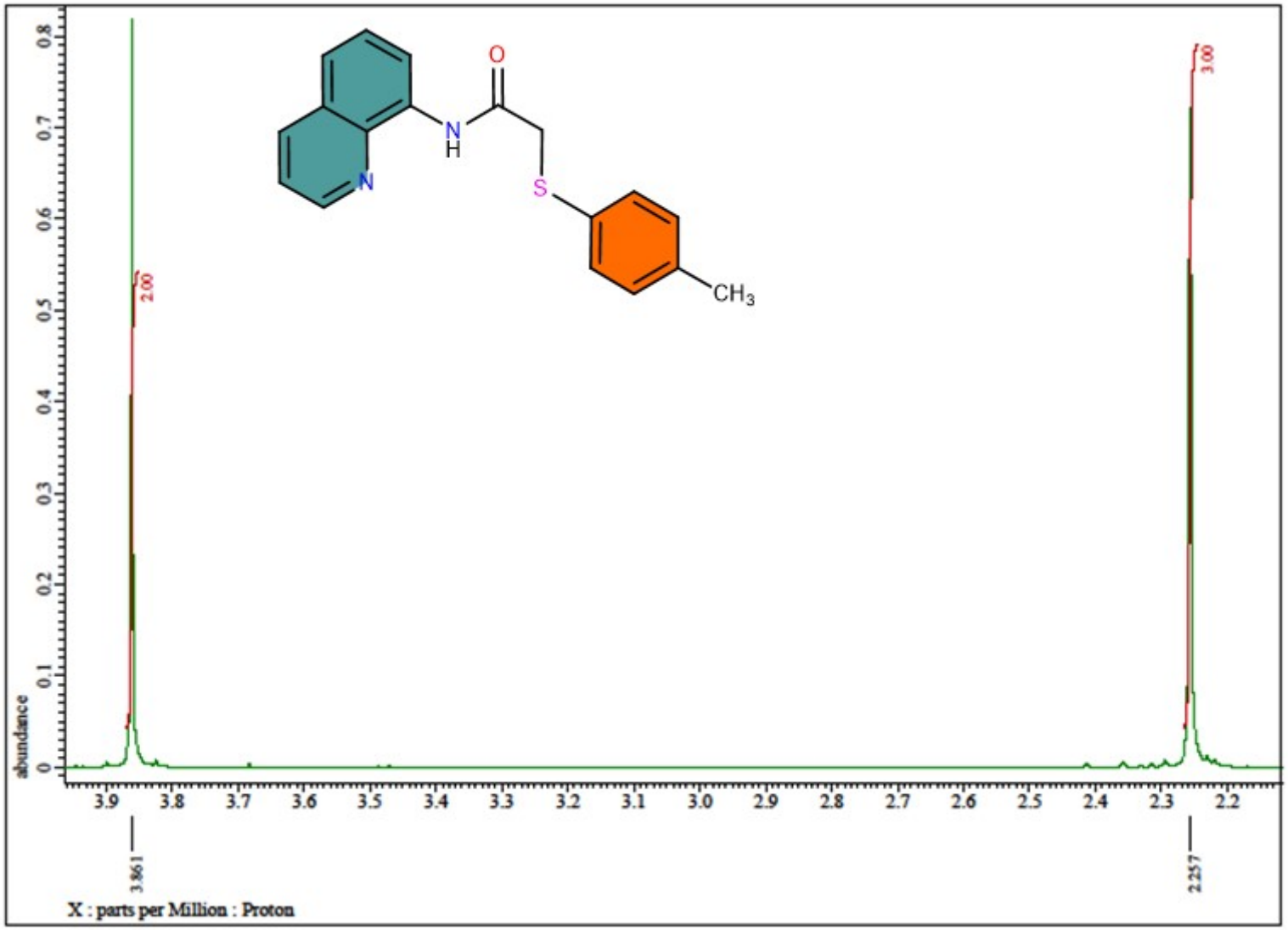

Fig. S12.[1]H NMR ($CDCl_3$, 400 MHz) spectrum of **L3** in alkyl region.

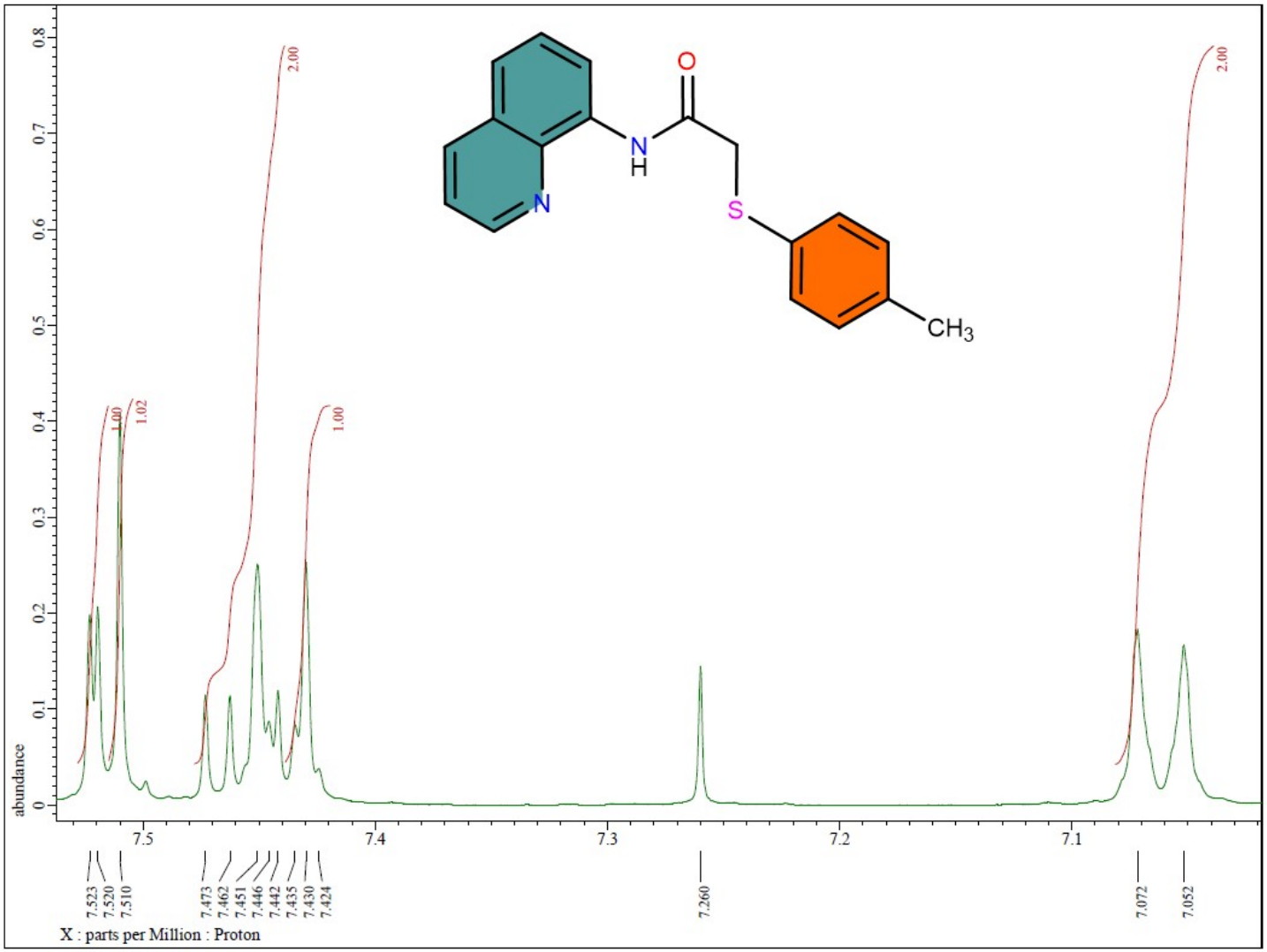

Fig. S13.[1]H NMR ($CDCl_3$, 400 MHz) spectrum of **L3** in aryl region.

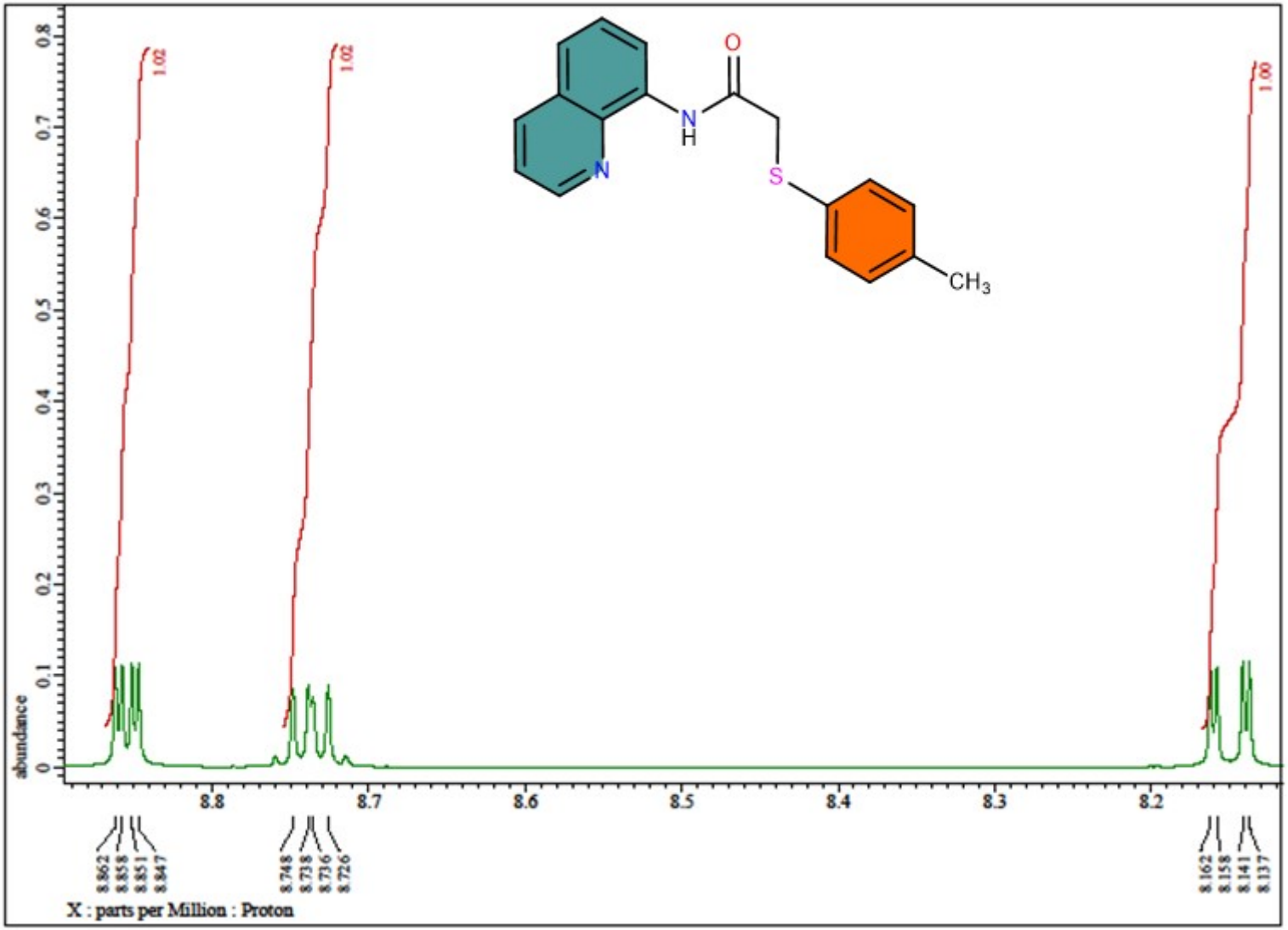

Fig. S14.[1]H NMR ($CDCl_3$, 400 MHz) spectrum of **L3** in aryl region.

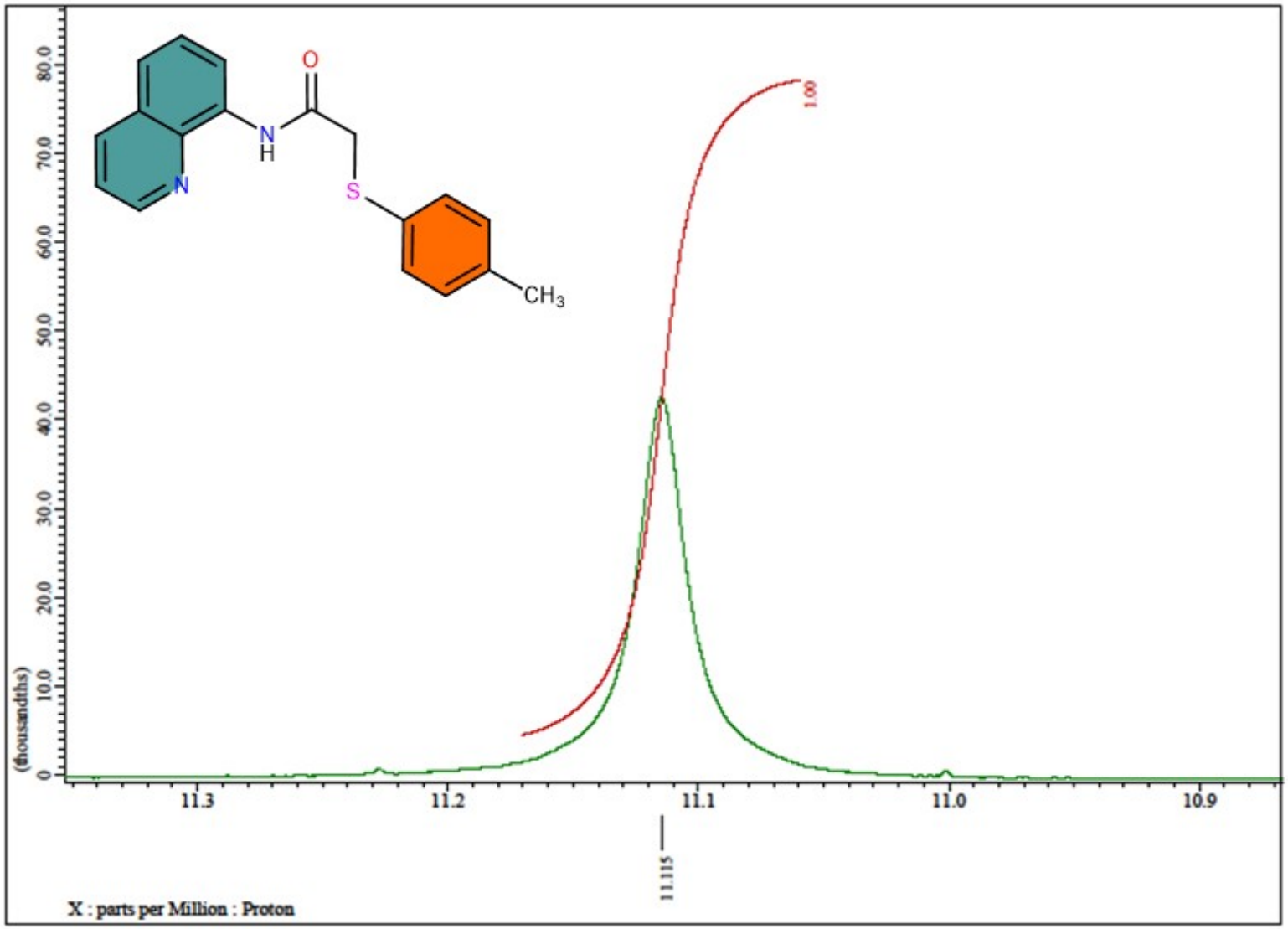

Fig. S15.[1]H NMR ($CDCl_3$, 400 MHz) spectrum of **L3** in aryl region.

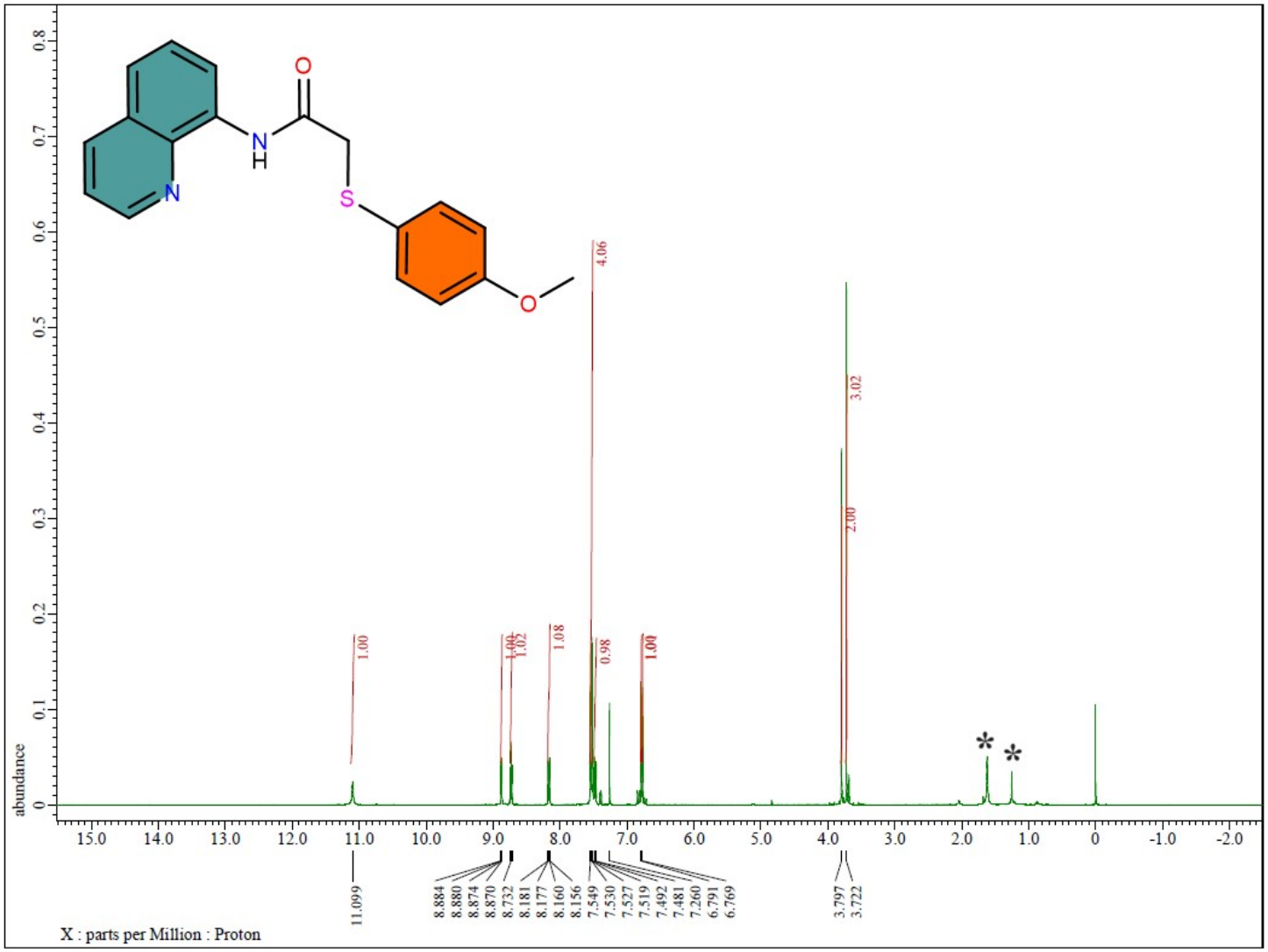

Fig. S16.[1]H NMR ($CDCl_3$, 400 MHz) spectrum of **L4** and asterisk (*) represents the solvents.

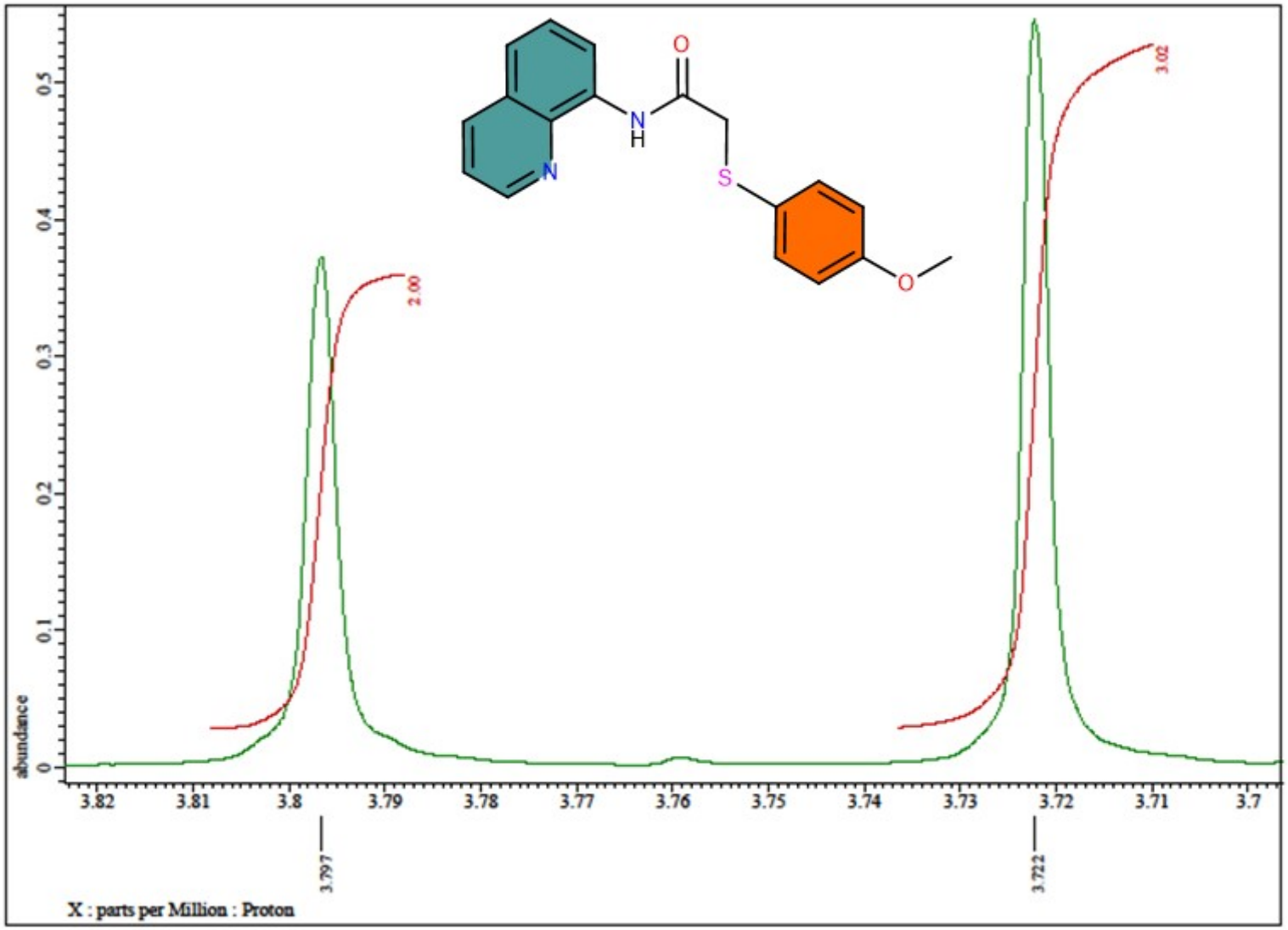

Fig. S17.[1]H NMR ($CDCl_3$, 400 MHz) spectrum of **L4** in alkyl region.

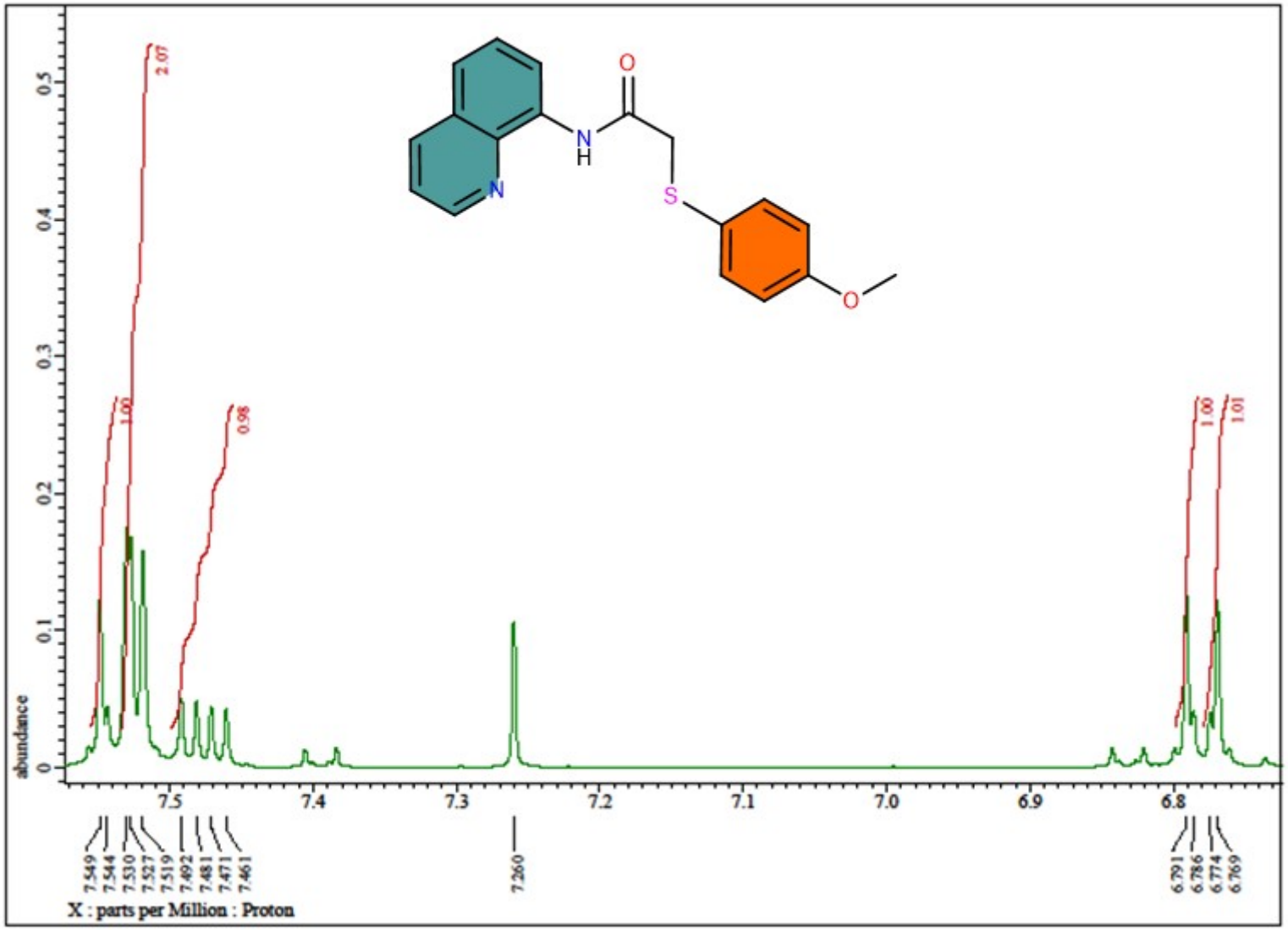

Fig. S18.[1]H NMR ($CDCl_3$, 400 MHz) spectrum of **L4** in aryl region.

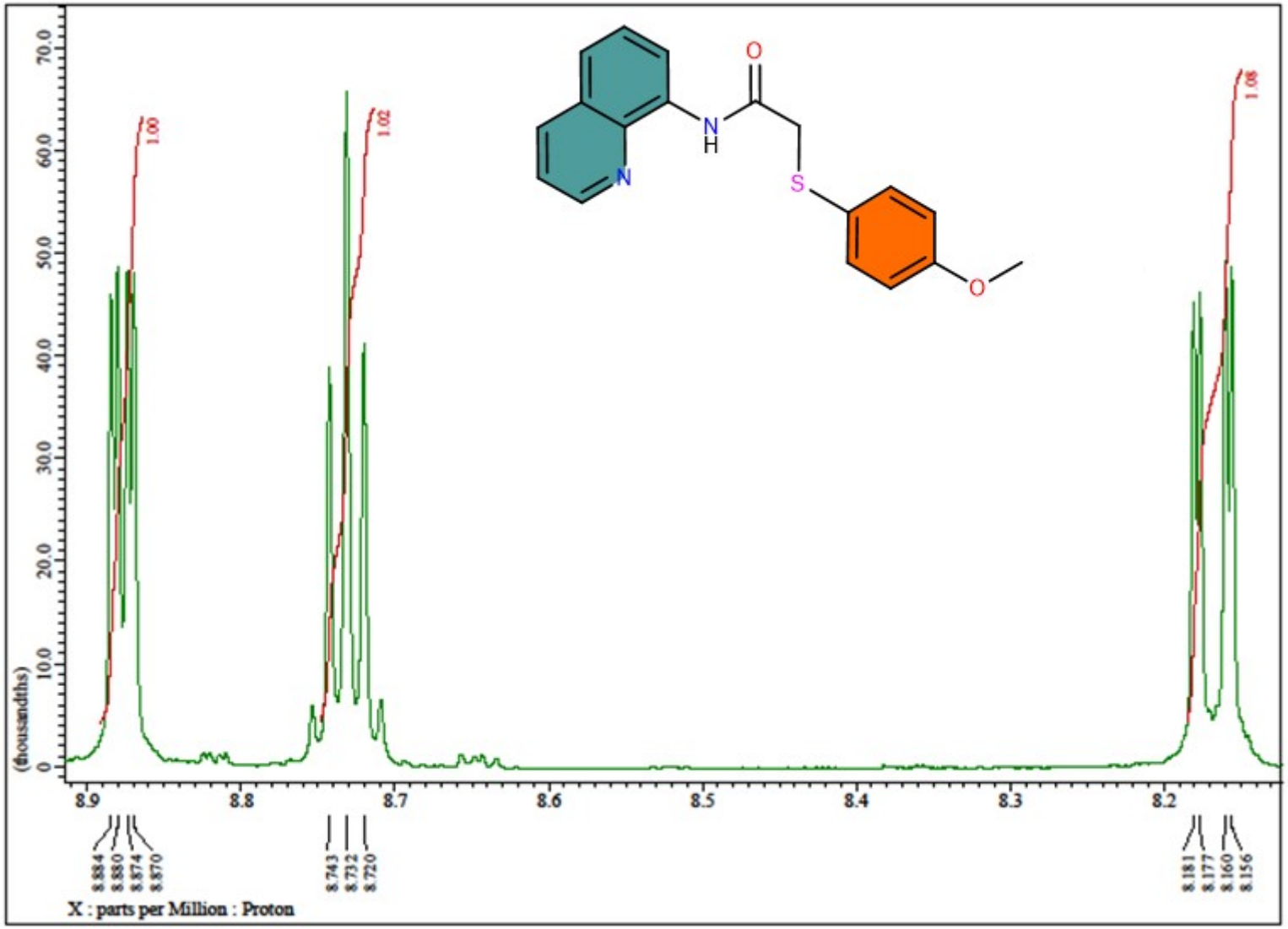

Fig. S19.[1]H NMR ($CDCl_3$, 400 MHz) spectrum of **L4** in aryl region.

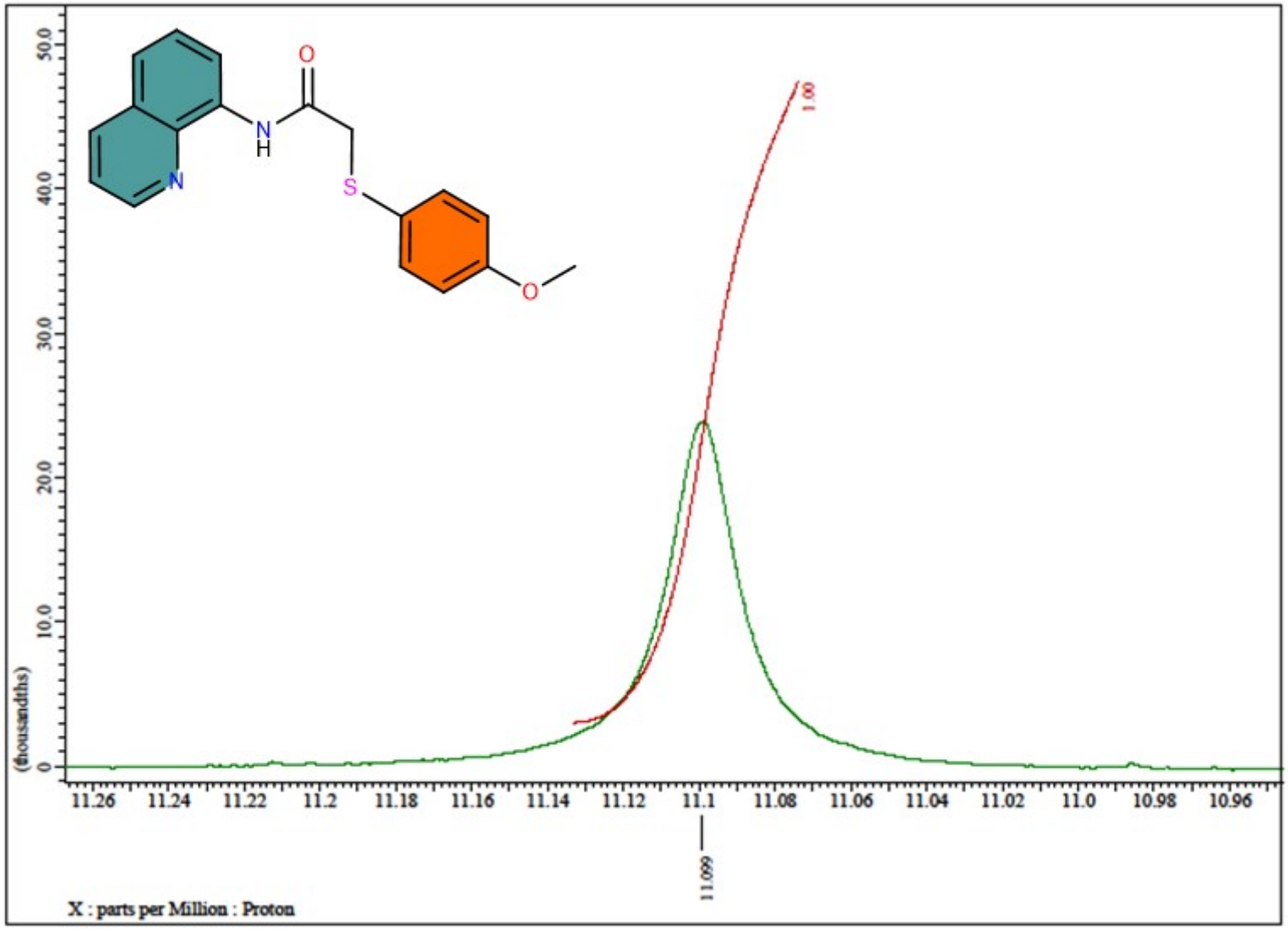

Fig. S20.[1]H NMR ($CDCl_3$, 400 MHz) spectrum of **L4** in aryl region.

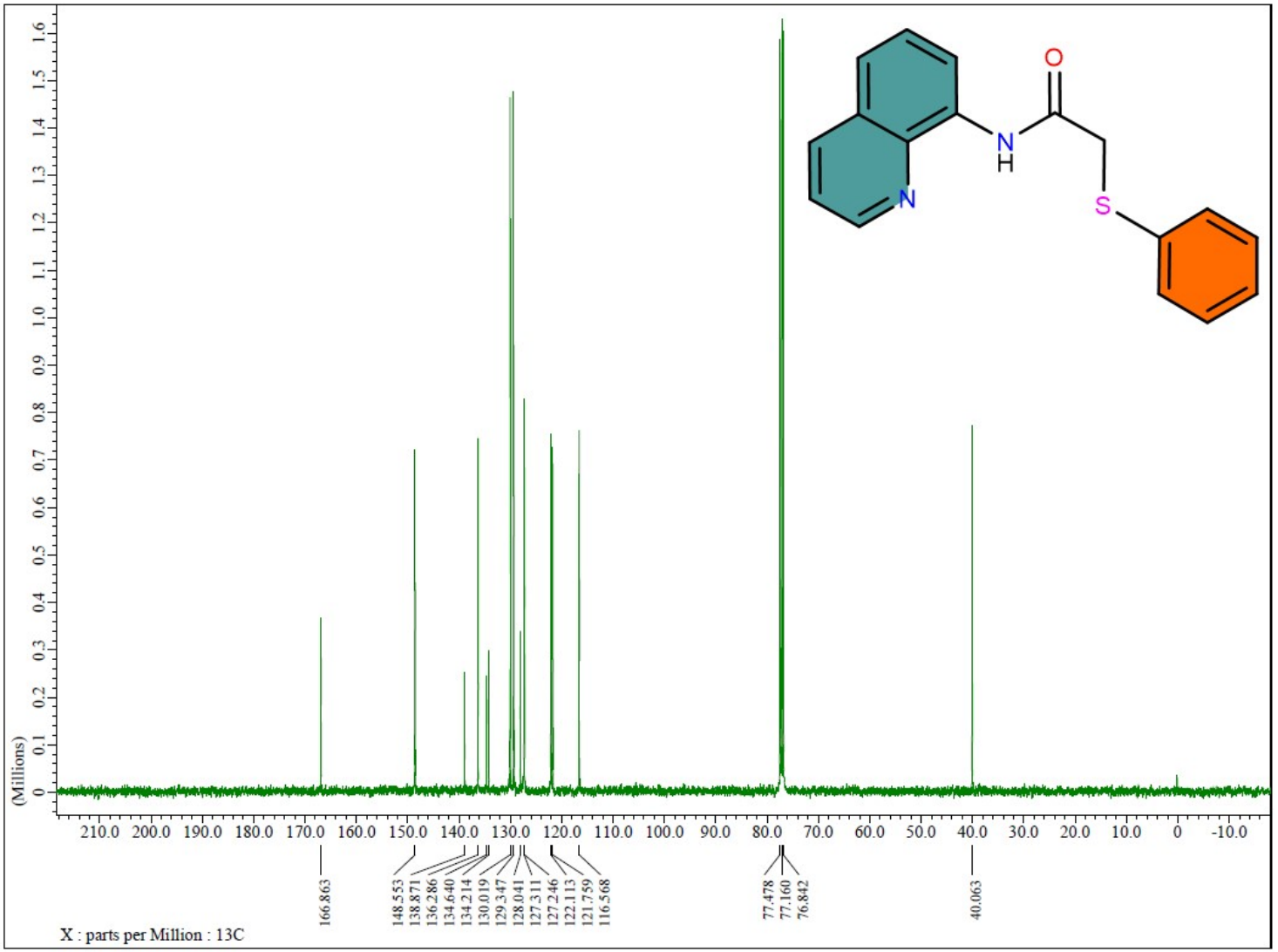

Fig. S21.$^{13}C\{^{1}H\}$ NMR ($CDCl_3$, 100.5 MHz) spectrum of **L1**.

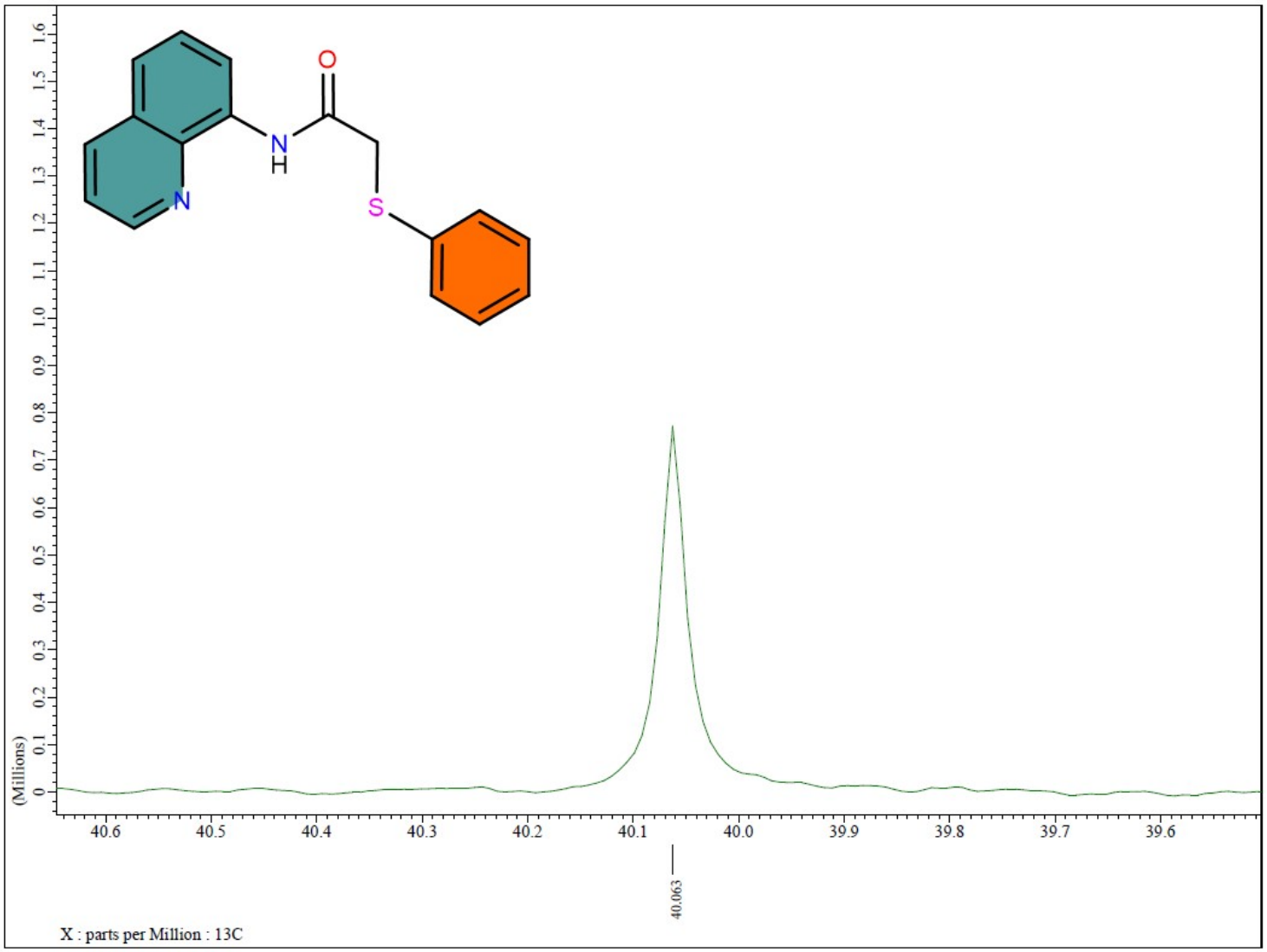

Fig. S22.$^{13}C\{^{1}H\}$ NMR ($CDCl_3$, 100.5 MHz) spectrum of **L1** in the alkyl region.

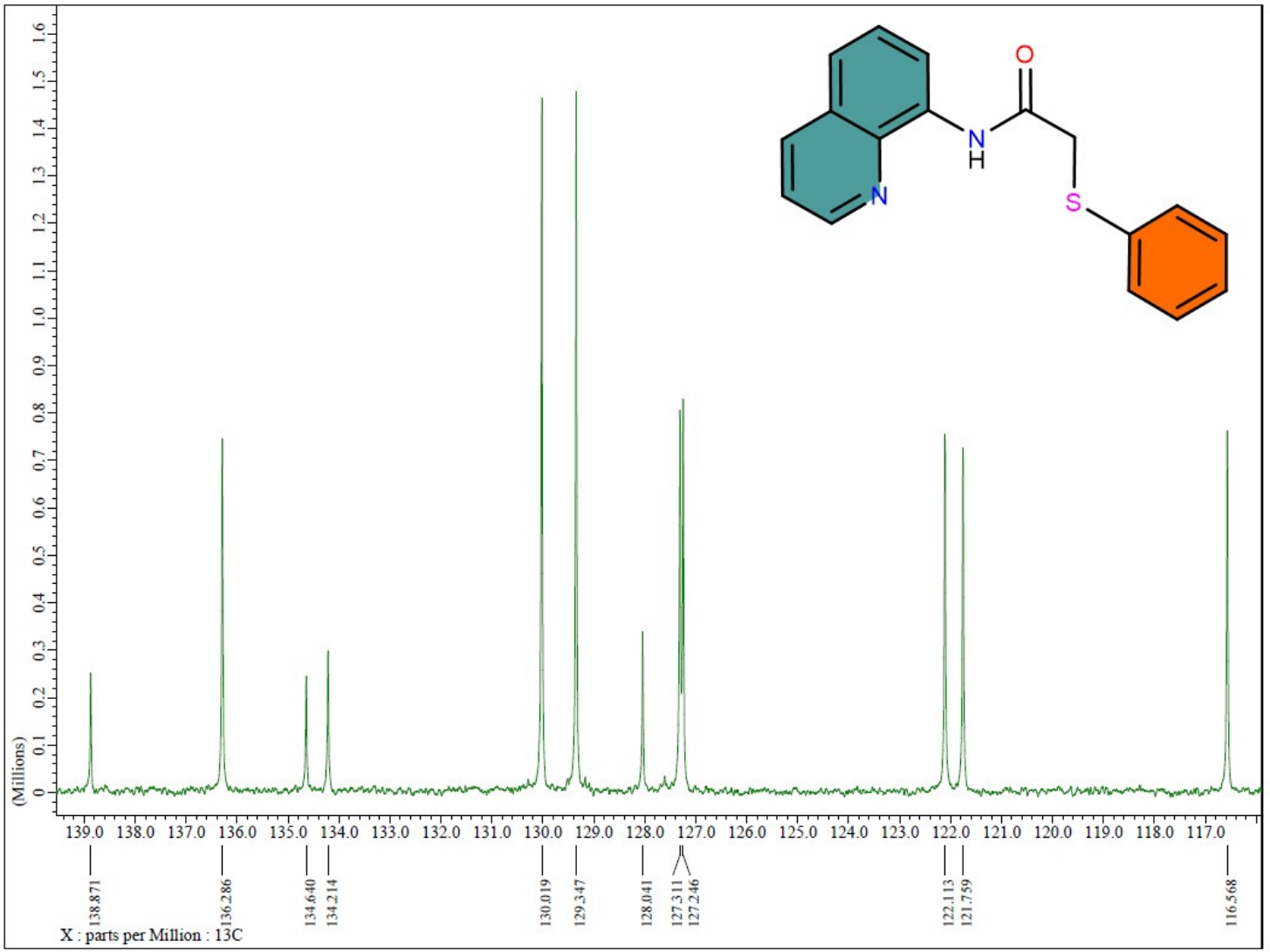

Fig. S23.$^{13}C\{^{1}H\}$ NMR ($CDCl_3$, 100.5 MHz) spectrum of **L1** in the aryl region.

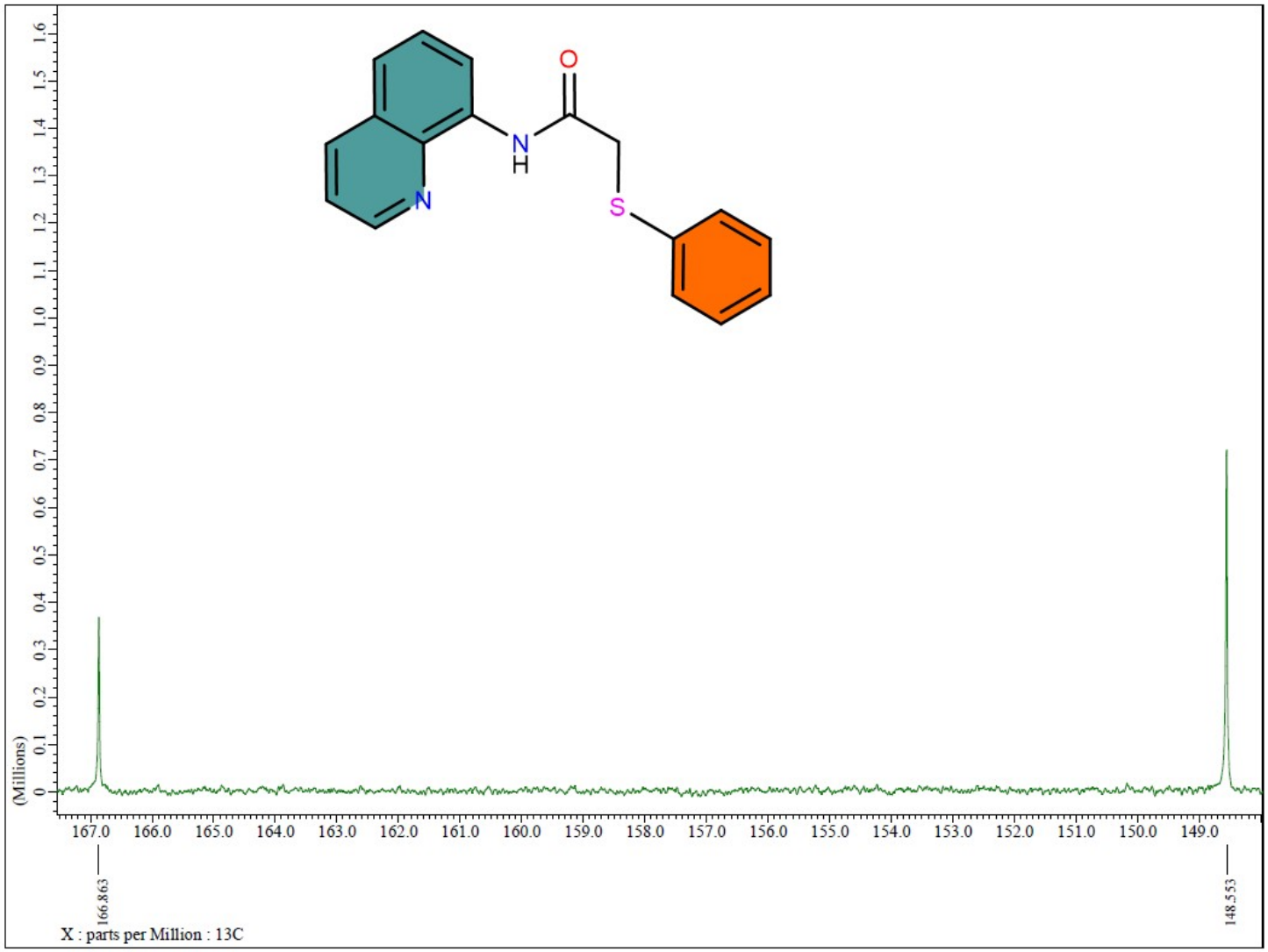

Fig. S24.$^{13}C\{^{1}H\}$ NMR ($CDCl_3$, 100.5 MHz) spectrum of **L1** in the aryl region.

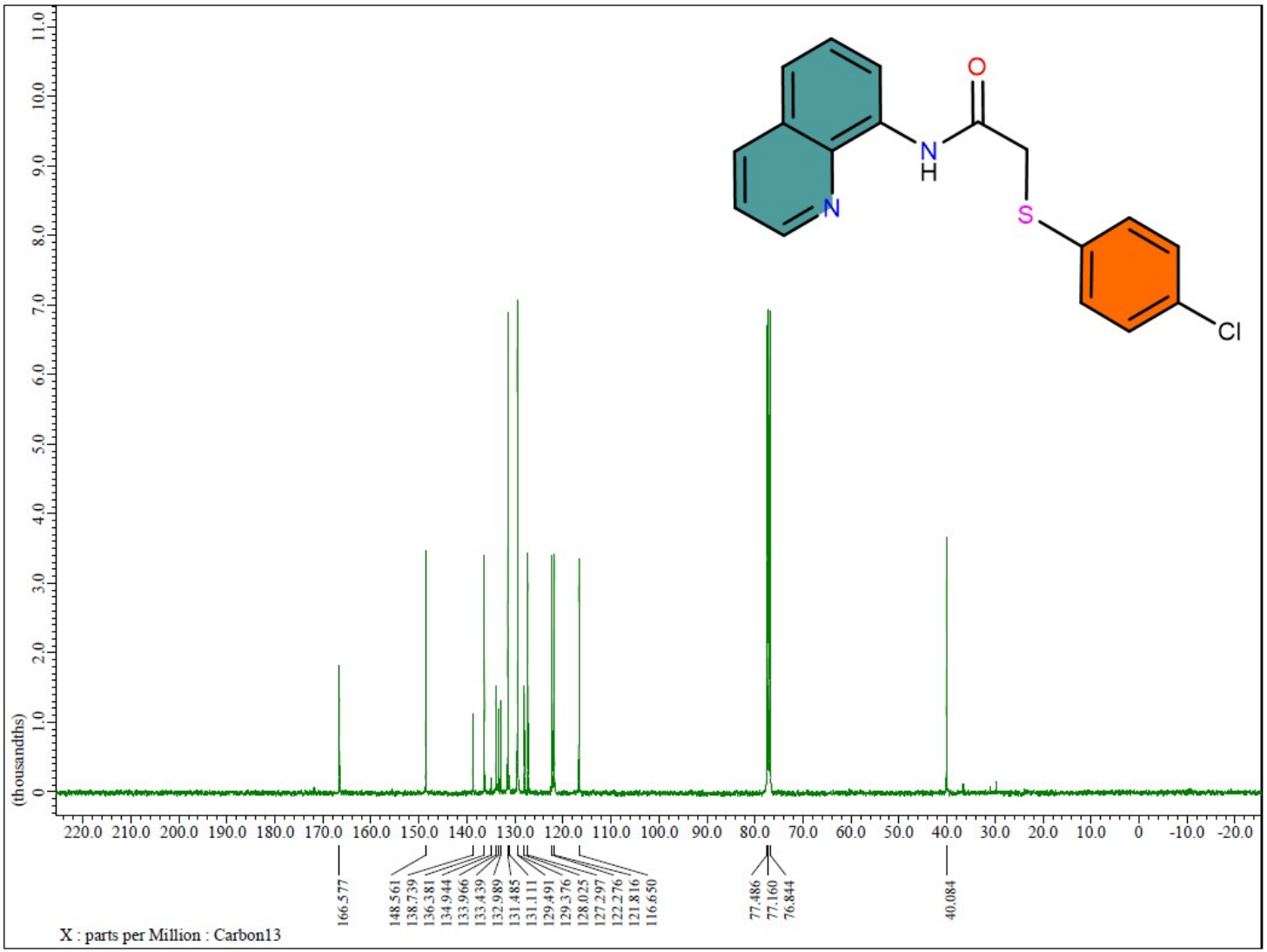

Fig. S25.$^{13}C\{^{1}H\}$ NMR ($CDCl_3$, 100.5 MHz) spectrum of **L2**.

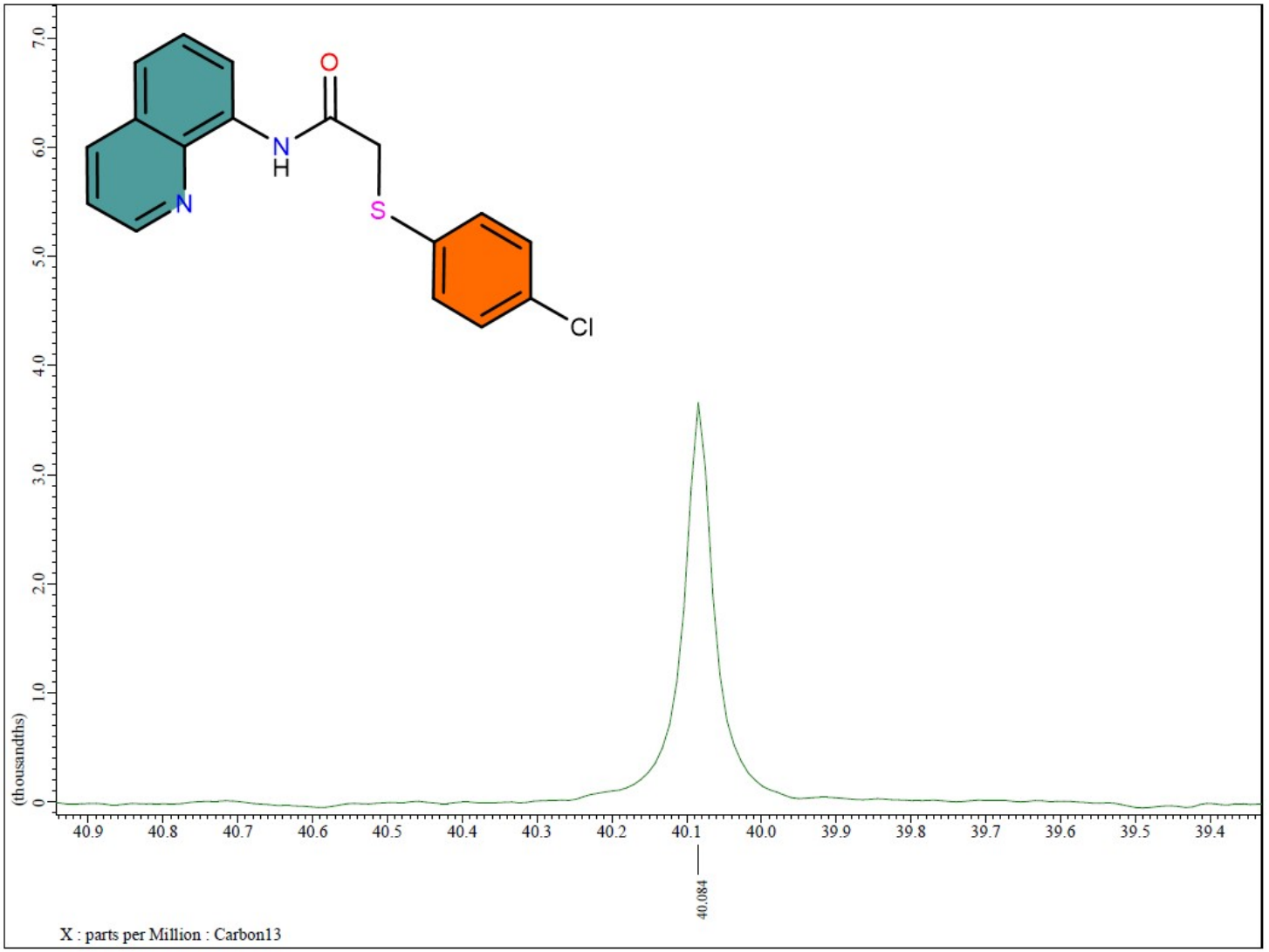

Fig. S26.$^{13}C\{^{1}H\}$ NMR ($CDCl_3$, 100.5 MHz) spectrum of **L2** in the alkyl region.

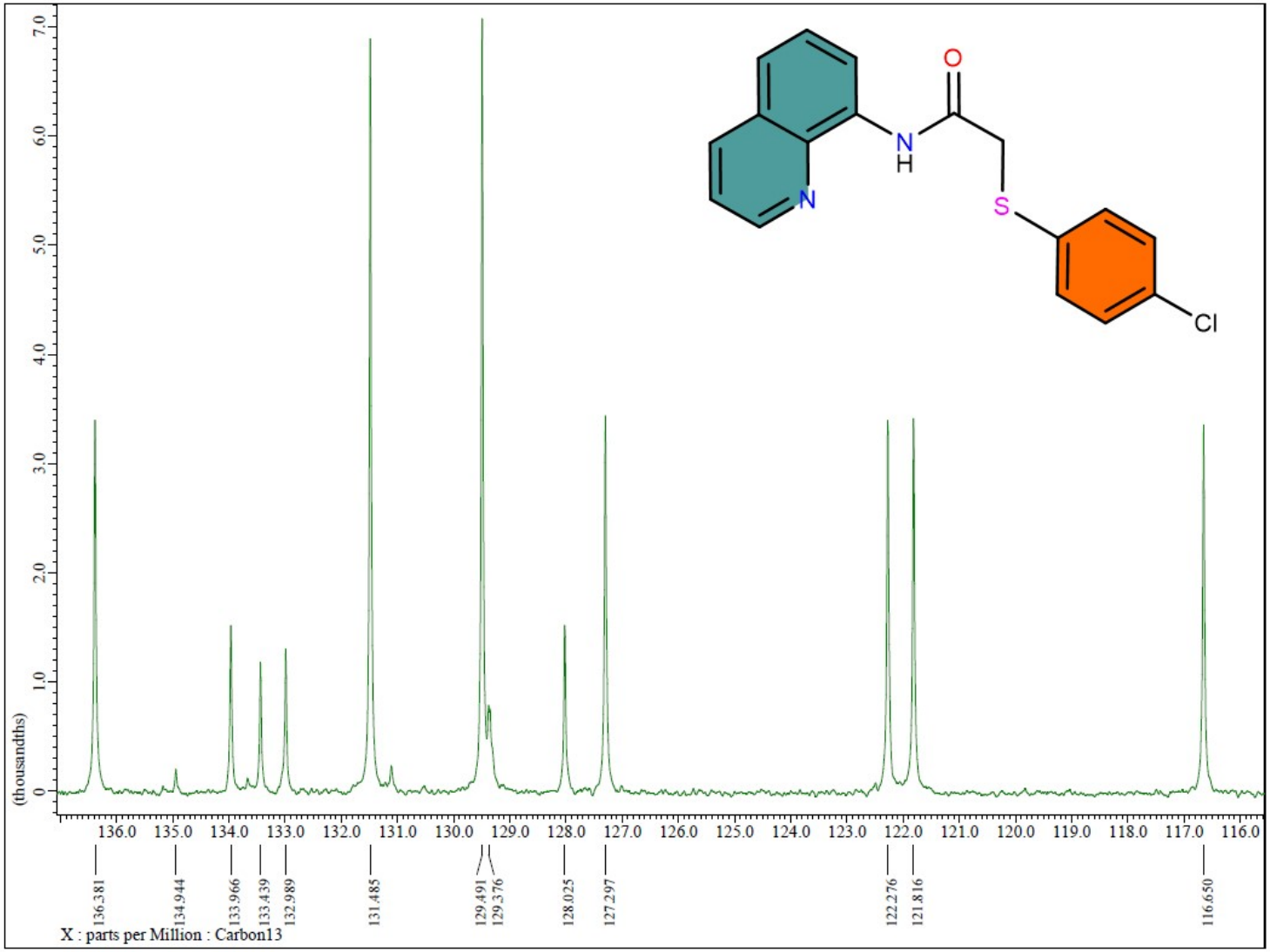

Fig. S27.$^{13}C\{^{1}H\}$ NMR ($CDCl_3$, 100.5 MHz) spectrum of **L2** in the aryl region.

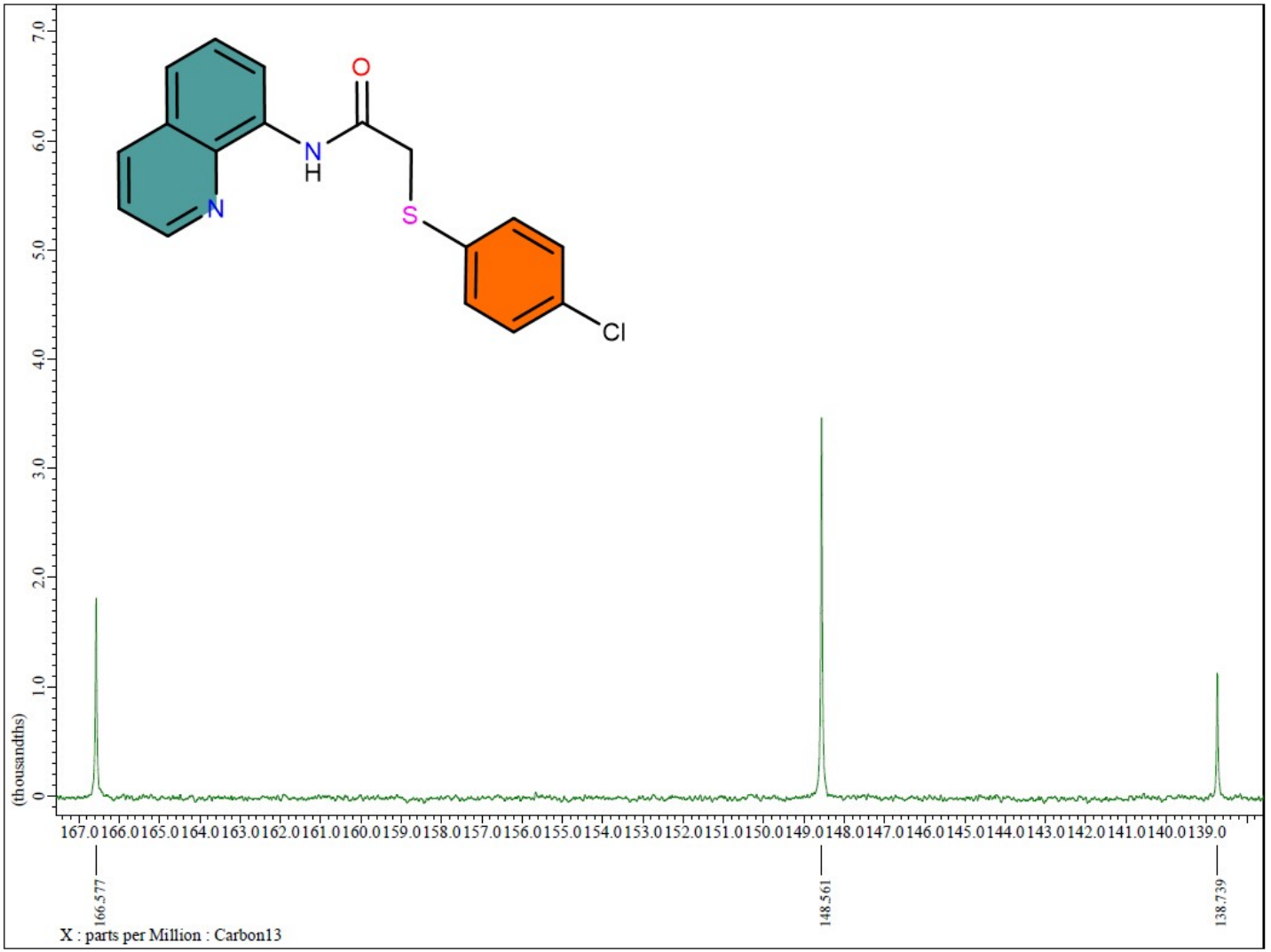

Fig. S28.$^{13}C\{^{1}H\}$ NMR ($CDCl_3$, 100.5 MHz) spectrum of **L2** in the aryl region.

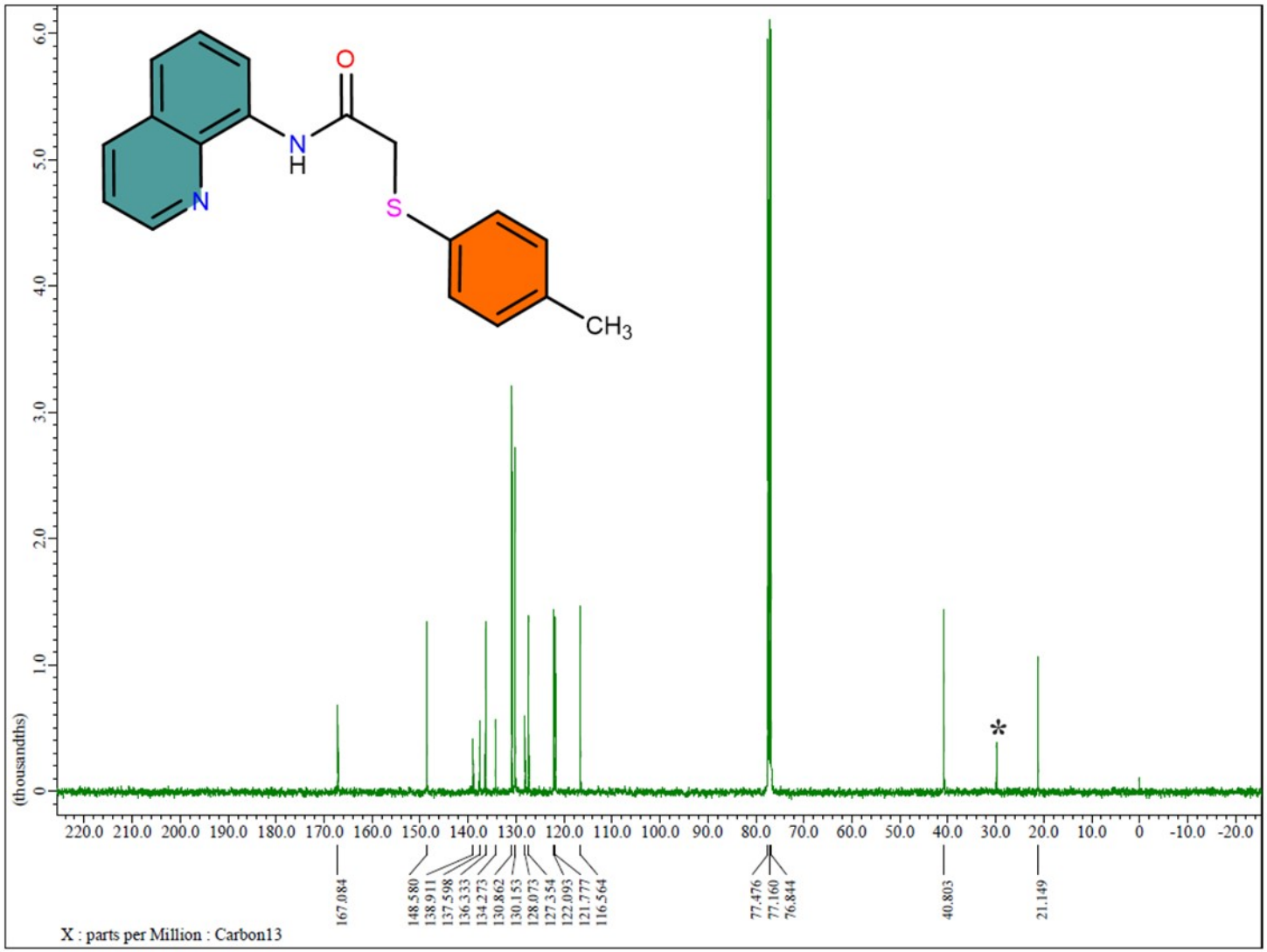

Fig. S29.$^{13}C\{^{1}H\}$ NMR ($CDCl_3$, 100.5 MHz) spectrum of **L3** and asterisk (*) represents the solvent.

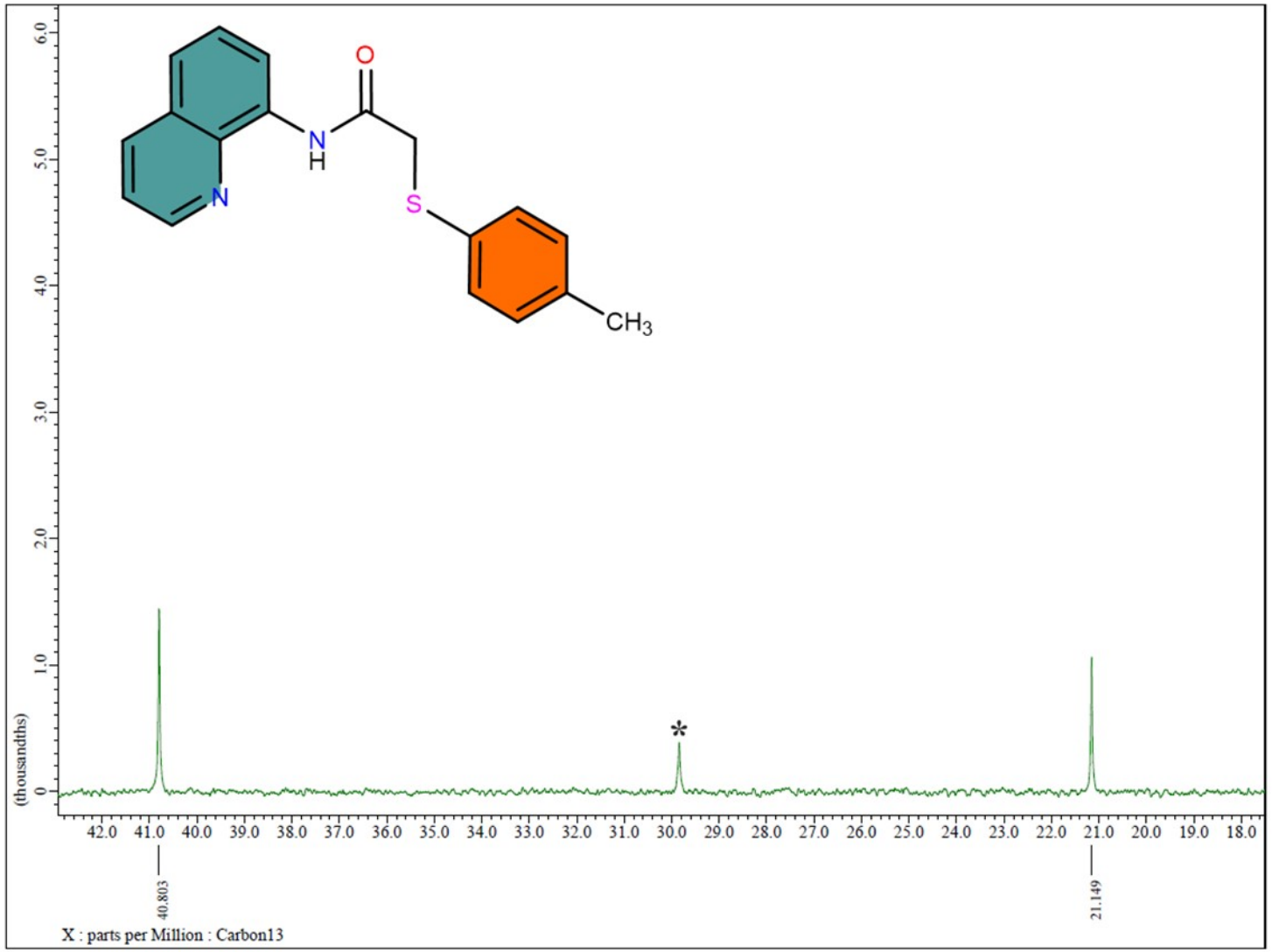

Fig. S30.$^{13}C\{^{1}H\}$ NMR ($CDCl_3$, 100.5 MHz) spectrum of **L3** in the alkyl region and asterisk (*) represents the solvent.

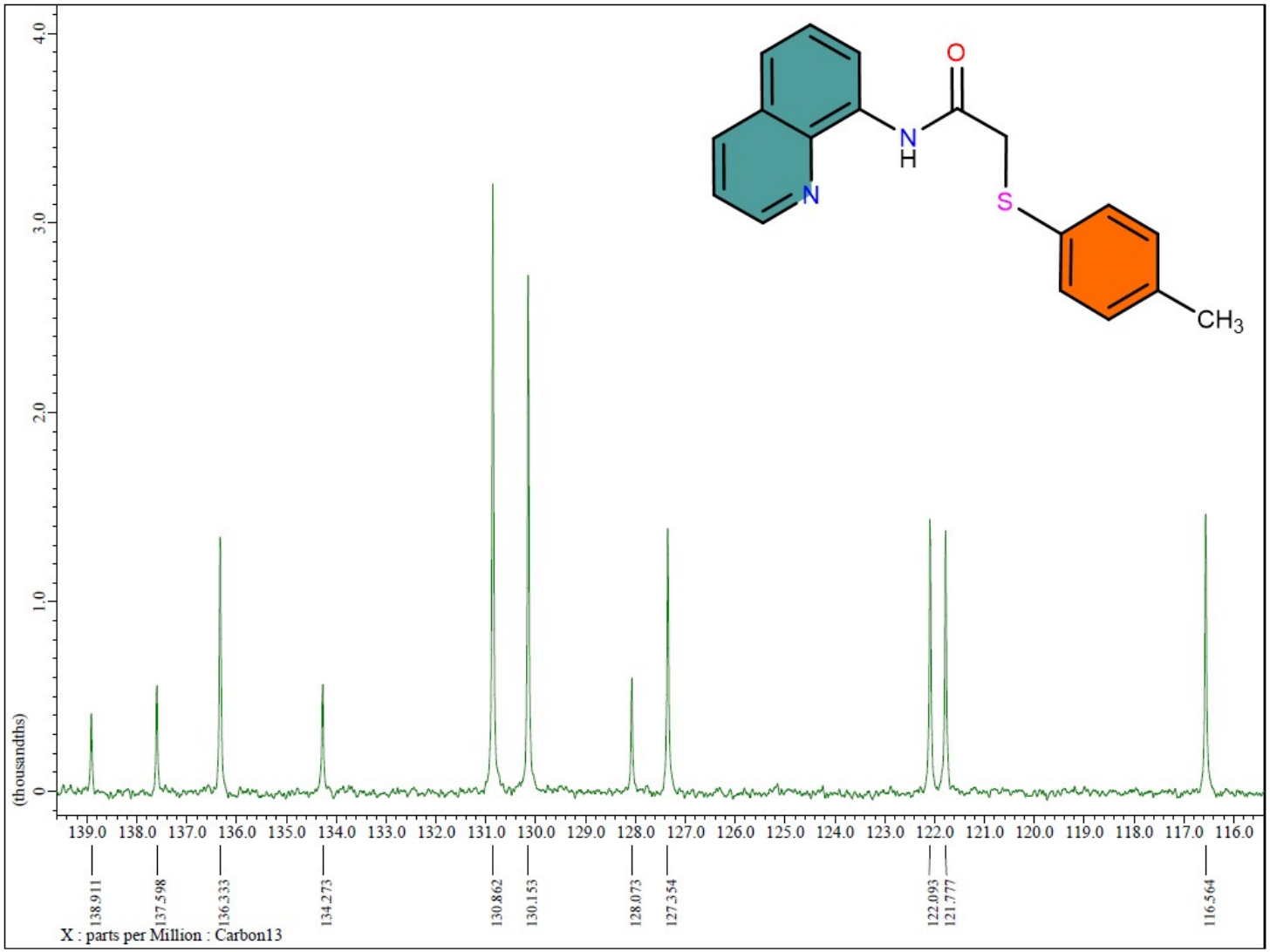

Fig. S31.$^{13}C\{^{1}H\}$ NMR ($CDCl_3$, 100.5 MHz) spectrum of **L3** in the aryl region.

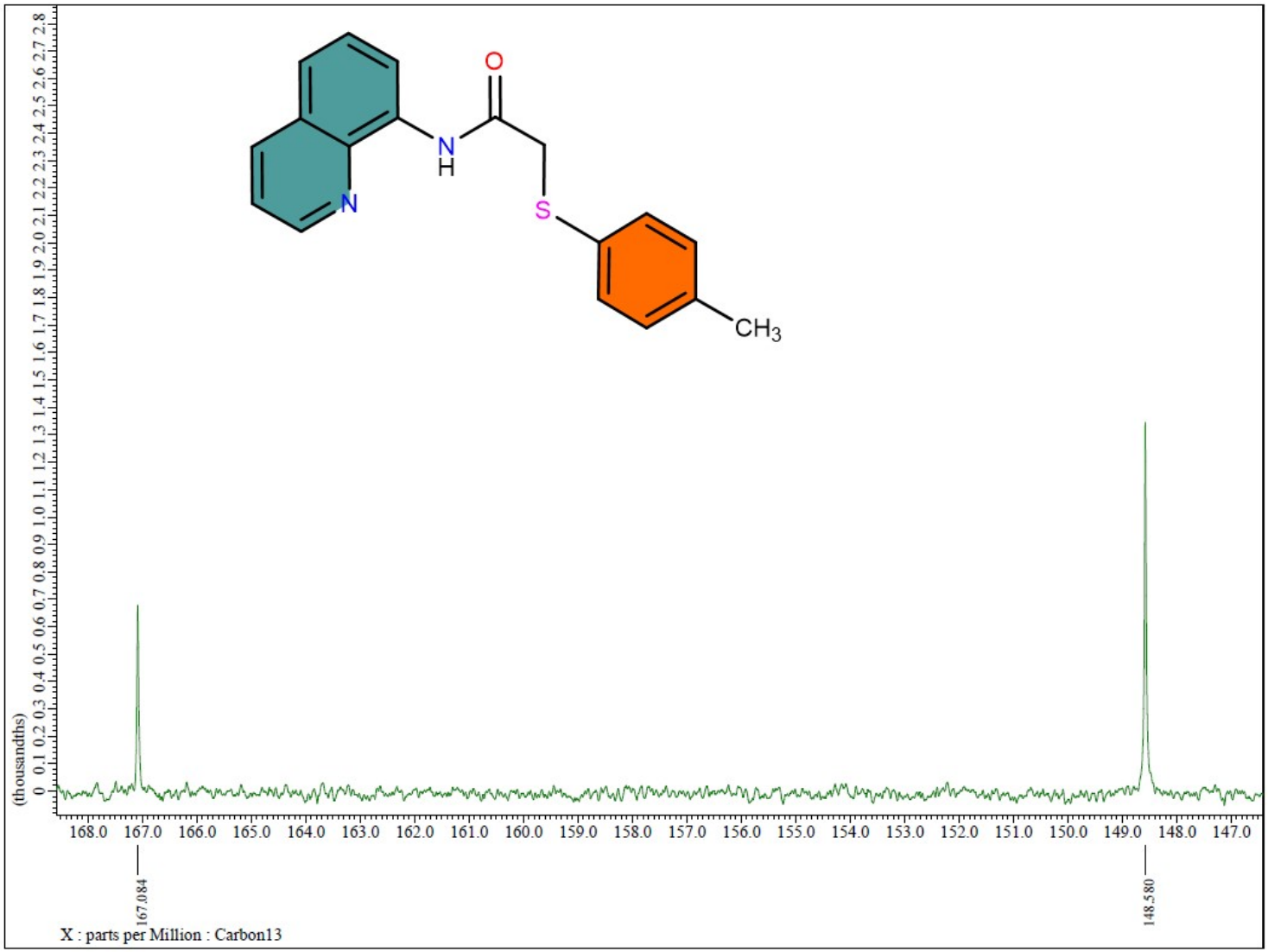

Fig. S32.$^{13}C\{^{1}H\}$ NMR ($CDCl_3$, 100.5 MHz) spectrum of **L3** in the aryl region.

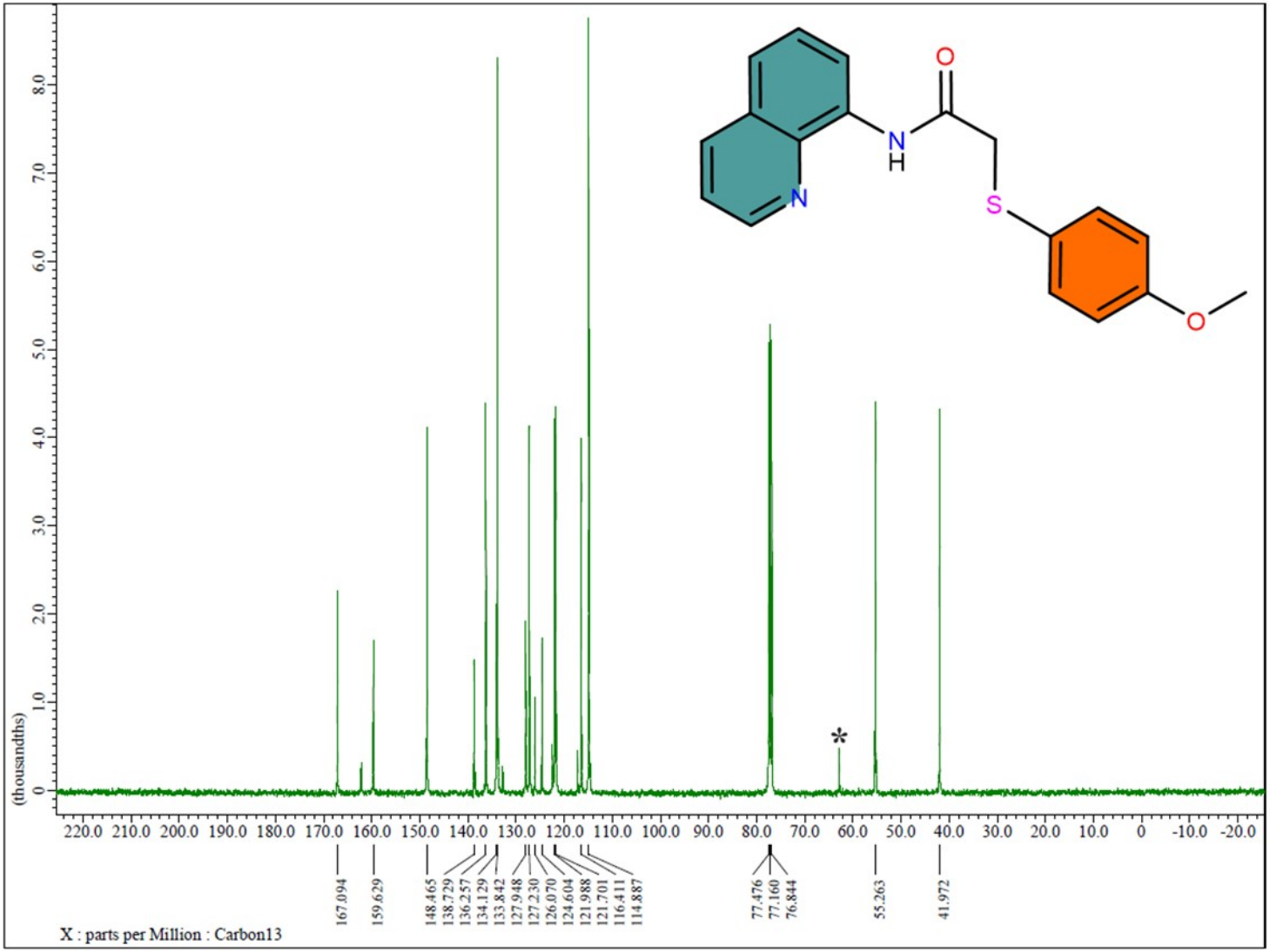

Fig. S33.$^{13}C\{^{1}H\}$ NMR ($CDCl_3$, 100.5 MHz) spectrum of **L4** and asterisk (*) represents the solvent.

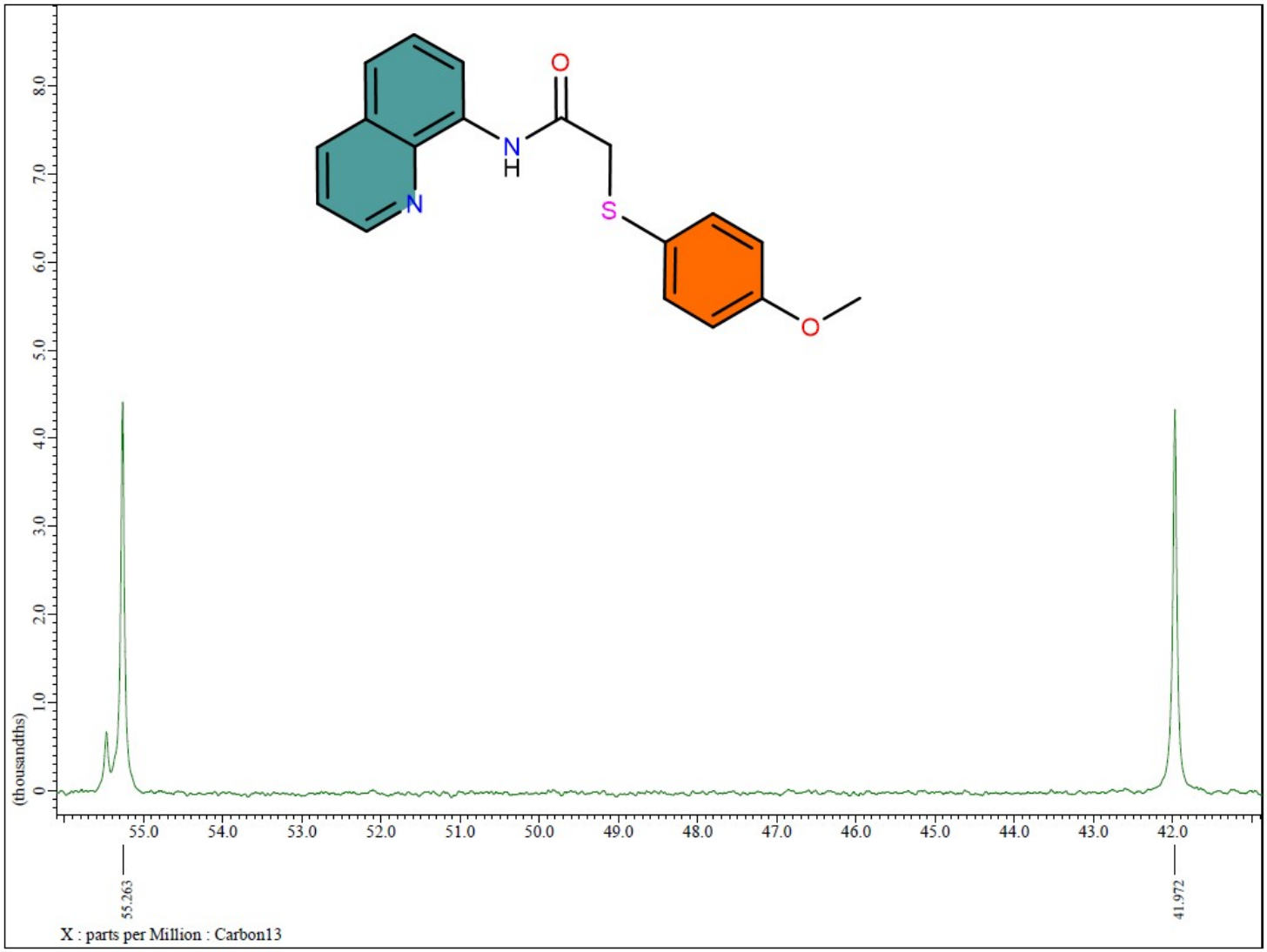

Fig. S34. $^{13}C\{^{1}H\}$ NMR ($CDCl_3$, 100.5 MHz) spectrum of **L4** in the alkyl region.

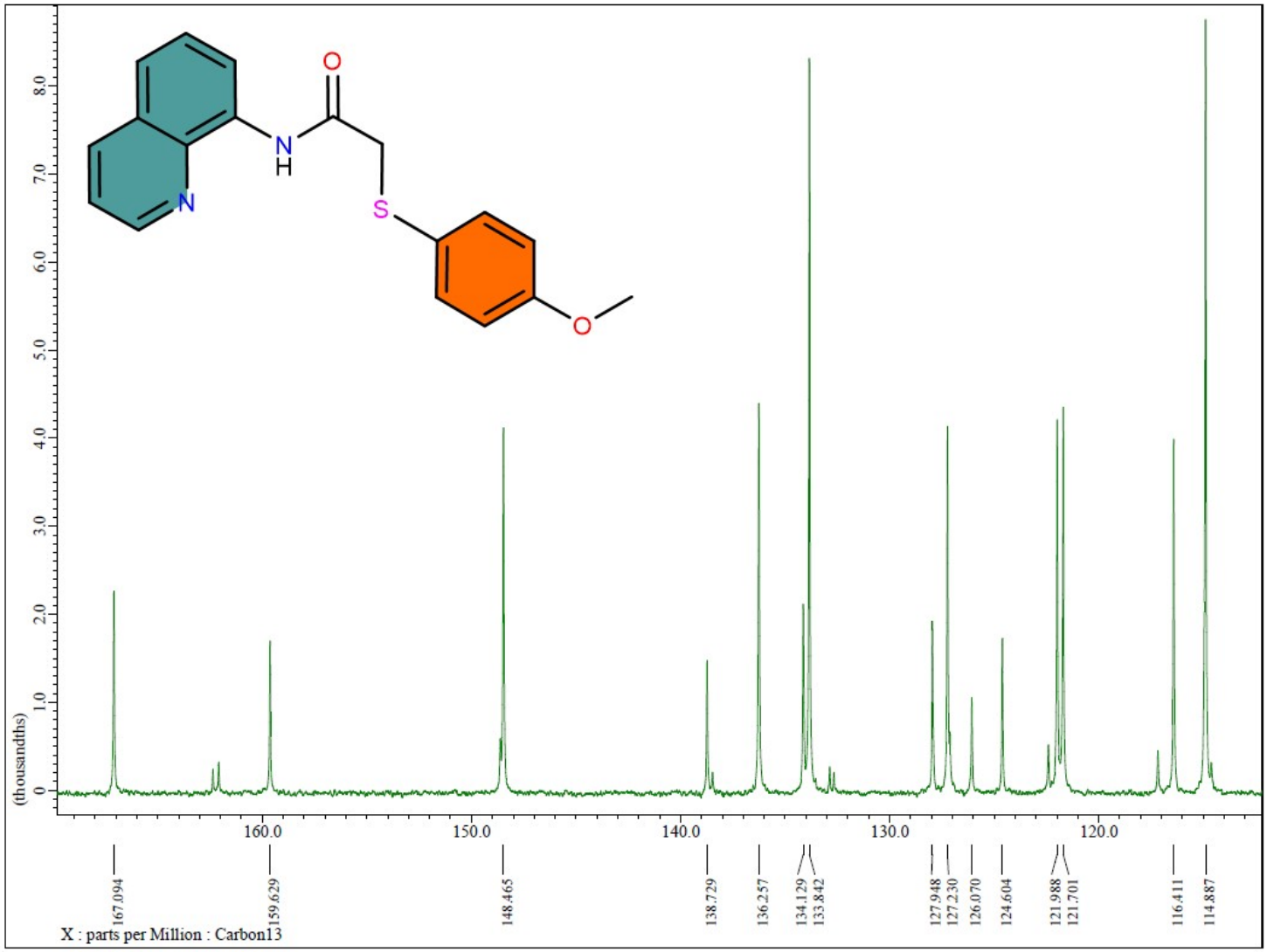

Fig. S35. $^{13}C\{^{1}H\}$ NMR ($CDCl_3$, 100.5 MHz) spectrum of **L4** in the aryl region.

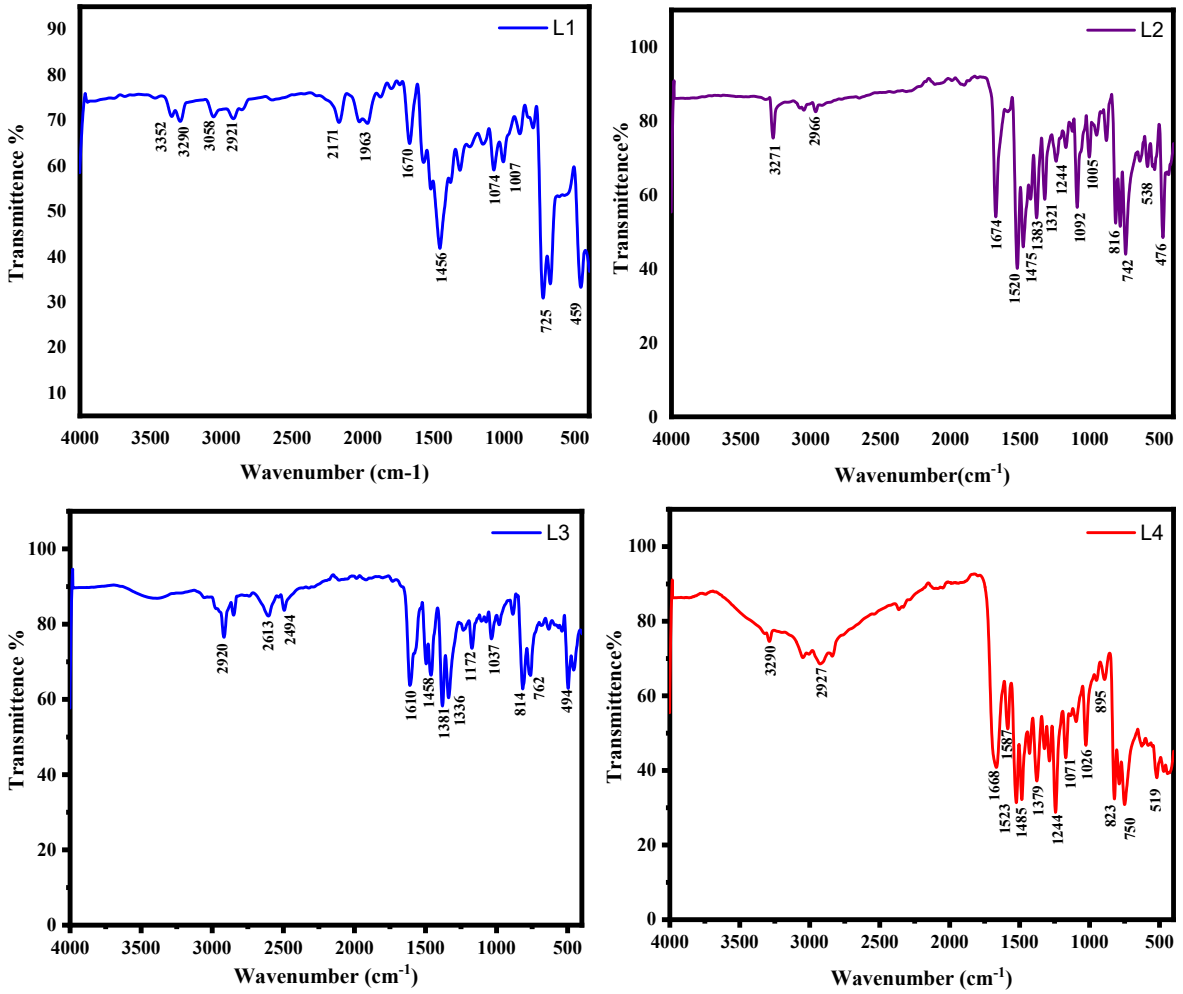

Fig. S36. FTIR spectra of **L1-L4.**

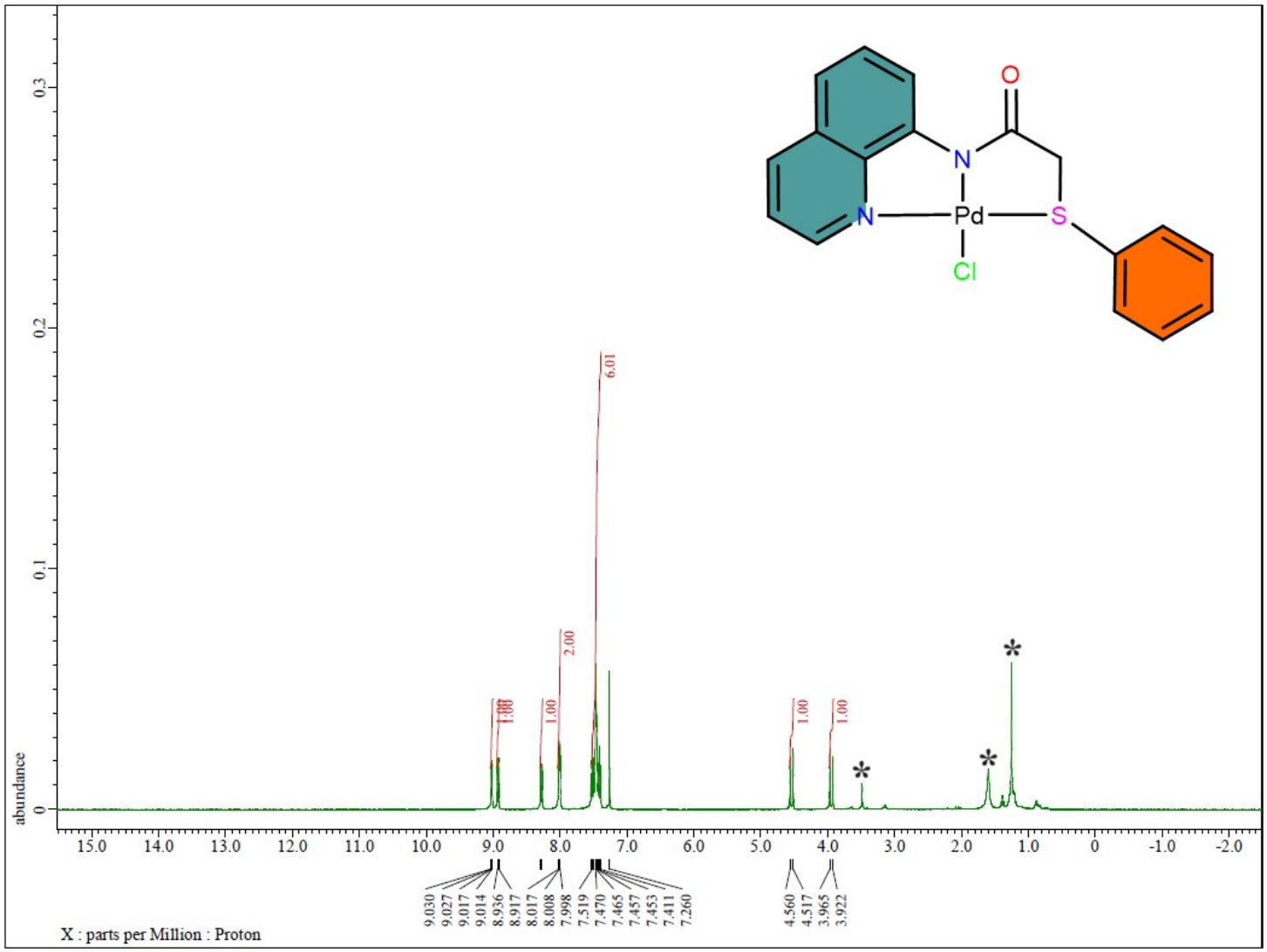

Fig. S37. ^{1}H NMR ($CDCl_3$, 400 MHz) spectrum of **C1** and asterisk (*) represents the solvents.

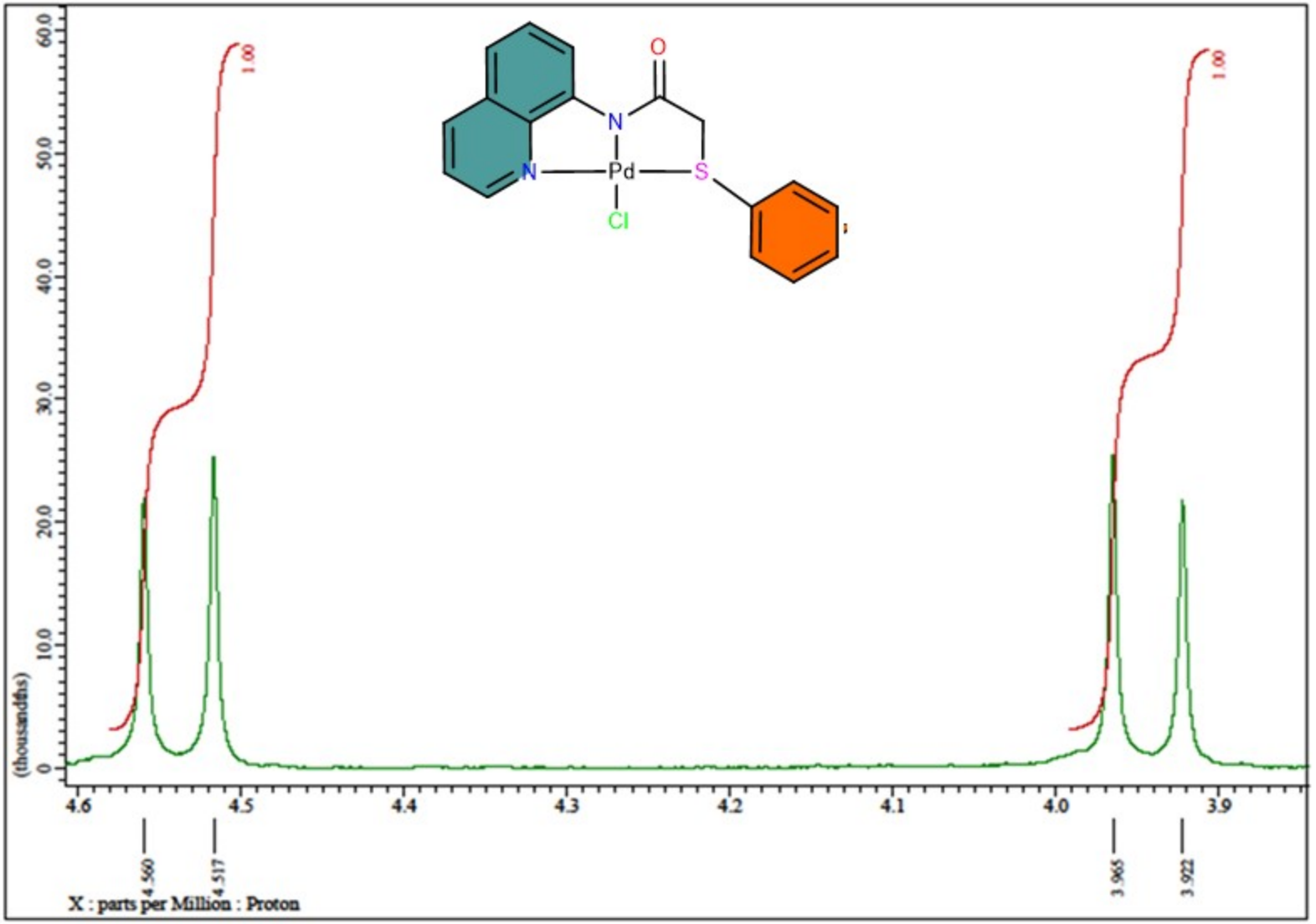

Fig. S38. ^{1}H NMR ($CDCl_3$, 400 MHz) spectrum of **C1** in alkyl region.

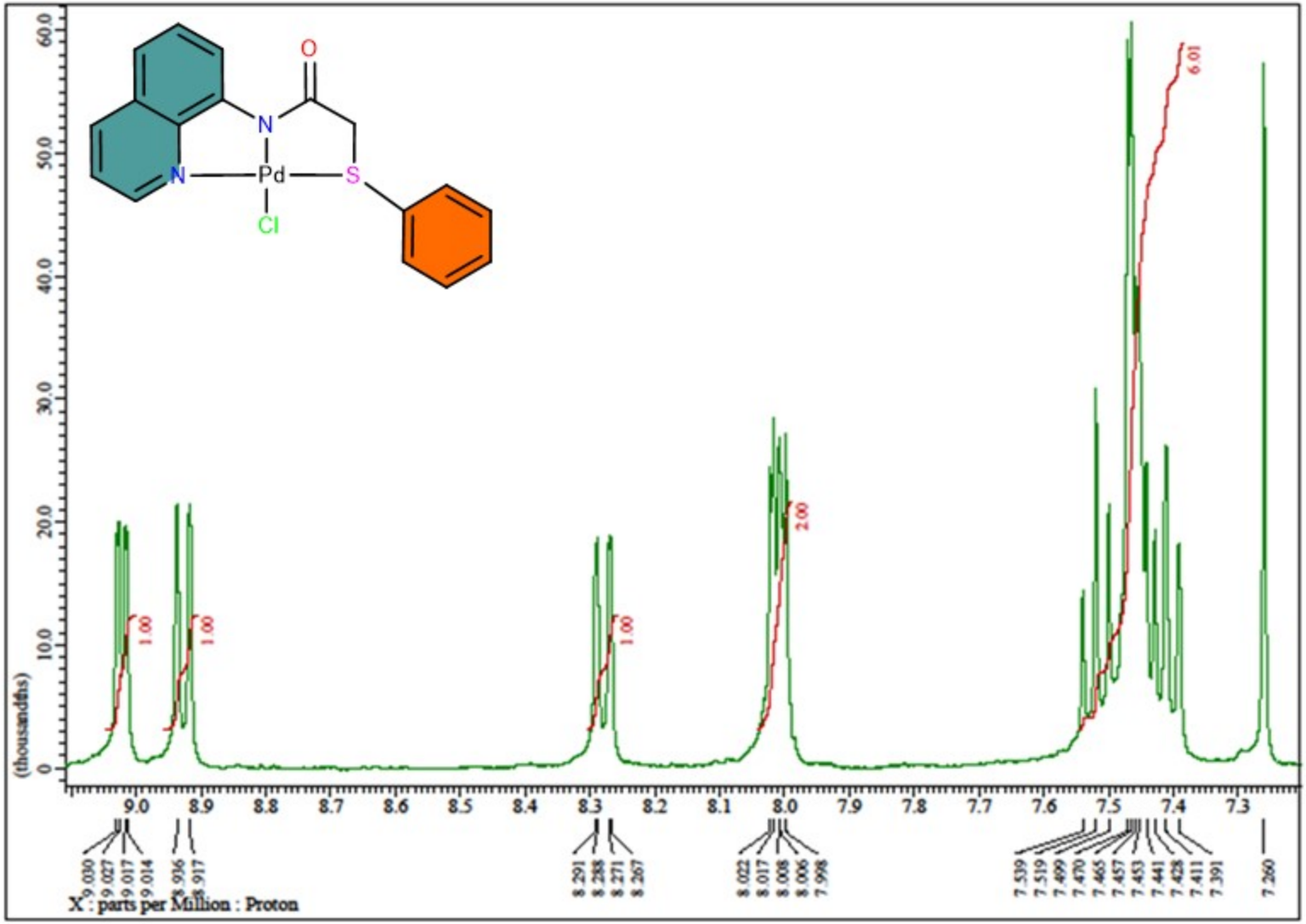

Fig. S39. ^{1}H NMR ($CDCl_3$, 400 MHz) spectrum of **C1** in aryl region.

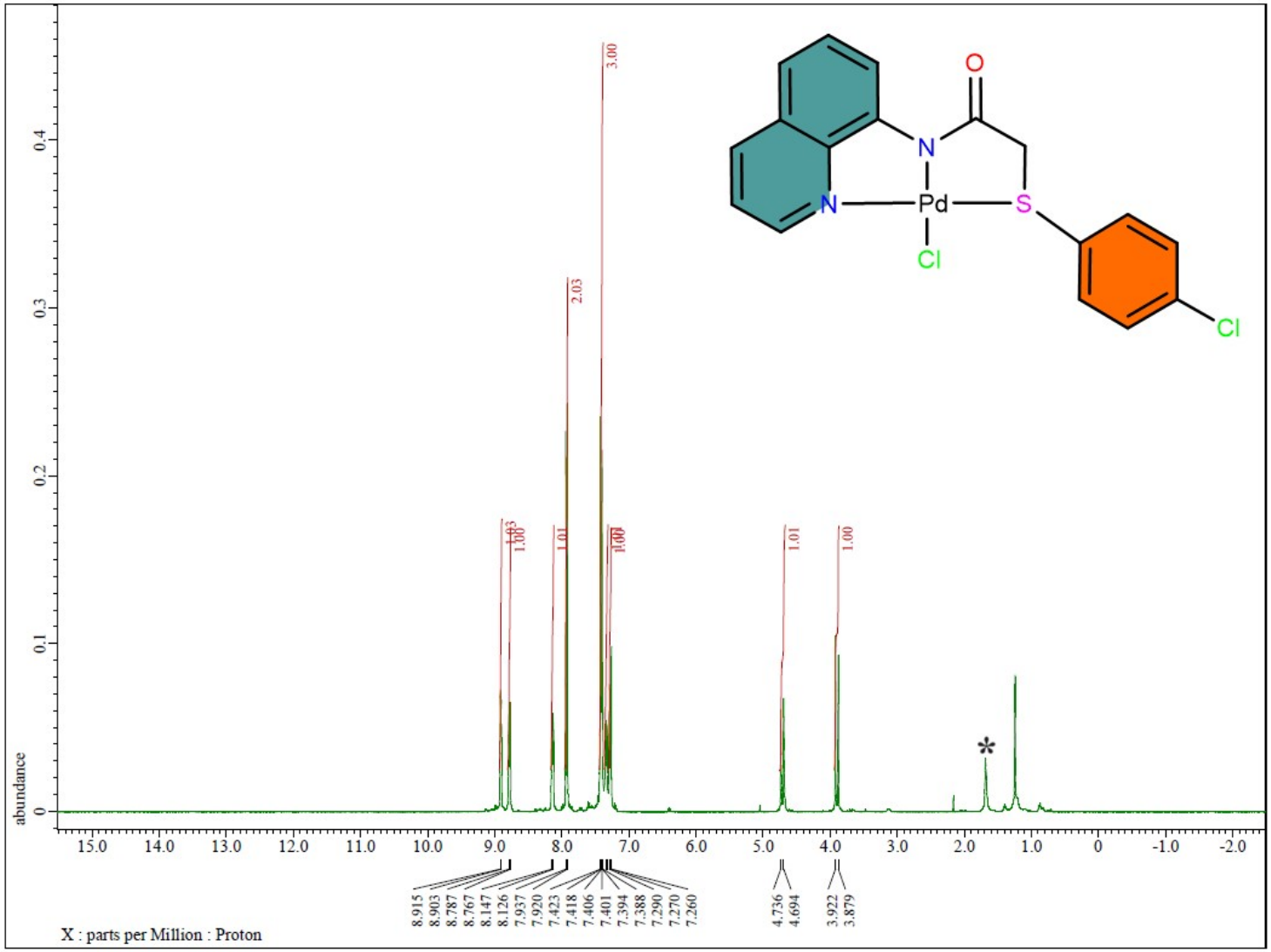

Fig. S40. ^{1}H NMR ($CDCl_3$, 400 MHz) spectrum of **C2** and asterisk (*) represents the solvent.

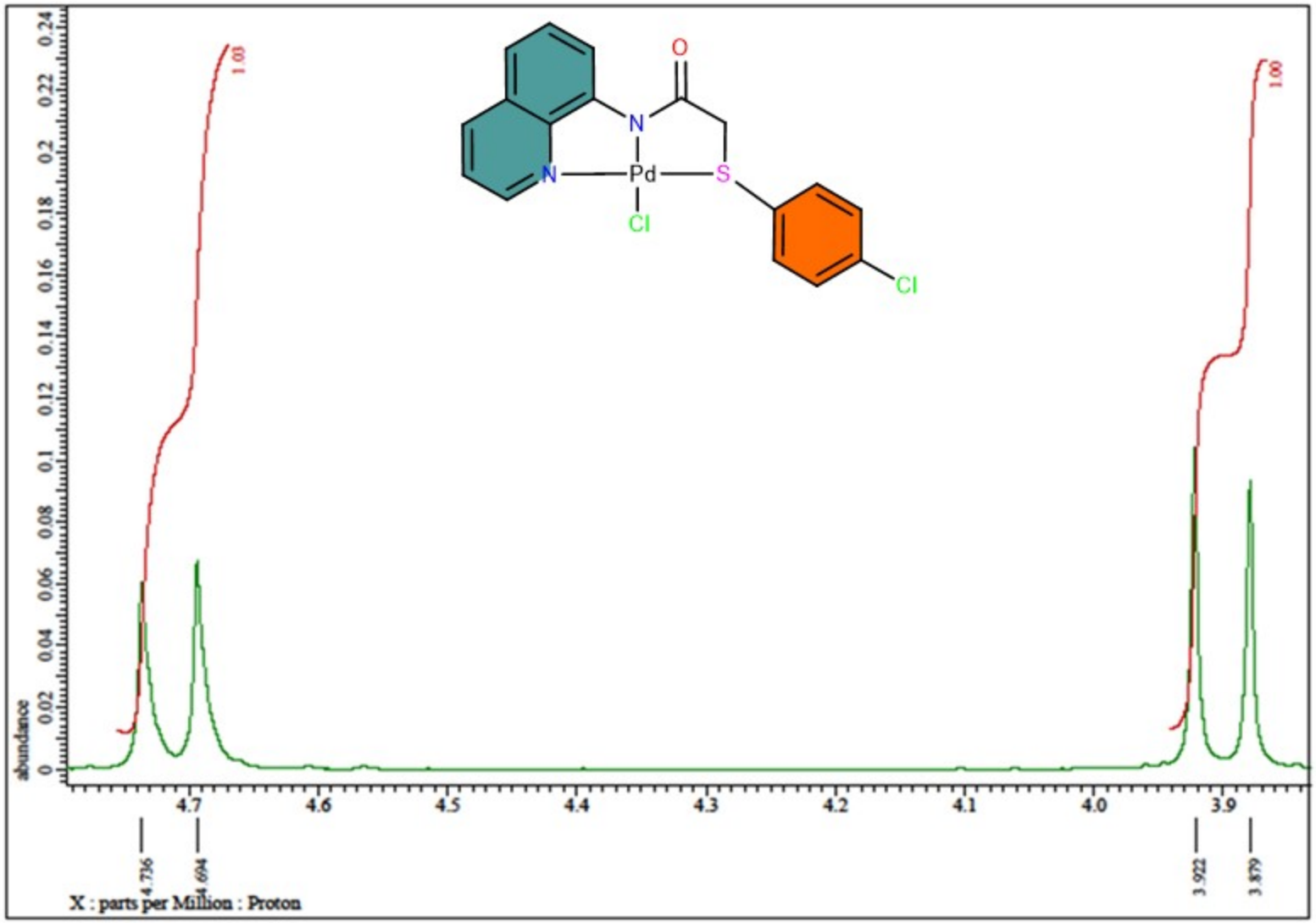

Fig. S41. ^{1}H NMR ($CDCl_3$, 400 MHz) spectrum of **C2** in alkyl region.

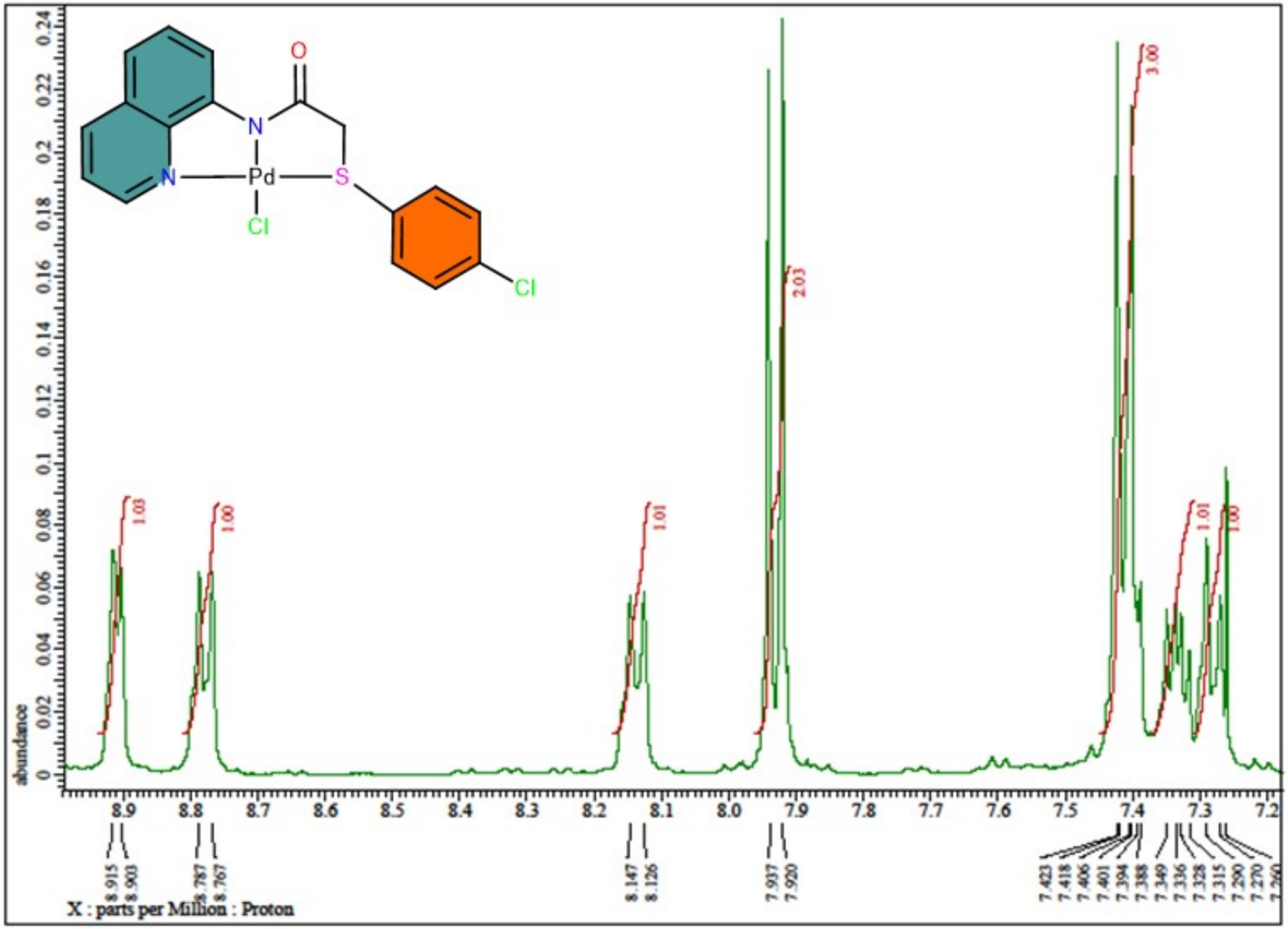

Fig. S42. ^{1}H NMR ($CDCl_3$, 400 MHz) spectrum of **C2** in aryl region.

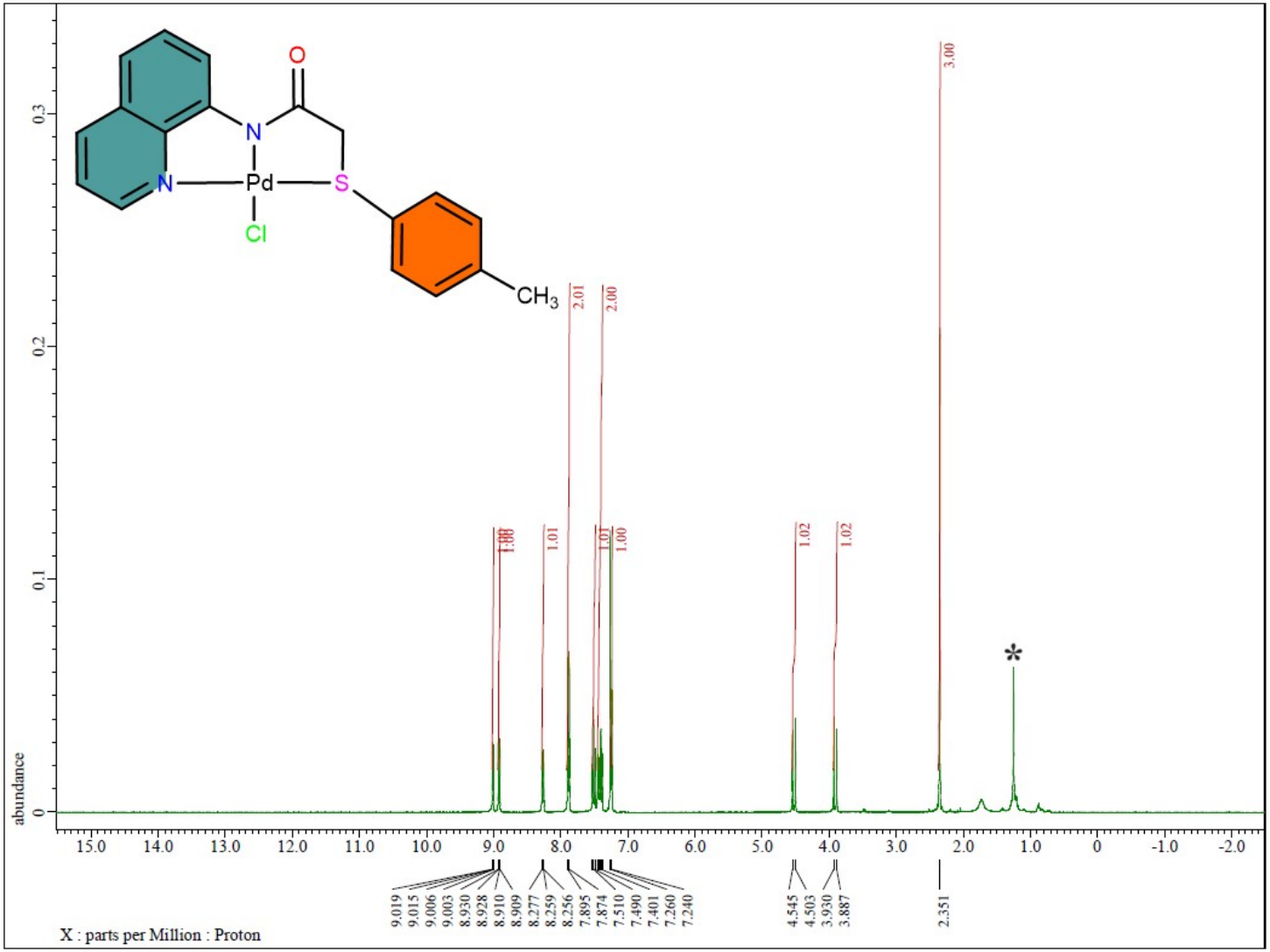

Fig. S43. ^{1}H NMR ($CDCl_3$, 400 MHz) spectrum of **C3** and asterisk (*) represents the solvent.

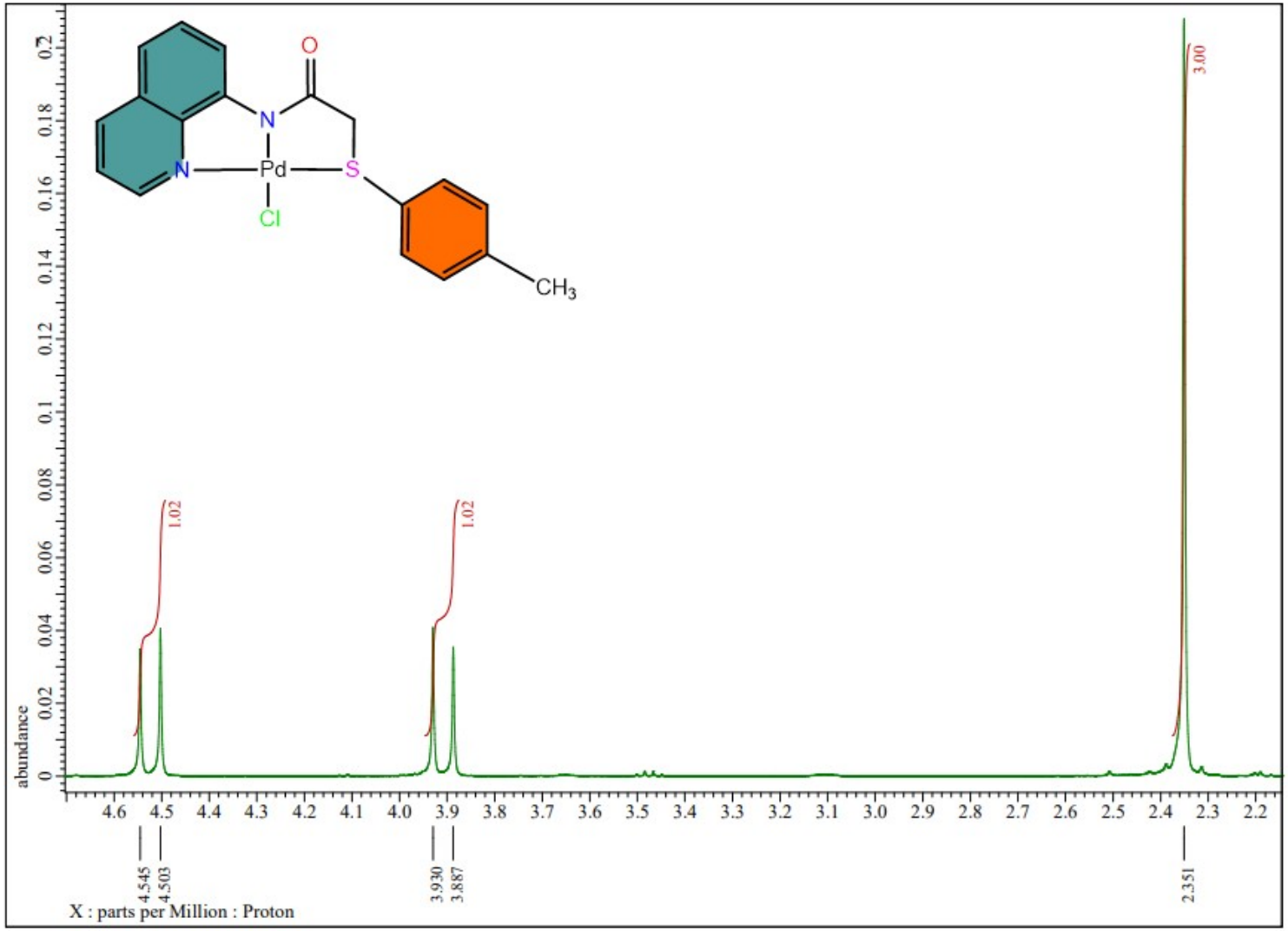

Fig. S44. ^{1}H NMR ($CDCl_3$, 400 MHz) spectrum of **C3** in alkyl region.

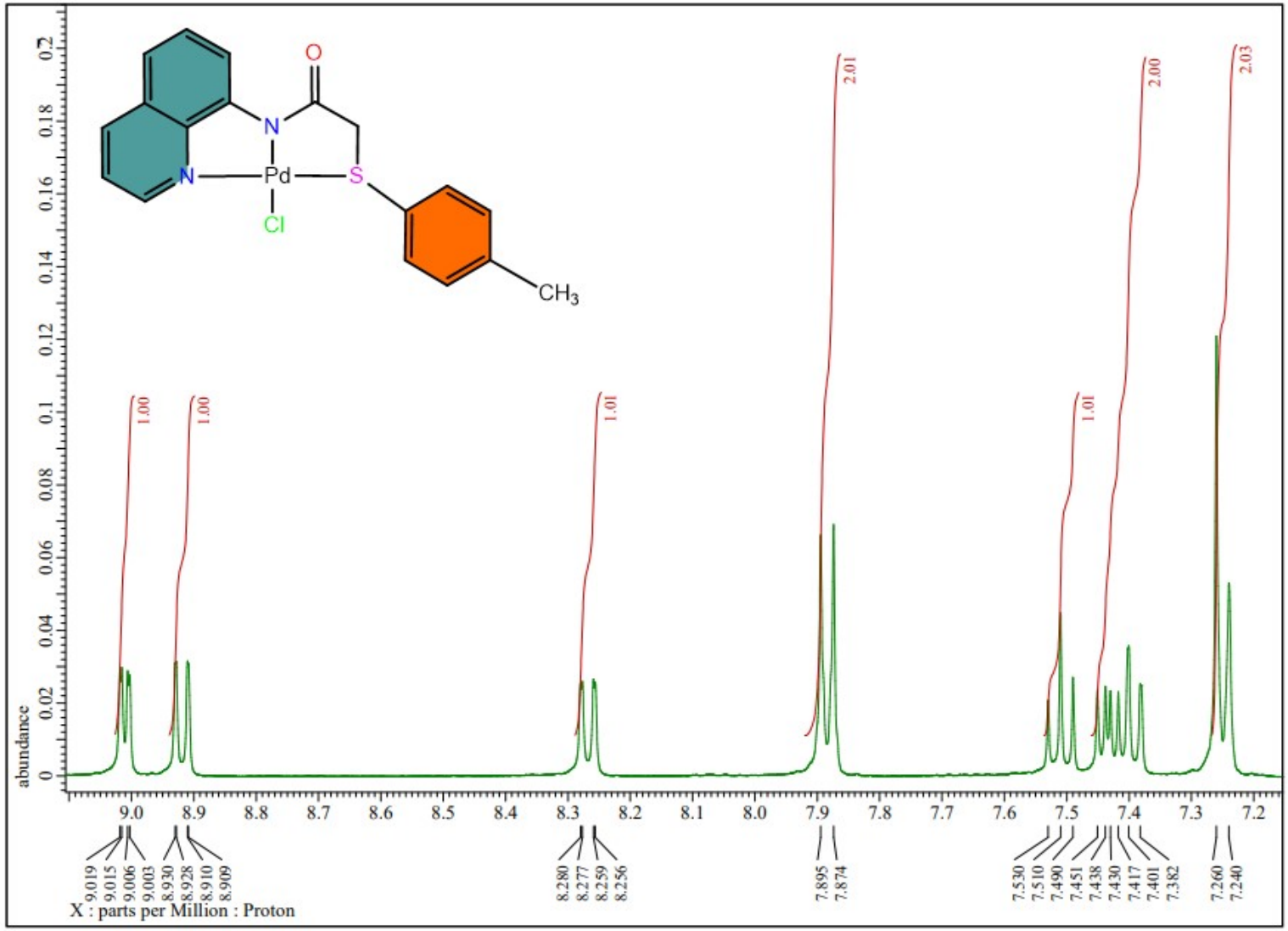

Fig. S45. ^{1}H NMR ($CDCl_3$, 400 MHz) spectrum of **C3** in aryl region.

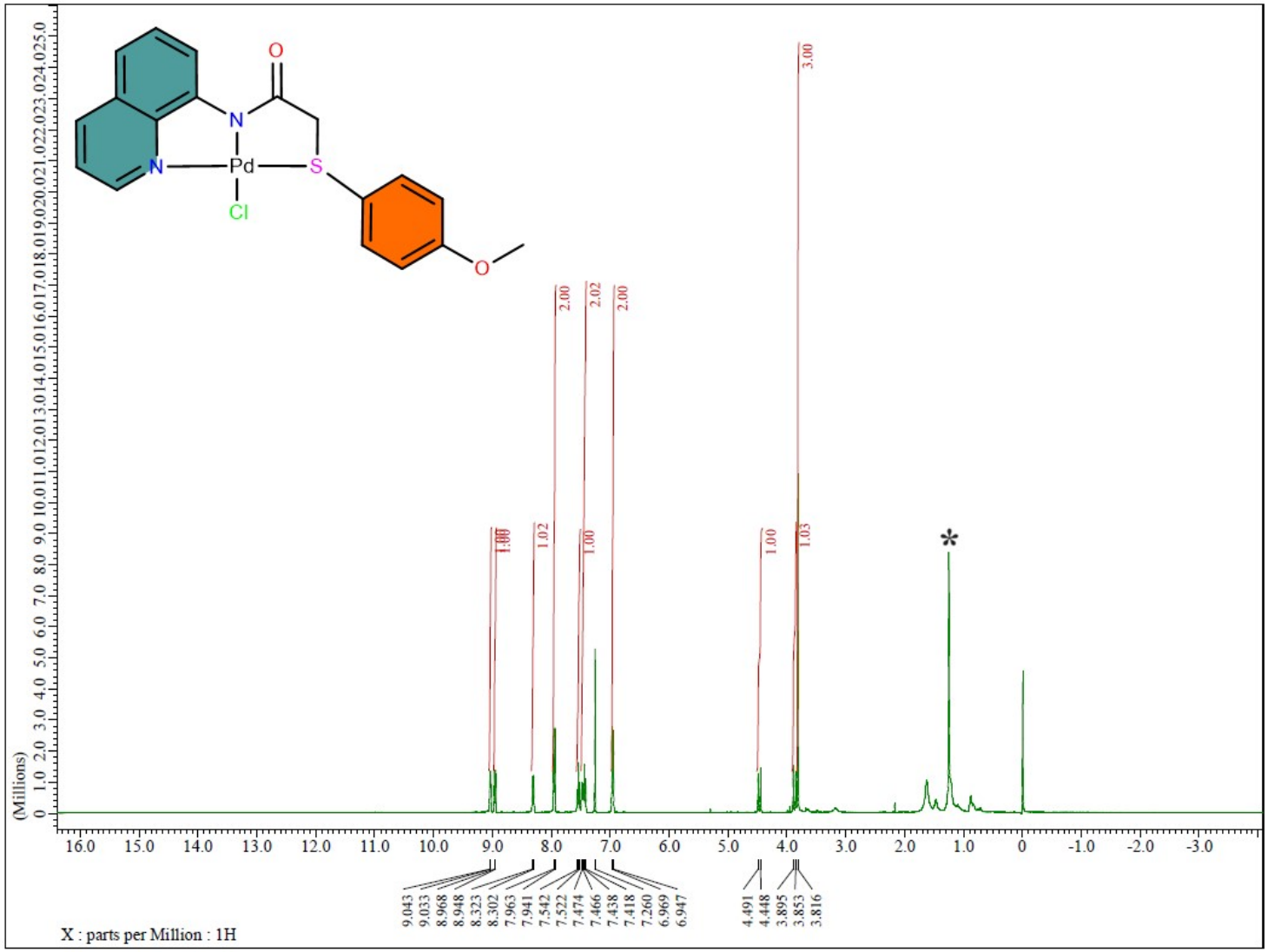

Fig. S46. ^{1}H NMR ($CDCl_3$, 400 MHz) spectrum of **C4** and asterisk (*) represents the solvent.

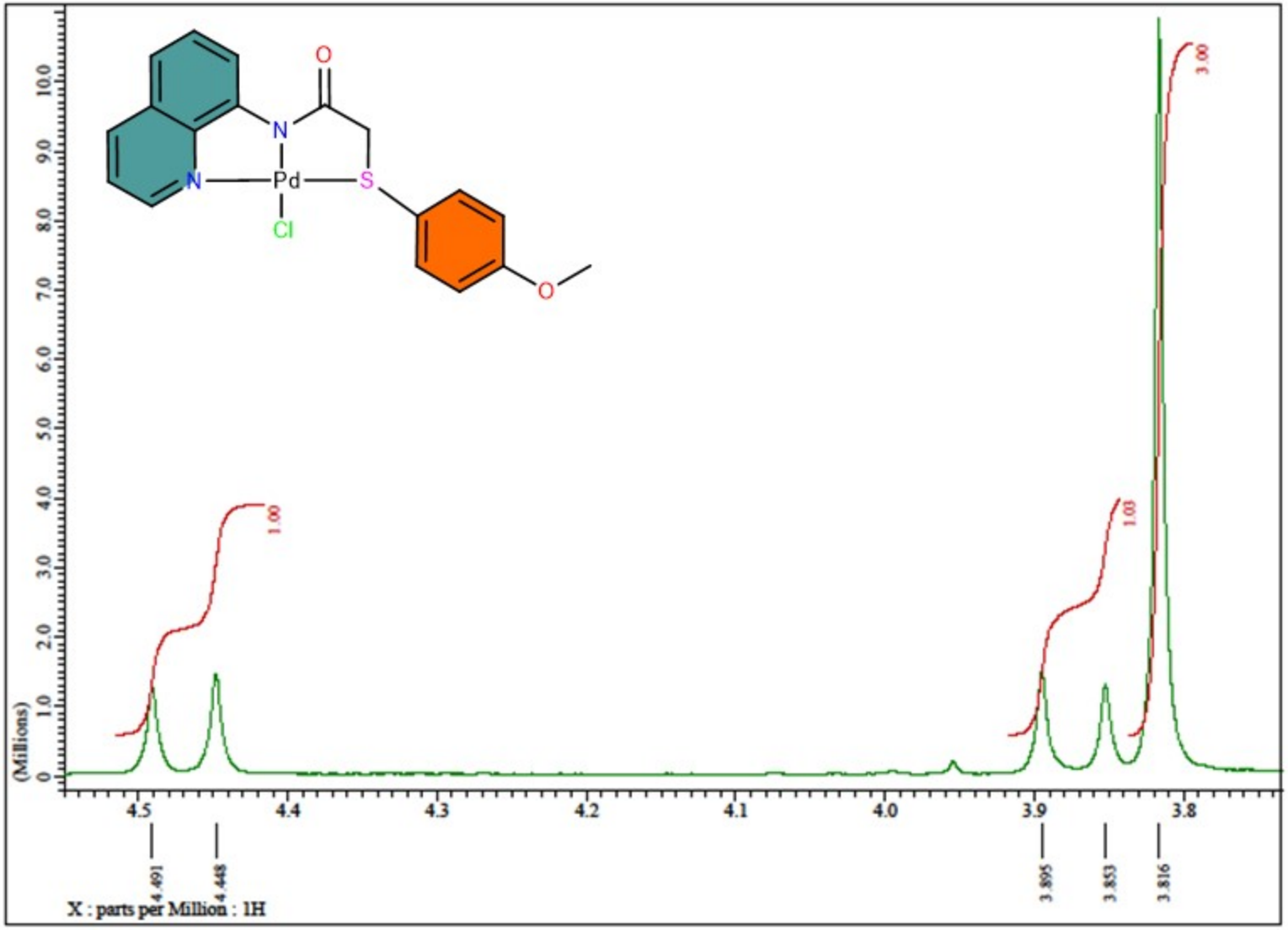

Fig. S47. ^{1}H NMR ($CDCl_3$, 400 MHz) spectrum of **C4** in alkyl region.

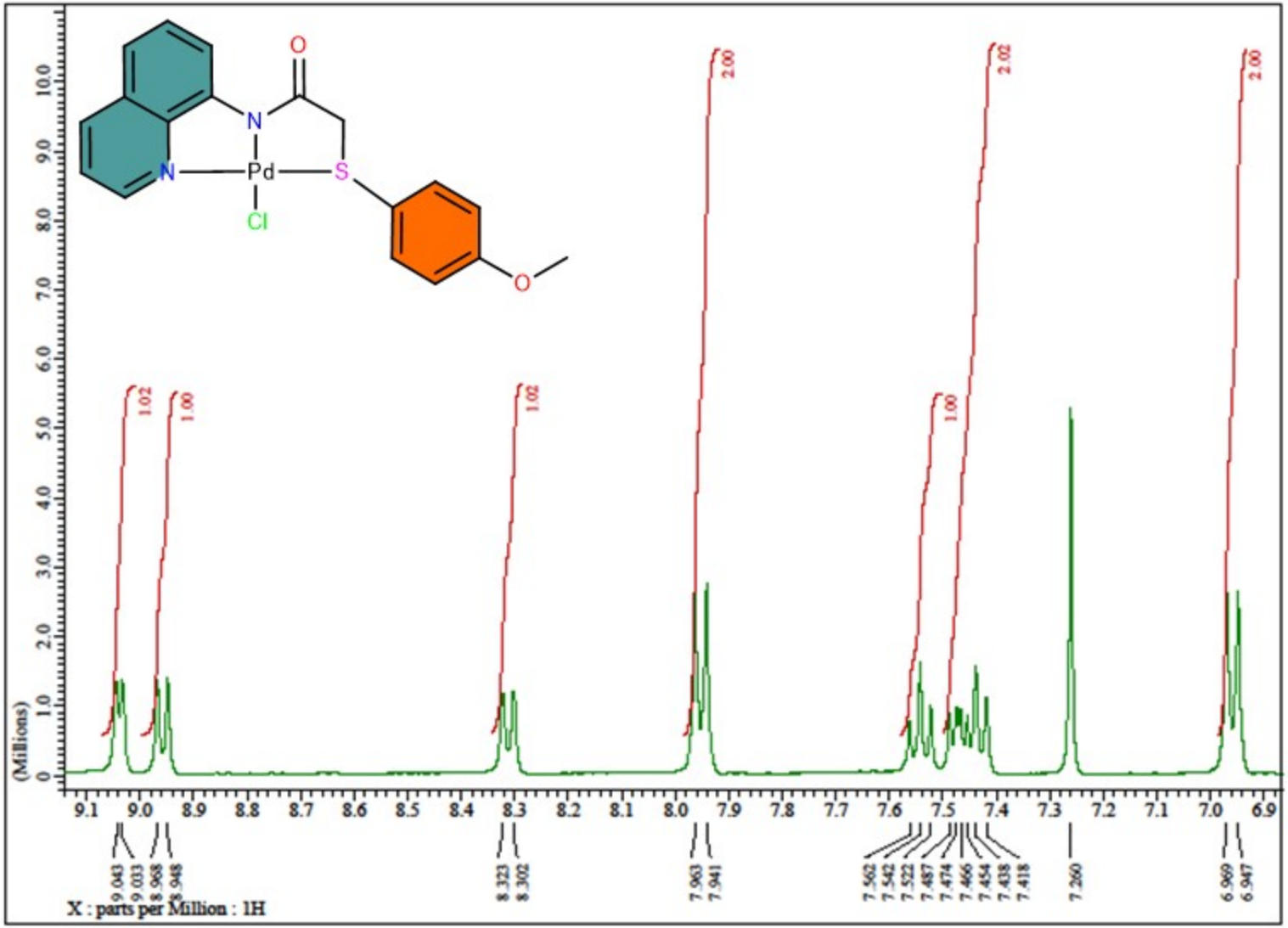

Fig. S48. ^{1}H NMR ($CDCl_3$, 400 MHz) spectrum of **C4** in aryl region.

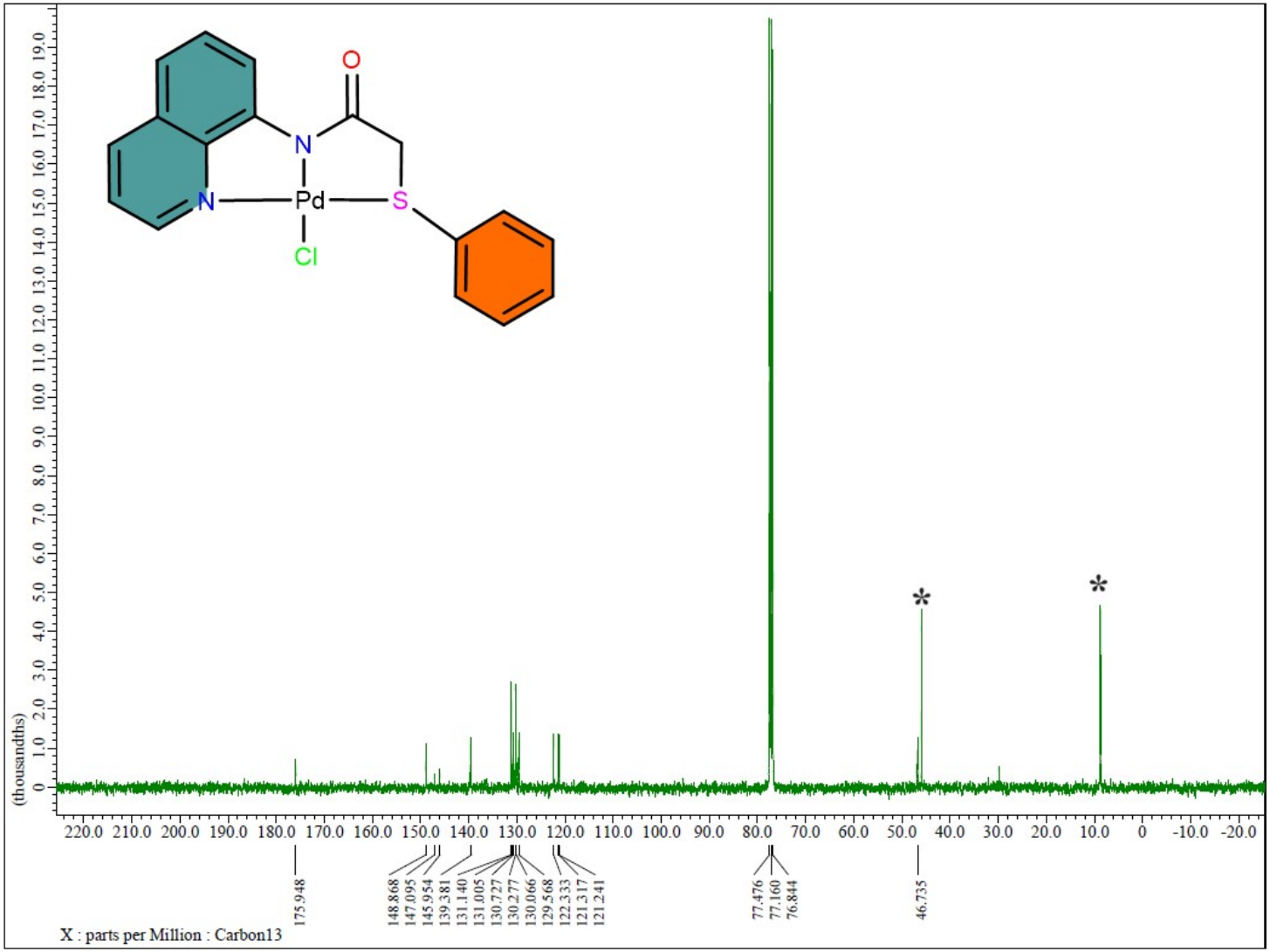

Fig. S49.$^{13}C\{^{1}H\}$ NMR ($CDCl_3$, 100.5 MHz) spectrum of **C1** and asterisk (*) represents the triethyl amine.

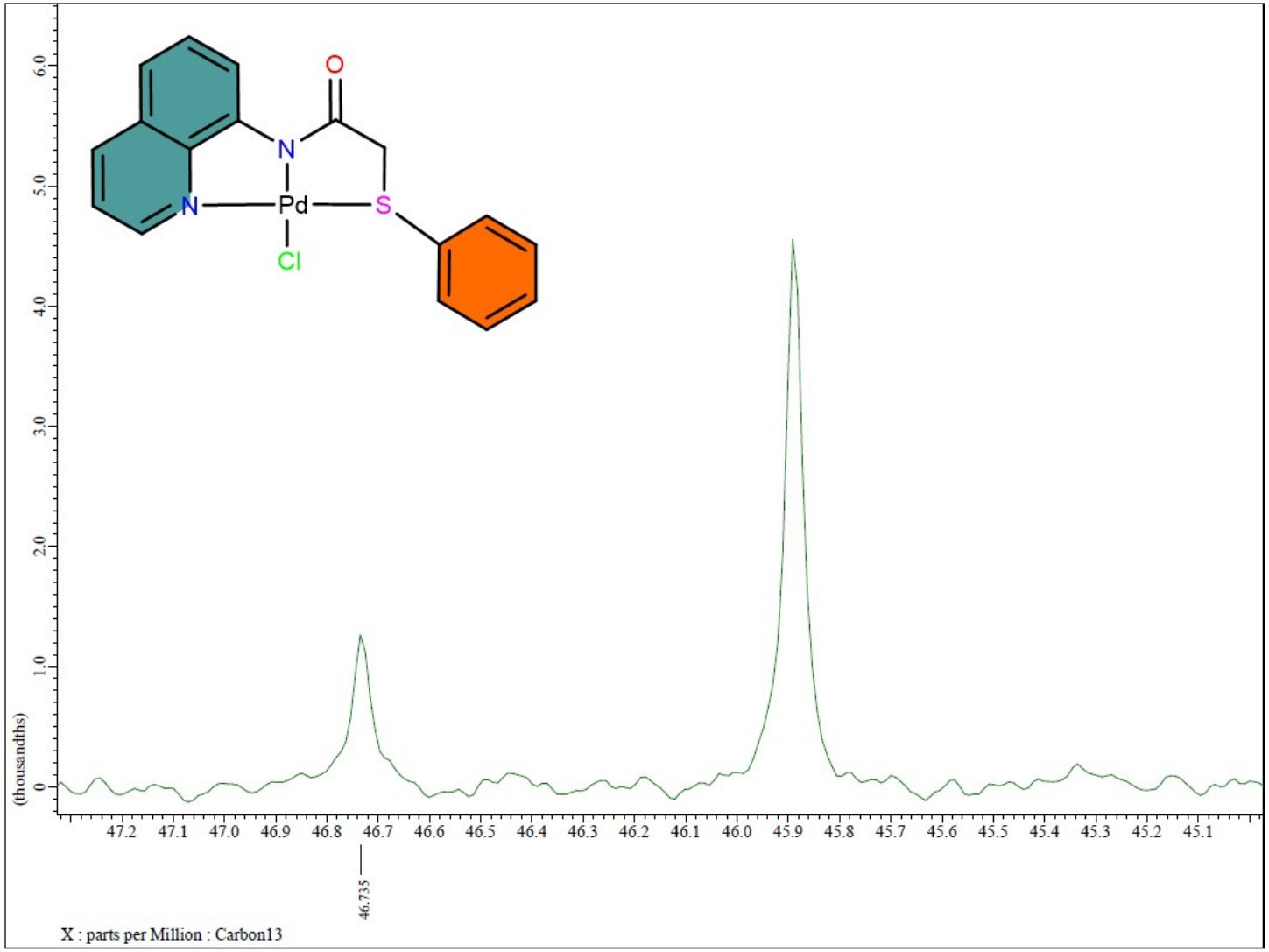

Fig. S50. $^{13}C\{^{1}H\}$ NMR ($CDCl_3$, 100.5 MHz) spectrum of **C1** in alkyl region.

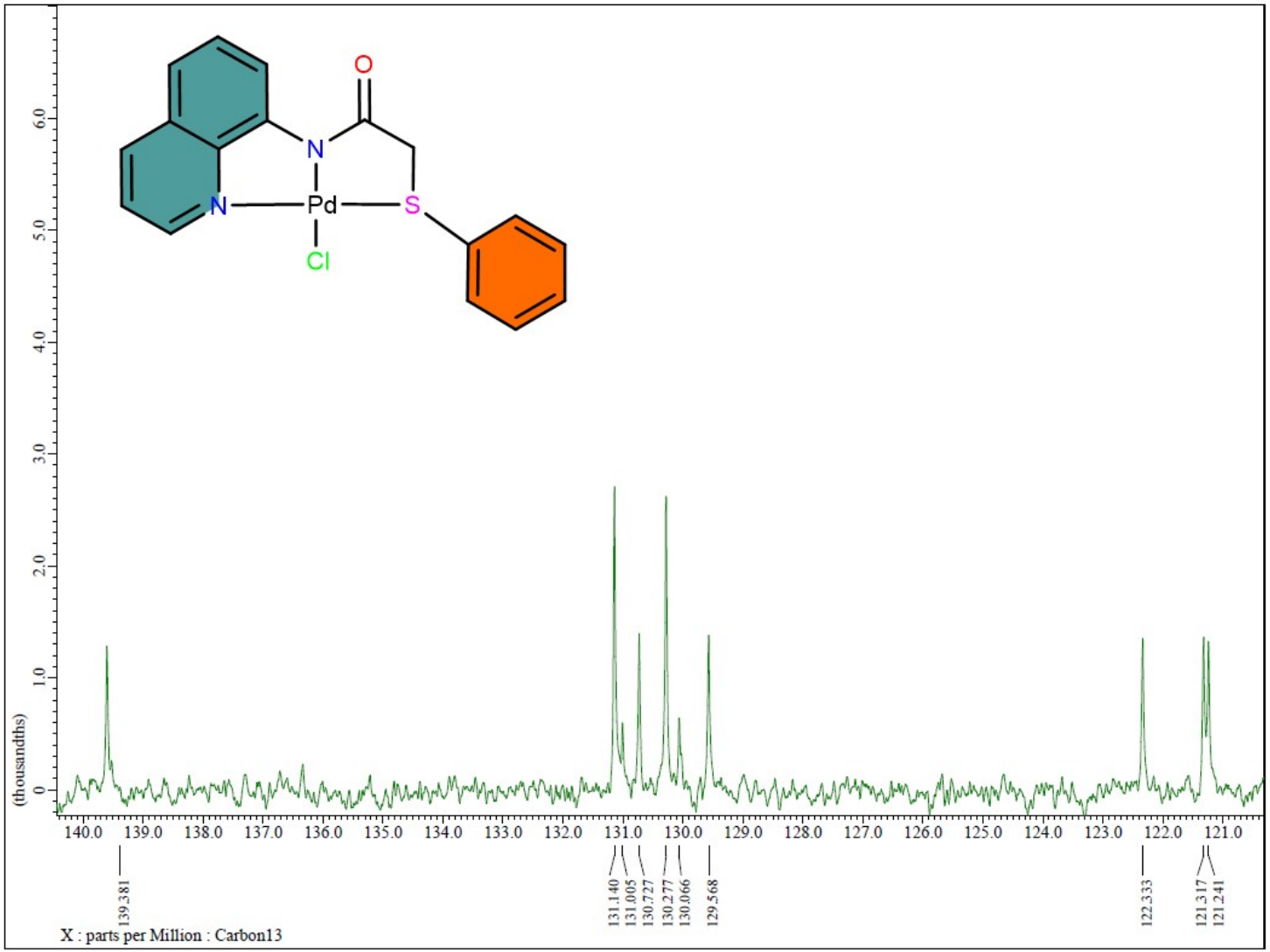

Fig. S51. $^{13}C\{^{1}H\}$ NMR ($CDCl_3$, 100.5 MHz) spectrum of **C1** in aryl region.

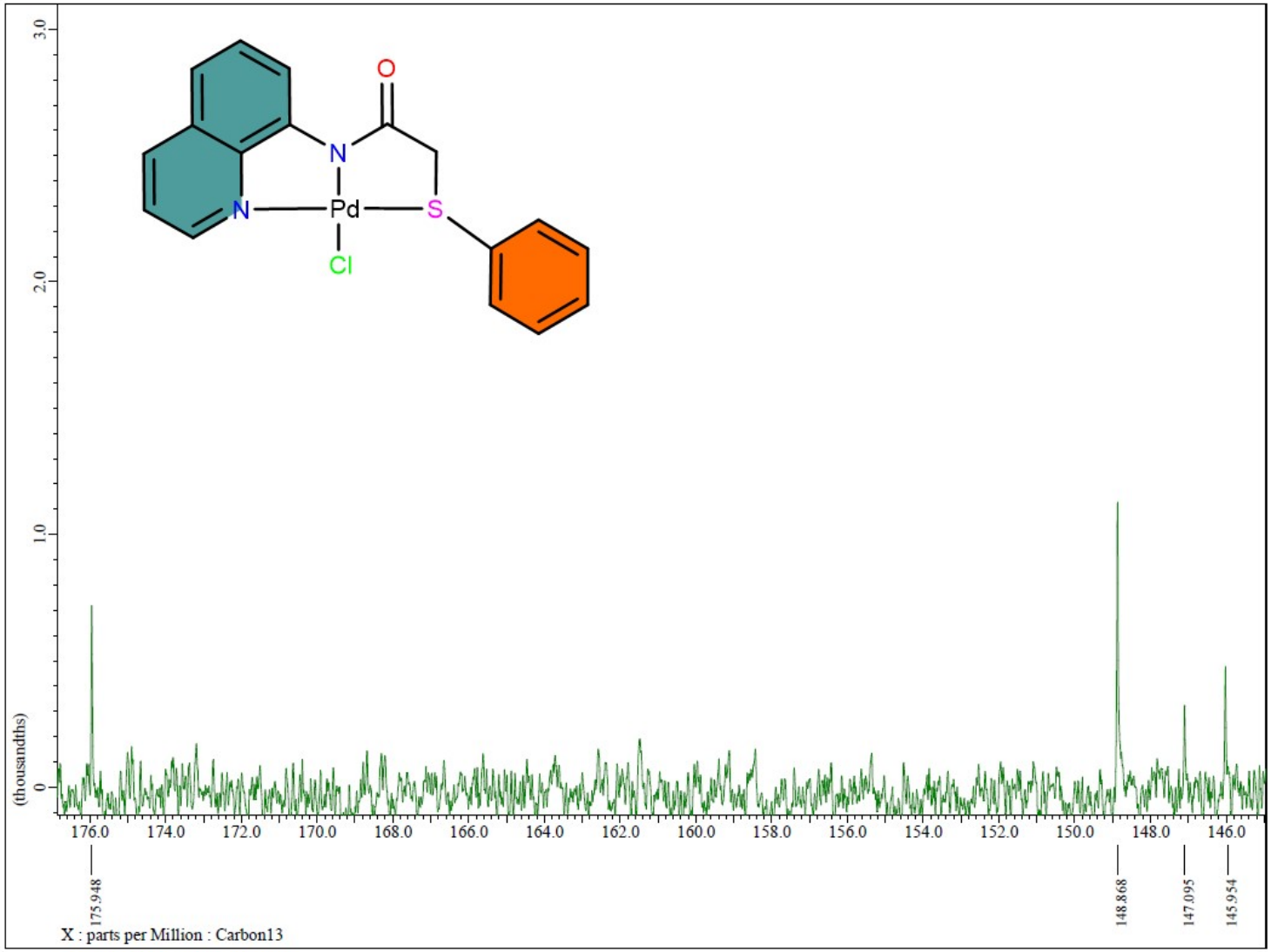

Fig. S52. $^{13}C\{^{1}H\}$ NMR ($CDCl_3$, 100.5 MHz) spectrum of **C1** in aryl region.

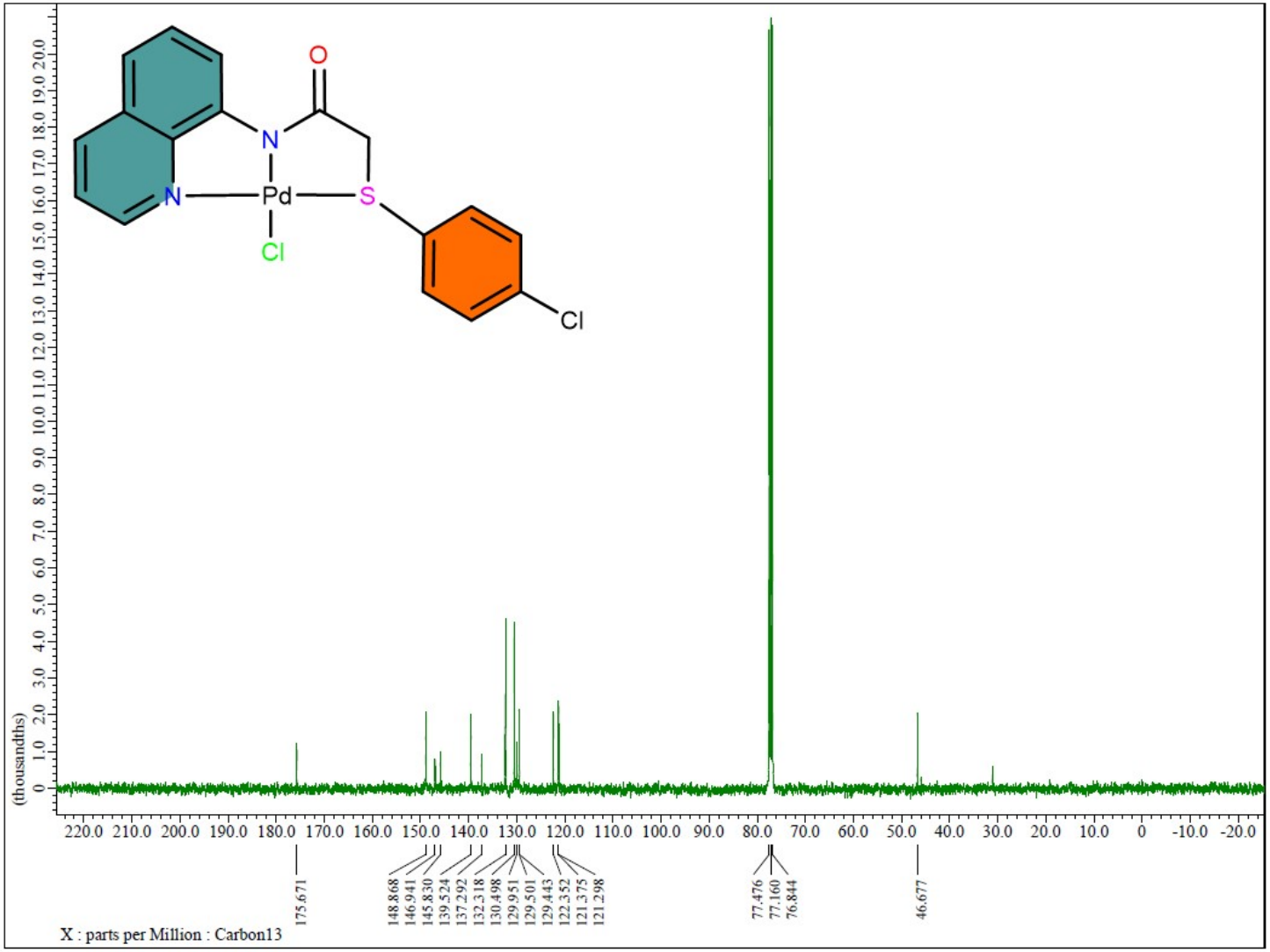

Fig. S53.$^{13}C\{^{1}H\}$ NMR ($CDCl_3$, 100.5 MHz) spectrum of **C2**.

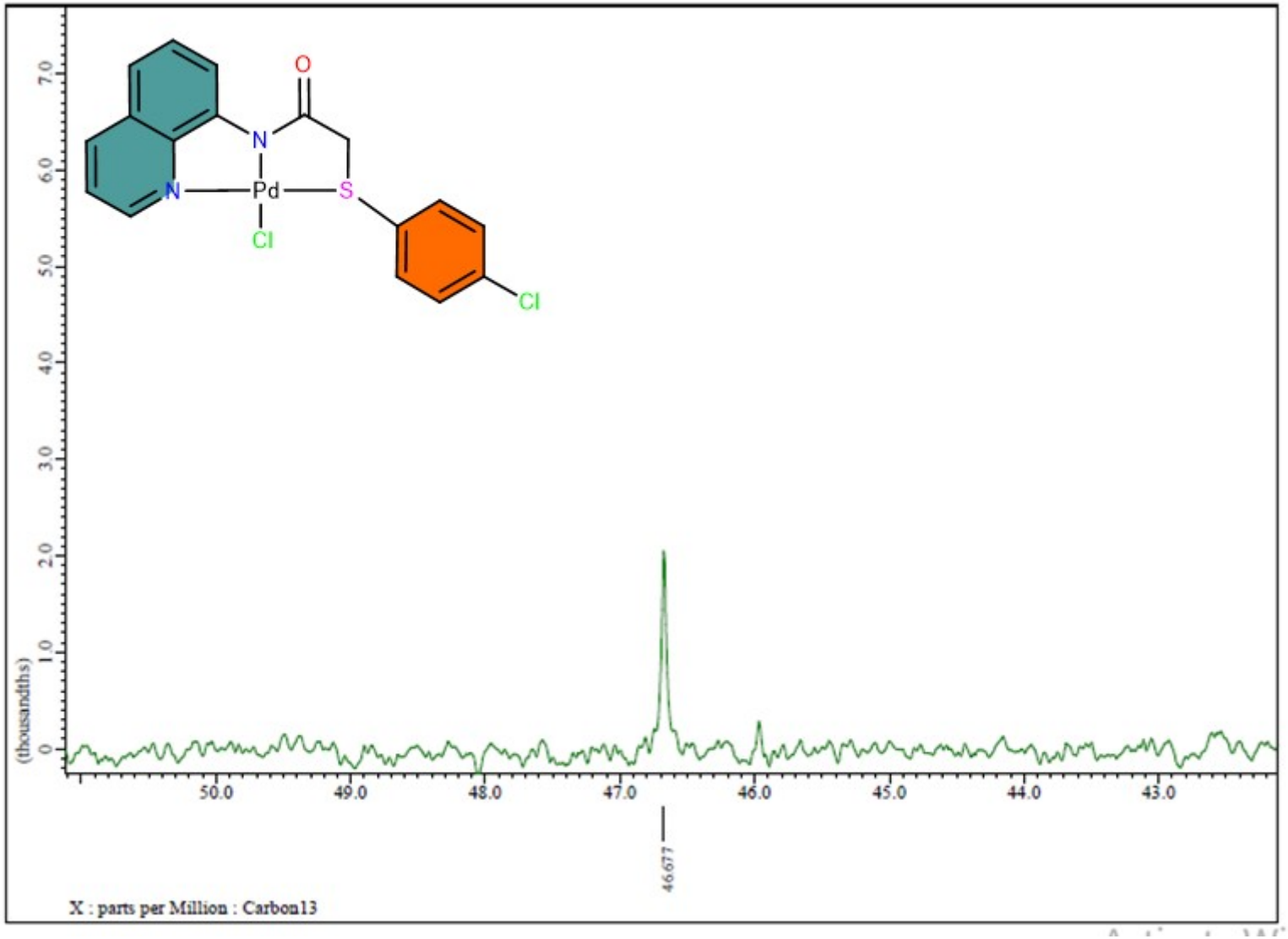

Fig. S54. $^{13}C\{^{1}H\}$ NMR ($CDCl_3$, 100.5 MHz) spectrum of **C2** in alkyl region.

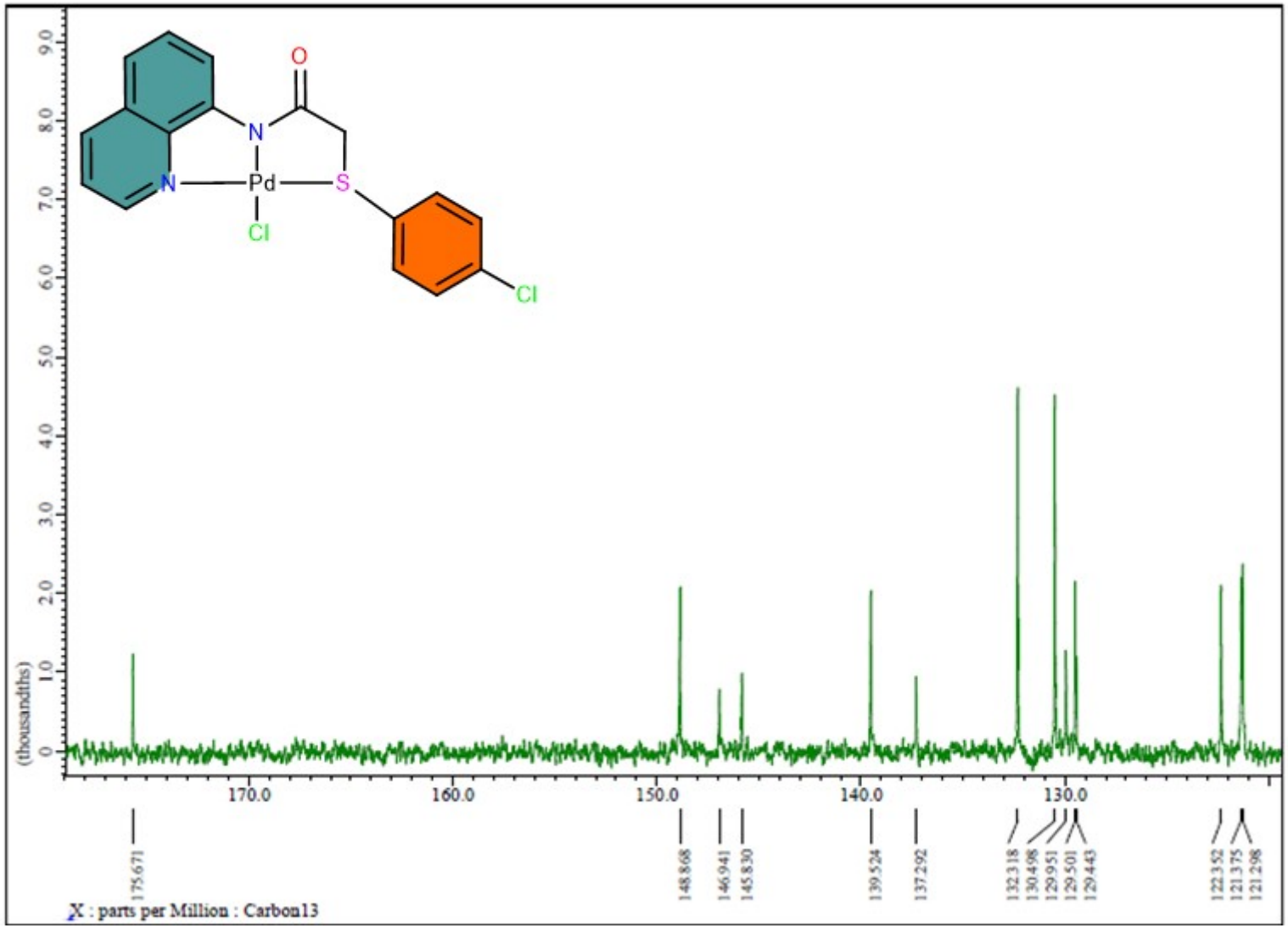

Fig. S55.$^{13}C\{^{1}H\}$ NMR ($CDCl_3$, 100.5 MHz) spectrum of **C2** in aryl region.

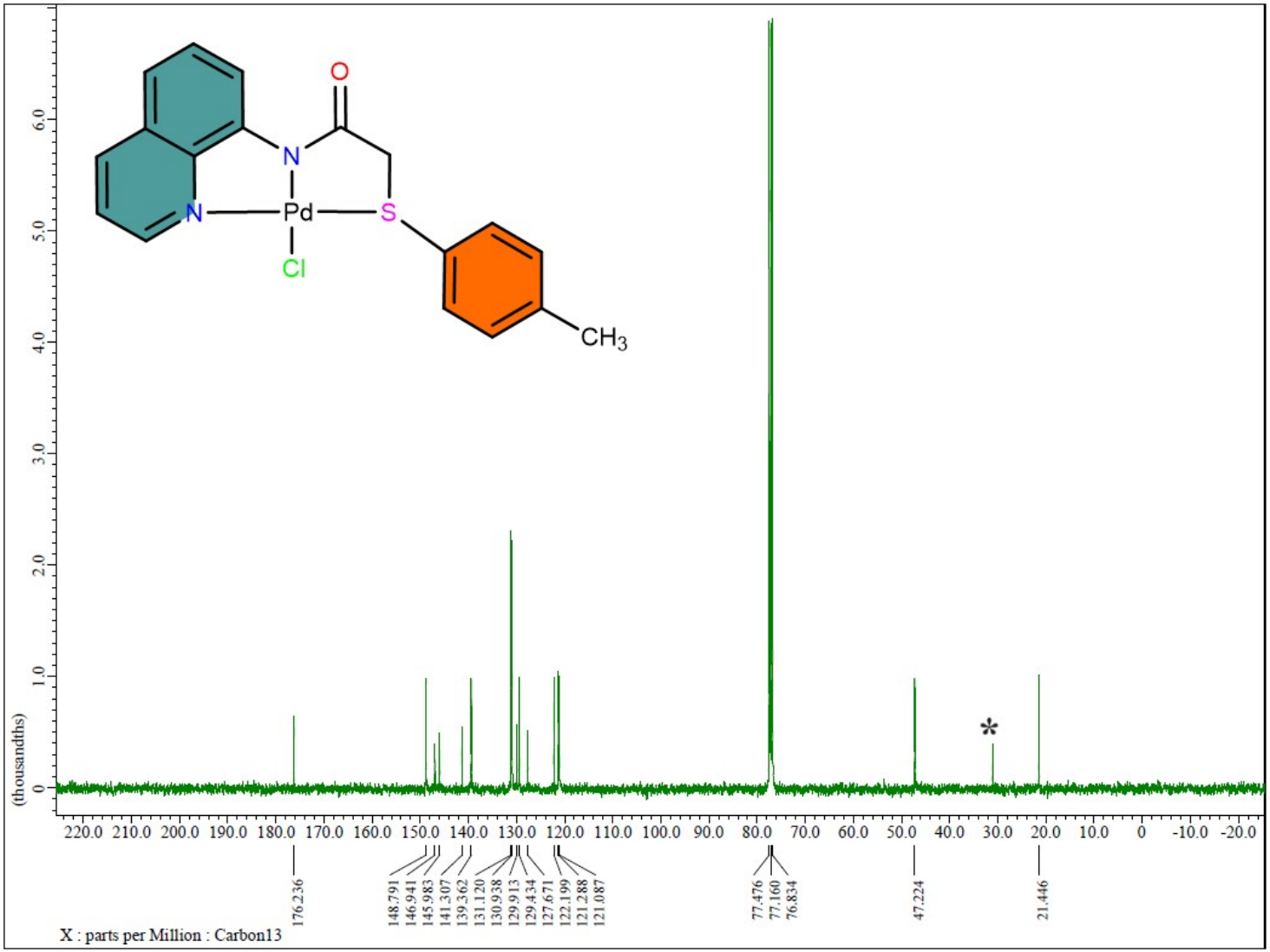

Fig. S56. $^{13}C\{^{1}H\}$ NMR ($CDCl_3$, 100.5 MHz) spectrum of **C3** and asterisk (*) represents the impurity.

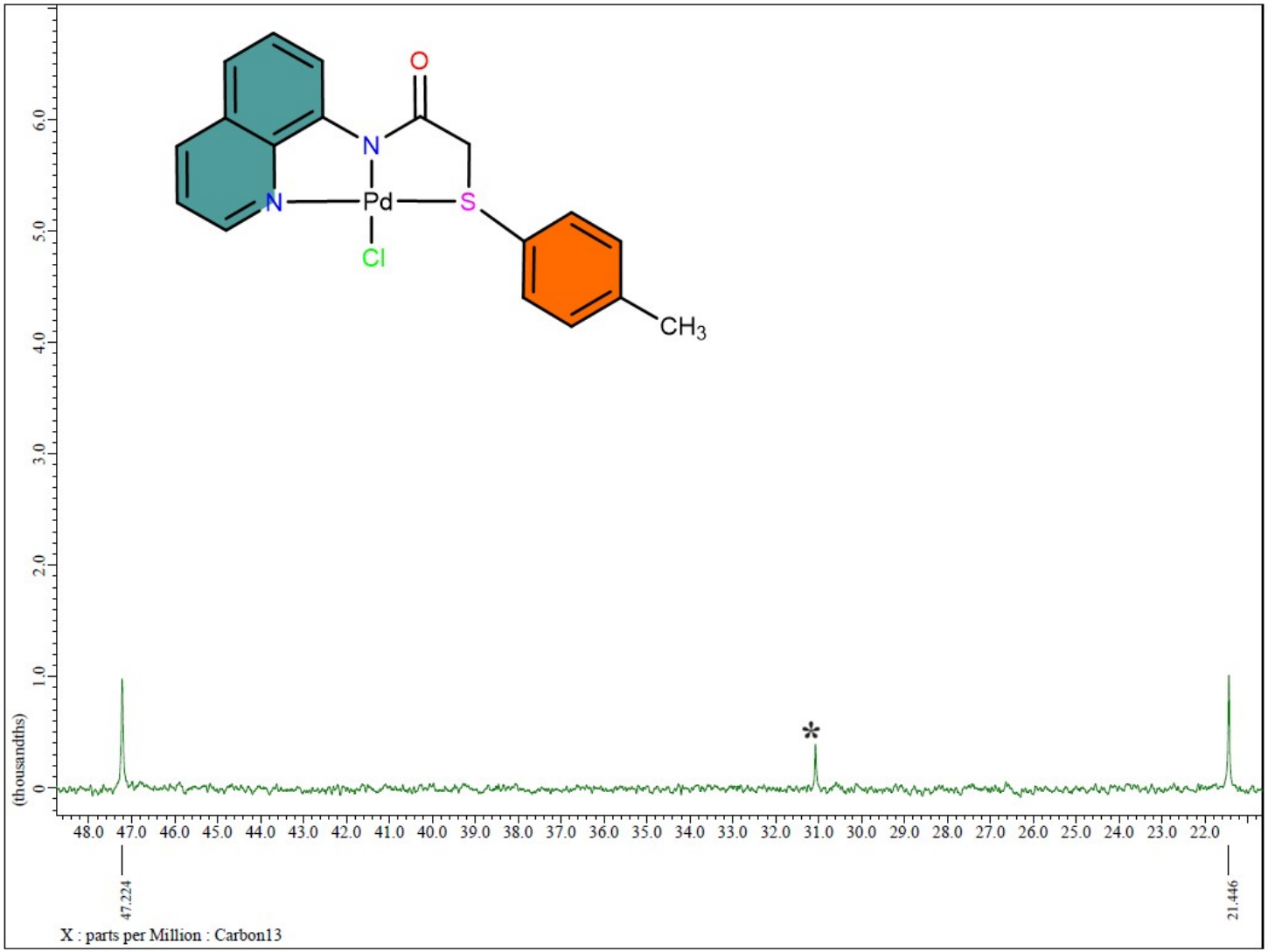

Fig. S57. $^{13}C\{^{1}H\}$ NMR ($CDCl_3$, 100.5 MHz) spectrum of **C3** in alkyl region and asterisk (*) represents the impurity.

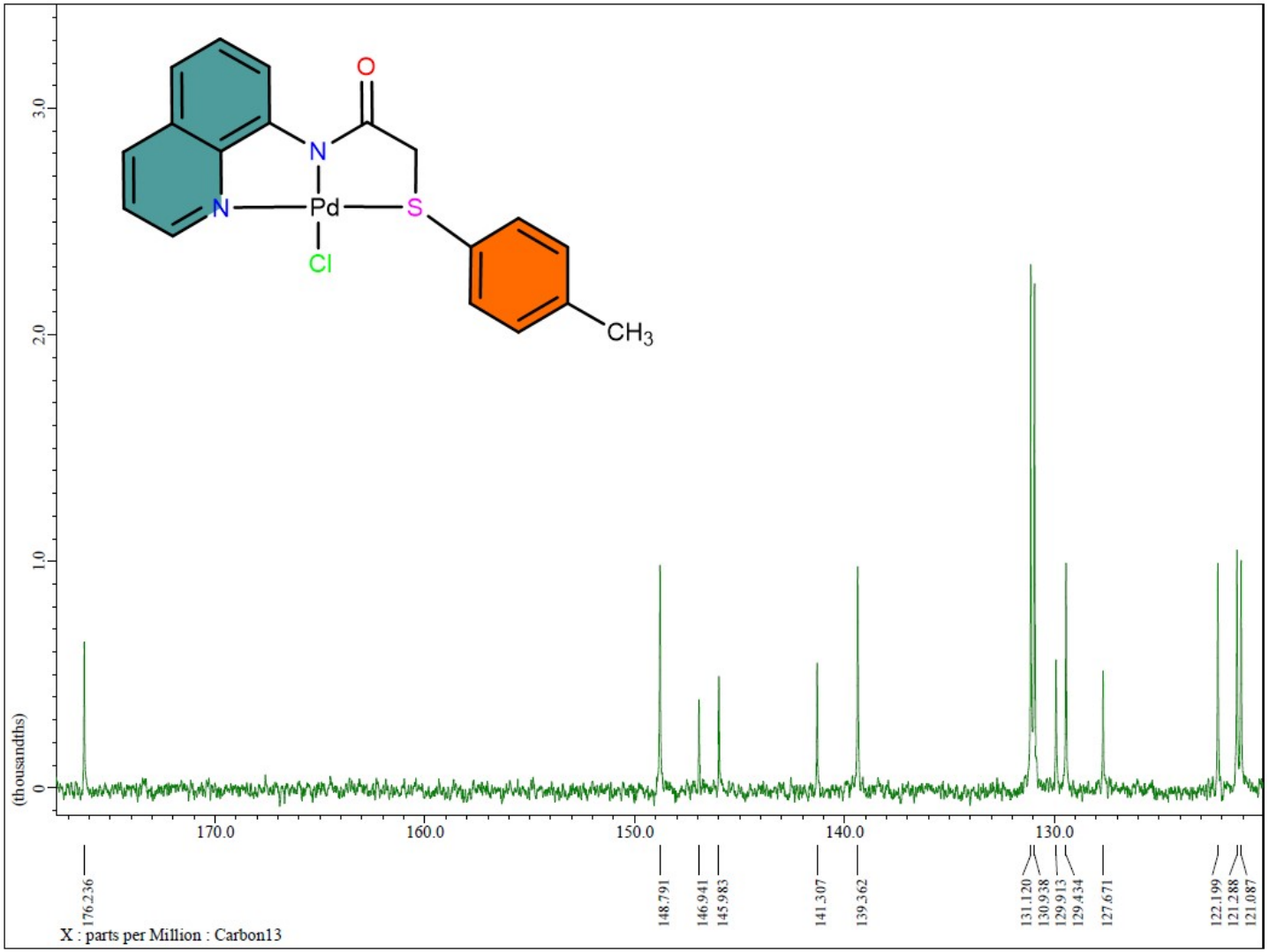

Fig. S58. $^{13}C\{^{1}H\}$ NMR ($CDCl_3$, 100.5 MHz) spectrum of **C3** in aryl region.

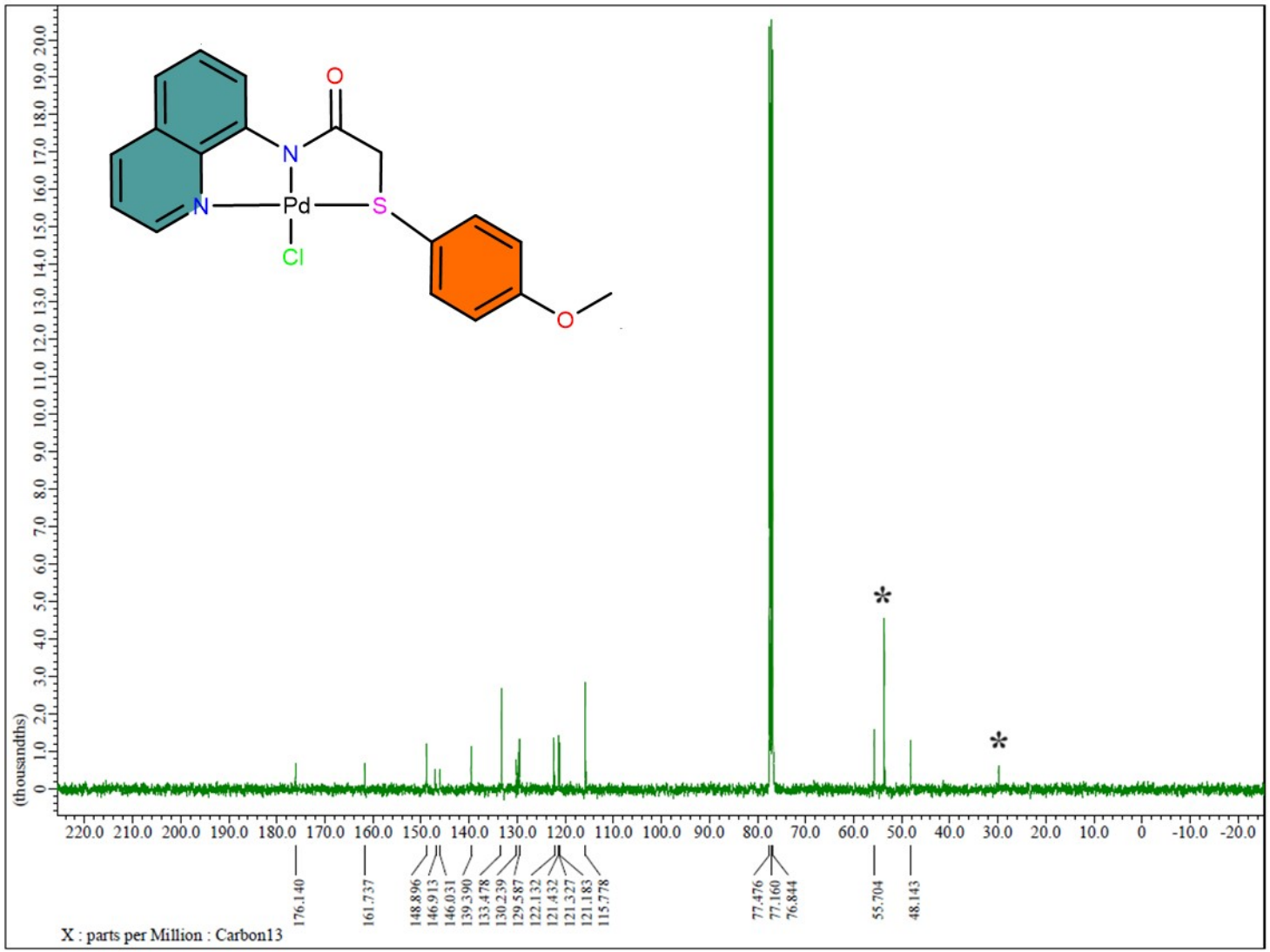

Fig. S59.$^{13}C\{^{1}H\}$ NMR ($CDCl_3$, 100.5 MHz) spectrum of **C4** and asterisk (*) represents the DCM.

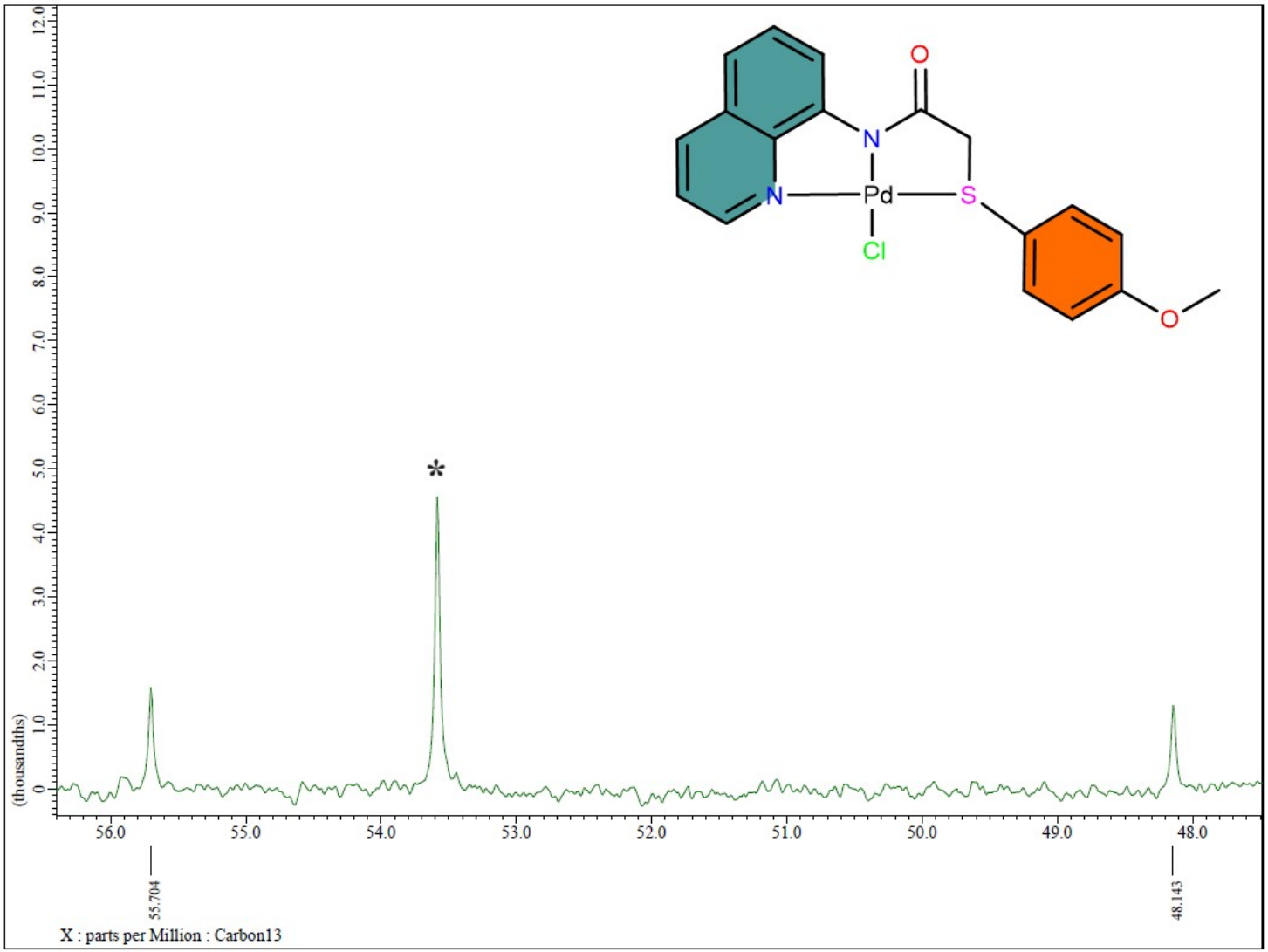

Fig. S60.$^{13}C\{^{1}H\}$ NMR ($CDCl_3$, 100.5 MHz) spectrum of **C4** in alkyl region and asterisk (*) represents the DCM.

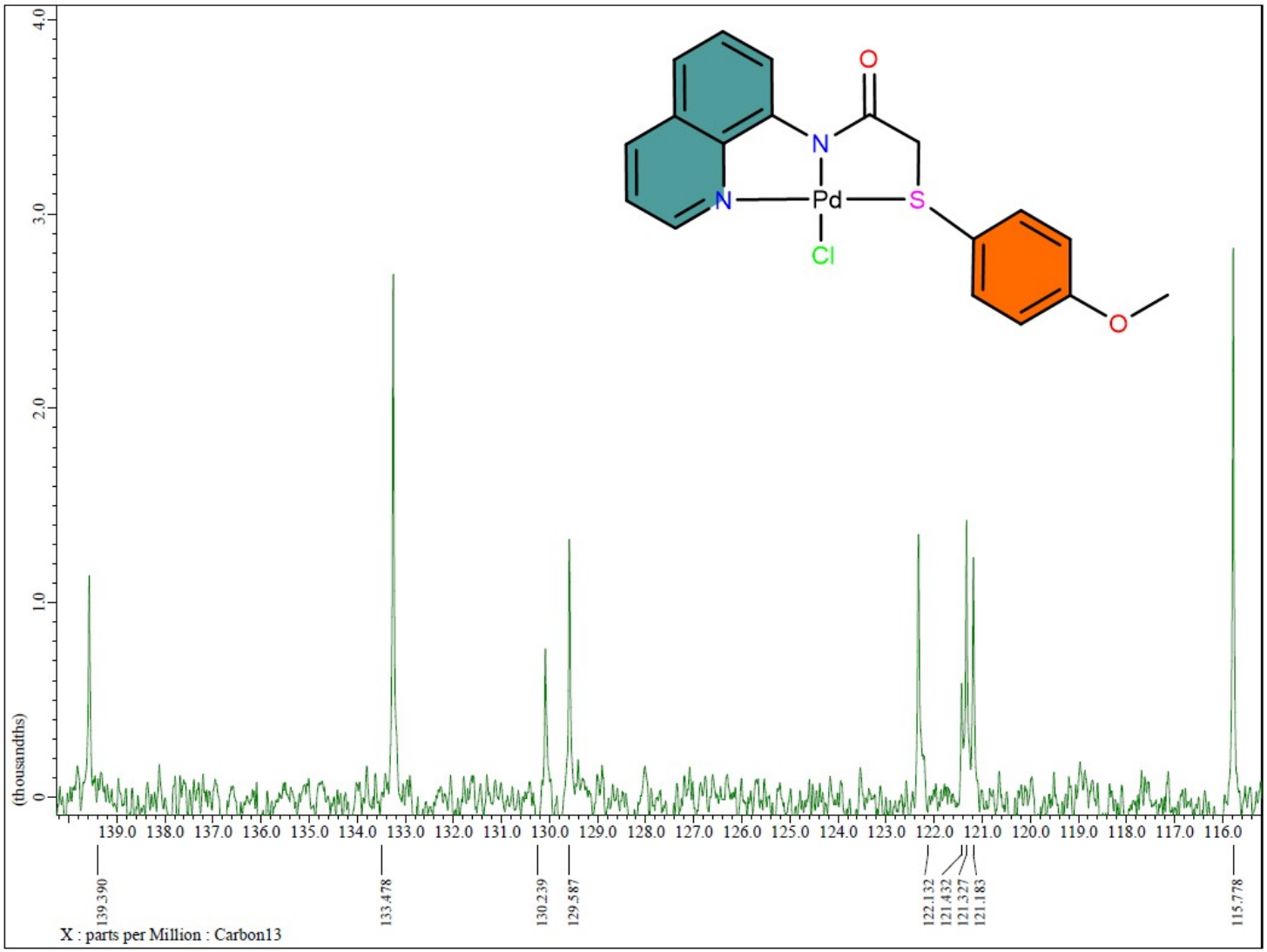

Fig. S61.$^{13}C\{^{1}H\}$ NMR ($CDCl_3$, 100.5 MHz) spectrum of **C4** in aryl region.

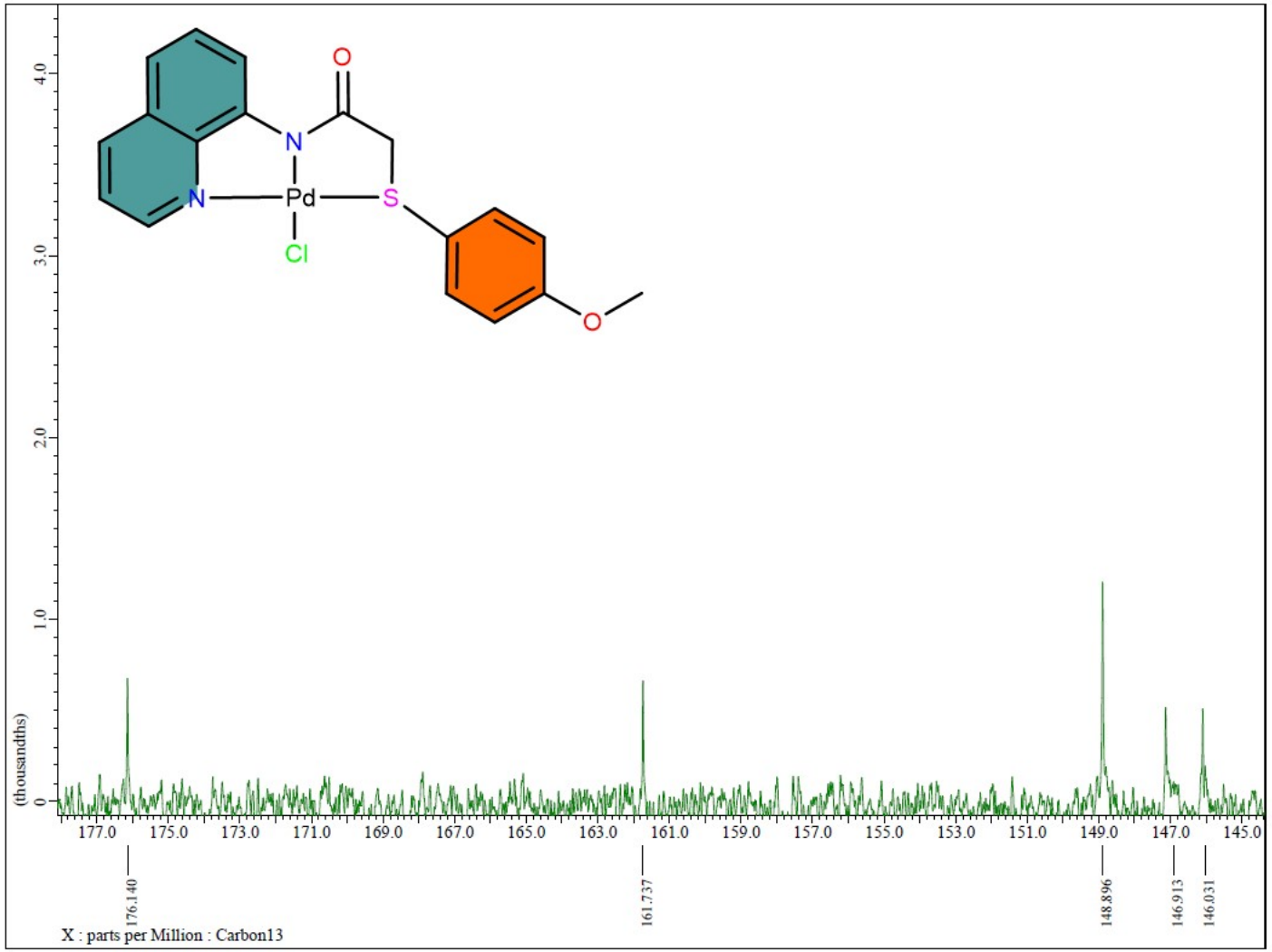

Fig. S62.$^{13}C\{^{1}H\}$ NMR ($CDCl_3$, 100.5 MHz) spectrum of **C4** in aryl region.

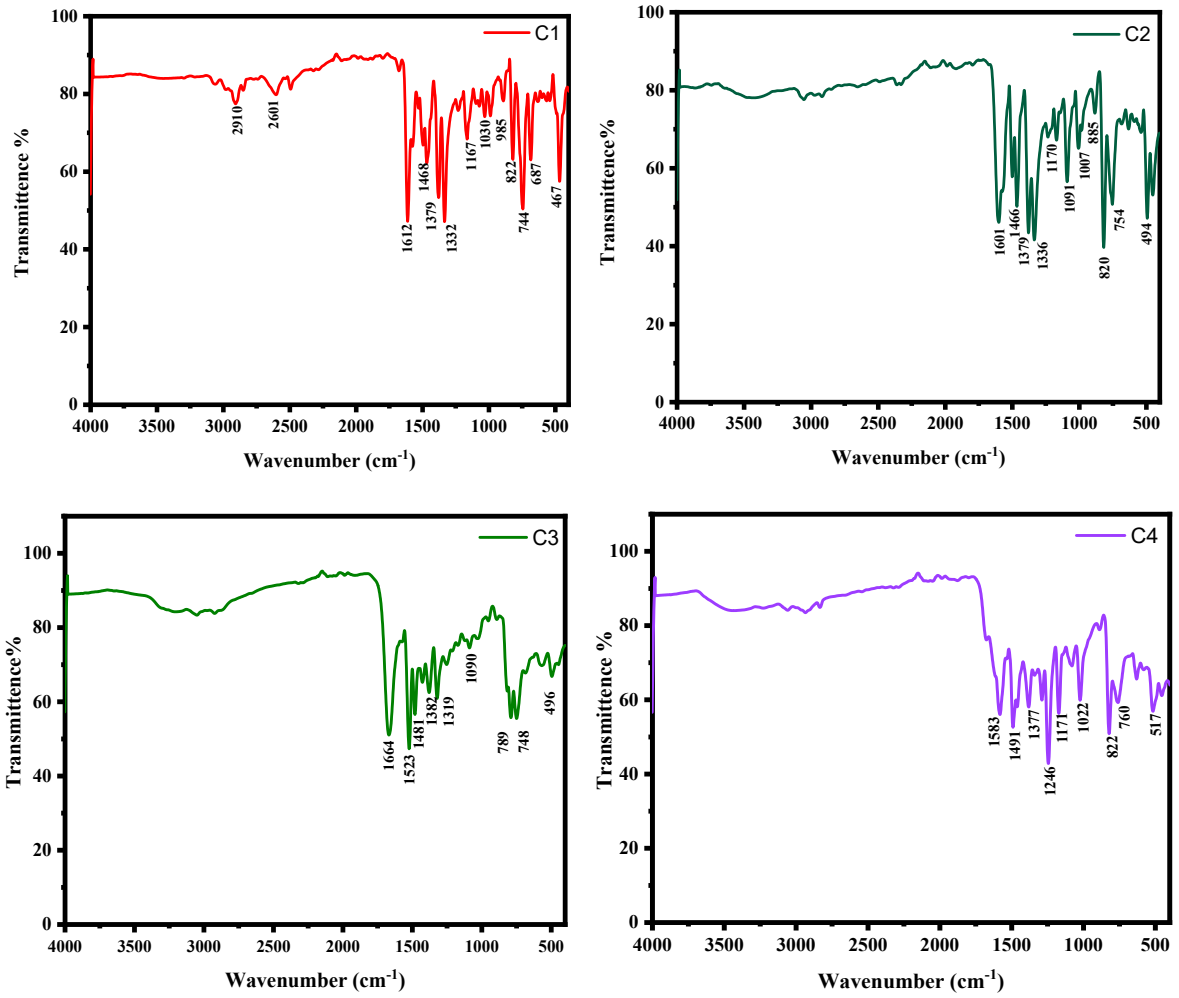

Fig. S63. FTIR spectra of **C1- C4.**

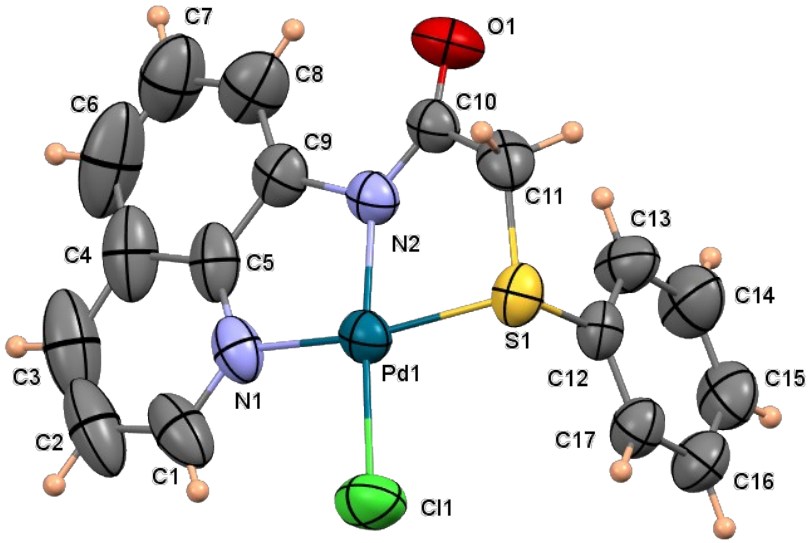

Figure 64: ORTEP of complex **1** with 50% probability ellipsoid. Selected bond lengths (Å) and angles (deg): Pd1–N1 2.018(6), Pd1–N2 1.945(5), Pd1–S1 2.2699(18), Pd1–Cl1 2.310(2); N1–Pd1–N2 86.3(3), N2–Pd1–S1 82.25(17), S1–Pd1–Cl1 93.69(9), N1–Pd1–Cl1 97.6(2), N1–Pd1–S1 167.31(18), N2–Pd1–Cl1 175.37(17).